STUDY ON CHANNEL ESTIMATION METHODS FOR OFDM BASED NEXT GENERATION WIRELESS COMMUNICATION SYSTEMS IN HIGHER TIME-VARYING FADING CHANNEL

MARCH 2016

TANAIRAT MATA

STUDY ON CHANNEL ESTIMATION METHODS
FOR OFDM BASED NEXT GENERATION
WIRELESS COMMUNICATION SYSTEMS
IN HIGHER TIME-VARYING FADING CHANNEL

by

Tanairat Mata, B.Eng., M.Eng.

Submitted in fulfillment of the requirements

for the Degree of Doctor of Engineering

Supervisor: Professor Hideo Kobayashi

Division of Systems Engineering

Graduate School of Engineering

Mie University

March 2016

三重大学

I declare that this chapter contains no material which has been accepted for a degree or diploma by the University or any other institution, except by way of background information and duly acknowledged in the thesis, and that, to the best of my knowledge and belief, this thesis contains no material previously published or written by another person, except where due acknowledgement is made in the text of the thesis.

Signed: _____

       Tanairat Mata

Date: _____

This thesis may be made available for loan and limited copying in accordance with the *Mie University Copyright Act 2016*

Signed: _____

Tanairat Mata

Date: _____

ABSTRACT

The Orthogonal Frequency Division Multiplexing (OFDM) technique has been received a lot of attentions especially in the wireless communication systems because of its efficient usage of frequency bandwidth and robustness to the multi-path fading. From these advantages, OFDM technique has been already adopted in many wireless communication systems as the standard transmission technique such as the wireless LAN (WLAN) system, broadband wireless communication system, the 4th generation mobile telecommunication (4G) system and the terrestrial digital broadcasting systems including the Digital Audio Broadcasting (DAB) and the Digital Video Broadcasting (DVB). Recently, many researchers proposed the various new systems based on OFDM technique such as Multi-Input and Multi-Output (MIMO)-OFDM system which can achieve higher data transmission rate or higher signal quality, uplink OFDM Access (OFDMA) system which can accommodate multiple users flexibly and efficiently, two-way relay communication system with broadband analogue network coding (ANC) which can increase the channel capacity and transmission efficiency. To achieve the potential capability for the proposed OFDM based wireless communication systems, there are still remaining many unsolved problems. In this thesis, several practical solutions are proposed to realize the above proposed OFDM based systems which can achieve higher signal quality and higher transmission efficiency in higher time-varying fading channel.

One of the limitations of using OFDM technique is the larger peak to average power ratio (PAPR) of its time domain signal which causes the severe degradations of bit error rate (BER) performance and undesirable spectrum re-growth due to the non-linear distortion occurring at the non-linear amplifier. In the wireless communication systems especially for the user terminal, a non-linear amplifier is usually employed at the transmitter which is required for the efficient usage of transmission power because of its battery operation. To solve this problem, the Partial Transmit Sequence (PTS) method was proposed as one of promising PAPR reduction methods which can achieve better PAPR performance with reasonable computation complexity. However the PTS method is required to inform the side information (SI) to the receiver for the correct demodulation of data information by using the separate channel which leads the complexity of transceiver and inefficient usage of frequency bandwidth. To solve this problem, this thesis proposes a new PAPR reduction method based on the packet-switched transmission systems in which all the clusters within the certain number of OFDM symbols have the sequential cluster ID numbers embedded in the header of each cluster. The proposed method enables the reduction of PAPR performance by re-ordering of clusters (ROC) in the frequency domain at the transmitter and reconstructs the original ordering of clusters by using the cluster ID numbers demodulated from each cluster at the receiver which requests no side information.

Intelligent Transport Systems (ITS) have been expanding with the popularization of Electrical Toll Collection System (ETC) and Vehicle Information and Communication System (VICS). The OFDM based Road to Vehicle Communication (RVC) system has been considered as one of the promising ITS technologies which can provide the drivers for safety and comfortable driving and collection of variable information from network in the real-time. This thesis proposes a RVC system of using the STBC (Space Time Block Coding) MIMO-OFDM technique which can achieve better BER performance even in higher time-varying fading channel. To achieve the potential capability in the proposed RVC system, it is the essential to realize the accurate channel estimation method. This thesis proposes a novel channel frequency response (CFR) estimation method by using the scattered pilot subcarriers in the frequency domain. From computer simulation results, this thesis demonstrates that the STBC MIMO-OFDM based RVC system of using the proposed CFR estimation method can

achieve higher channel estimation accuracy and better BER performance even in the time varying fading channel.

To achieve a potential capability of MIMO-OFDM system, it is the essential to realize an efficient and accurate channel estimation method. The conventional Discrete Fourier Transform Interpolation-based channel estimation (DFTI-CE) method of using the scattered pilot symbol can achieve higher estimation accuracy only when the transmission OFDM signal is sampled by the Nyquist rate. However the estimation accuracy of using the conventional DFTI-CE method would be degraded relatively when null subcarriers (zero padding) are inserted at both ends of data subcarrier to reject the aliasing occurring at the output of Digital to Analogue (D/A) converter which corresponds to the non-Nyquist sampling rate. To solve this problem, the Maximum Likelihood (ML) channel estimation method was proposed for MIMO-OFDM system which can achieve better estimation accuracy than the conventional DFTI-CE method. However its estimation accuracy would be degraded at around the both ends of data subcarrier at the non-Nyquist rate especially when increasing the number of transmit antennas and zero padding. To solve the above problem, this thesis proposes the ML based time domain channel estimation (TD-CE) method for MIMO-OFDM system which can achieve higher estimation accuracy even when the non-Nyquist rate and increasing the number of transmit antennas. From computer simulation results, this thesis demonstrates the effectiveness of propose ML based TD-CE method for MIMO-OFDM system.

OFDMA technique is considered as one of promising wireless access techniques which can accommodate multiple users flexibly and efficiently. In the uplink OFDMA system, since all users transmit their information data symbols to the base station (BS) simultaneously, it is required to estimate all user's channel frequency responses all together at the BS before receiving the information data symbols. The estimation of multiple users' channels in the uplink OFDMA system is similar to that the estimation of multiple channels between the transmit antenna and the receive antenna in the MIMO-OFDM system. From computer simulation results, this thesis also demonstrates the effectiveness of above proposed ML based TD-CE method when employing in the uplink OFDMA system.

Broadband ANC of using the OFDM technique has been widely investigated to increase the capacity of two-way relay communication. In the two-way relay communication, it can be simply modeled by two user terminals (UTs) and one relay station (RS) in which each UT sends his information data to the other UT through the RS by using two timeslots. Each UT can demodulate the other user's information data by removing its self-information data with frequency domain equalization (FDE). To conduct the removal of self-information data and the FDE precisely, it is the essential to realize the accurate channel estimation method for the combined CFR in the 1st and 2nd timeslots from the superimposed received signal sent from both UTs at each UT. To solve this problem, this thesis proposes the ML based combined CFR estimation method for two-way relay communication system by using a novel scattered pilot assignment method including the null subcarriers to avoid the collision of pilot subcarriers sent from both UTs. From the various computer simulation results, this thesis demonstrates the effectiveness of proposed ML based combined CFR estimation method which can achieve higher estimation accuracy and better BER performance even in higher time-varying fading channel.

This thesis also demonstrates the effectiveness of proposed ML based combined CFR estimation method when employing the two-way communication system of using the SFBC (Space-Frequency Block Coding) MIMO-OFDM technique to improve the BER performance. The salient feature of proposed CFR estimation method is to employ the pilot subcarriers with Walsh code to differentiate the pilot subcarriers sent from both UTs. From computer simulation results, this thesis confirms that the proposed SFBC MIMO-OFDM system of using the ML based combined CFR estimation method can achieve higher CFR estimation accuracy and better BER performance with higher transmission efficiency even in higher time-varying fading channel.

From the numerous computer simulation results, it is confirmed that the proposed methods presented in this thesis can be employed as the practical solutions to realize the next generation OFDM based wireless communication systems.

ACKNOWLEDGEMENTS

TABLE OF CONTENTS

LIST OF TABLES

LIST OF FIGURES

LIST OF FIGURES

CHAPTER 1

INTRODUCTION

This chapter presents an overview of OFDM (Orthogonal Frequency Division Multiplexing) technique in Section 1.1 including the general structure of an OFDM system, standardized system of using the OFDM technique in the wireless communications systems, and the PAPR problems which is the main disadvantage of OFDM signal and several solutions for PAPR problems. Section 1.2 briefly explains an overview of MIMO (Multi Input Multi Output) Based OFDM signal. Section 1.3 introduces the uplink OFDMA (Orthogonal Frequency Division Multiple Access) method. Then, the Broadband ANC (Analog Network Coding) based wireless two-way relay communication is presented in Section 1.4. Subsequently, the background of all topics included in this research is presented in Section 1.5. Finally, it describes the organization of thesis contents in Section 1.6.

1.1 Overview of OFDM System

Orthogonal Frequency Division Multiplexing (OFDM) is a multicarrier transmission technology in wireless communication which was developed from the conventional FDM (Frequency Division Multiplexing) technique to increase the bandwidth efficiency. The basic concept of OFDM is to divide the available bandwidth into several narrowband subcarriers and keep their frequency responses overlap and orthogonal. Up to today, the OFDM technique has been received a lot of attentions because of its efficient usage of frequency bandwidth and robustness to multipath fading. From these advantages, many standard transmission techniques employ the OFDM technique such as in the Wireless LAN, in the digital audio and video broadcasting (DAB and DVB), in the next generation of mobile communication system (LTE: Long Term Evaluation), and etc.. However, one of the limitations of using OFDM technique is the larger peak to average power ratio (PAPR) signal of its time domain signal which causes the severe degradation of system performance due to the inter-modulation noise occurring at the non-linear amplifier. The process of generating an OFDM signal will be described step by step in this section.

1.1.1 OFDM Basics

Figure 1.1 shows the spectrum of an OFDM symbol which each subcarrier can still be separated from the others because of the orthogonality guarantees which can get higher bandwidth efficiency. Moreover, the orthogonality of subcarriers' spectra can reduce the Inter-Symbol Interference (ISI) and Inter-Carrier Interference (ICI). However, when the OFDM signal is passed thought a time dispersive channel, it also makes that orthogonality of the subcarrier is lost, resulting inter carrier interference (ICI). To solve this problem, the cyclic prefix (CP) or guard interval (GI) is inserted at the top of OFDM symbol as shown in Figure 1.2. Figure 1.2 shows a structure of guard interval inserted in OFDM symbol which the GI is a copy of the last part of OFDM symbols that is deliberate to the transmitted symbol and is removed at the receiver before the demodulation. By using the GI, the subcarrier can maintain orthogonality of frequency responses each other even over time-varying channel. As long as keeping the length of GI longer than the time delay of reflected signal, the composite signal can reduce the influence of the ISI and ICI significantly and also improve the transmission quality over fading channel. However, the transmitted energy increases with the length of the cyclic prefix. There is loss power due to the insertion of the GI.
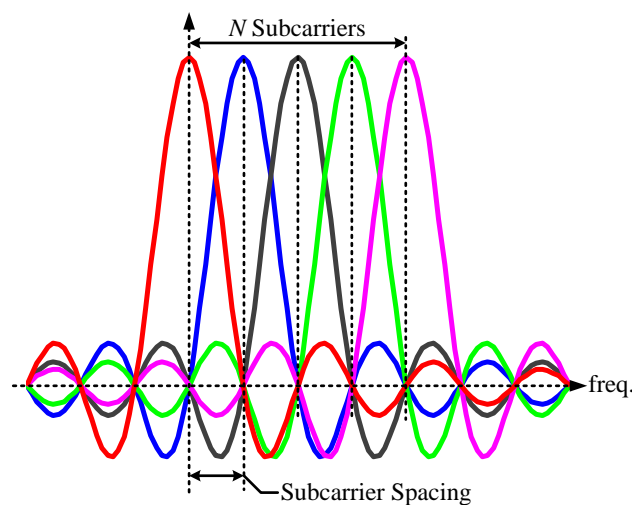
Figure 1.1: Spectrum of an OFDM symbol.
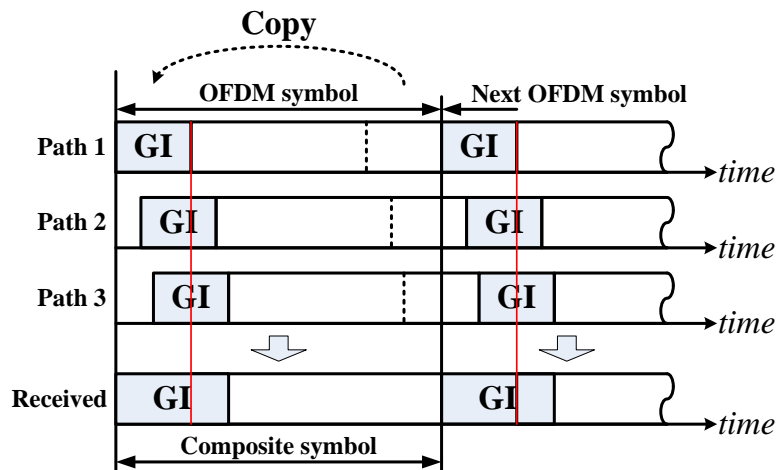
Figure 1.2: Structure of guard interval in OFDM symbol.

Figure 1.3 shows the structure of wireless OFDM transceiver. At the transmitter, X_n which is the modulated signal of information data D_n at the n-th subcarrier in the frequency domain is converted into time domain signal x_k by using IFFT processing which can be expressed by,

$$x_k = \frac{1}{\sqrt{N}} \sum_{n=1}^{N} X_n \cdot e^{j\frac{2\pi(k-1)(n-1)}{N}}, 1 \le k \le N \qquad (1.1)$$

where N is the number of IFFT-points. The time domain OFDM signal x_k after adding the guard interval (GI) to will be converted to the analogue signal by the digital-to-analogue converter (D/A) and then transmitted the signal s_t to the receiver which is passed through the multipath fading channel.

At the receiver, the time domain received signal y_t with adding the Addition white Gaussian noise z_t is removed the GI after A/D converter to get the received signal r_k. Then it will be transformed by FFT processing into the frequency domain which can obtain the frequency domain received signal $\hat{X}_n$ then $\hat{X}_n$ will be demodulated which can output the demodulated data $\hat{D}_n$ on each subcarrier.
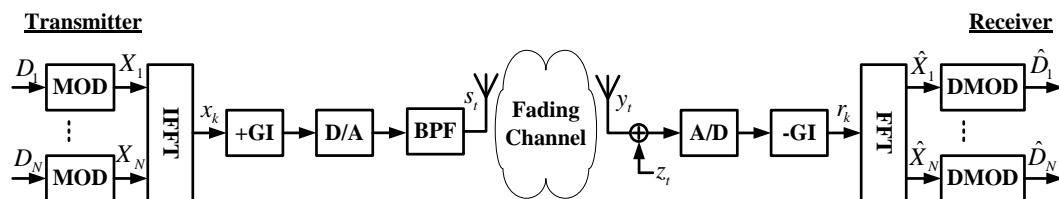
Figure 1.3: Overview of wireless OFDM transceiver

1.1.2   OFDM Standards

At present, OFDM has been widely incorporated in various wireless communication systems especially in three main applications including in Terrestrial Digital Video Broadcasting (DVB-T), Wireless Local Area Network (WLAN) and Mobile Broadband Wireless Access (MBWA) which are described in this section.

1.1.2.1   Terrestrial Digital Video Broadcasting (DVB-T)

In 1997, the Digital Television Broadcasting - Terrestrial (DVB-T) with using of OFDM, was standardized by the European Telecommunication Standards Institute (ETSI). Then it first broadcasts in the UK in 1998 [1]. Up to today, the DVB-T is the most widely used digital

television standard in use around the globe for terrestrial television transmissions. Recently, the DVB-T is developed the second generation digital terrestrial television broadcasting system as known as DVB-T2 which can offer more robustness, flexibility and 50% more efficiency than any other Digital Terrestrial television (DTT) systems [2].

1.1.2.2 Wireless Local Area Network (WLAN)

In 1998, IEEE selected OFDM as the basis for the new 802.11a 5GHz standard in the U.S. targeting a range of data rates up to 54Mbps [3]. In Europe, ETSI BRAN adopted OFDM in the standard of HIPERLAN/2 [4]. The physical layer of HIPERLAN/2 is quite similar to IEEE 802.11a WLAN. The main differences between IEEE 802.11a and HIPERLAN type 2 are in the medium access control (MAC). The IEEE 802.11a uses distributed MAC based on carrier sense multiple access with collision avoidance (CSMA/CA), whereas the HIPERLAN type 2 uses a centralized and scheduled MAC based on time division multiple access with dynamic slot assignment (TDMA/DSA). The MMAC support both of these MACs. In terms of the physical layer (PHY), there are only a few minor differences among the three standards.

1.1.2.3 Mobile Broadband Wireless Access (MBWA)

In 2008, IEEE specified the IEEE 802.20 or Mobile Broadband Wireless Access (MBWA) systems based OFDM for Mobile wireless internet access network [5] which is operated in the 3.5GHz and supported mobility classes up to 250km/h. IEEE 802.20 TDD Wideband and 625k-MC Modes was applied in Japan which is published by ARIB Standard in order to ensure fairness and transparency in the defining stage, the standard was set by consensus of the standard council with participation of interested parties including radio equipment manufacturers, telecommunications operators, broadcasters, testing organizations, general users, etc. with impartiality [6].

1.1.3   Peak-to-Average Power Ratio

One of the major disadvantages of OFDM technique is the high PAPR in the time domain signal because of independently modulated subcarriers which the instantaneous power is very larger than the average power of the signal. The larger PAPR signal would cause the fatal degradation of BER performance and un-desirable spectrum re-growth in the non-linear channel.

1.1.3.1   Mathematical Definition

The PAPR of the time domain OFDM signal x_i given in (1.1) is defined as the ratio of the maximum peak power divided by the average power of the OFDM signal which can be expressed by,

$$PAPR(x_k) \triangleq \frac{\underset{1 \leq k \leq N}{Max}\left[|x_k|^2\right]}{P_{av}(x_k)} \qquad (1.2)$$

with

$$P_{av}(x_k) = \frac{1}{N}\sum_{k=1}^{N}E\left[|x_k|^2\right] \qquad (1.3)$$

where $E[\cdot]$ denotes the expected value.

1.1.3.2   Distribution of PAPR

The PAPR performance for the time domain OFDM signal from the statistical point of view is evaluated by using the complementary cumulative distribution function (CCDF) which can be used to represent the probability of exceeding a given threshold $PAPR_0$,

$$CCDF\left(PAPR_0\right) = \Pr\left(PAPR\left(x_k\right) > PAPR_0\right) \tag{1.4}$$
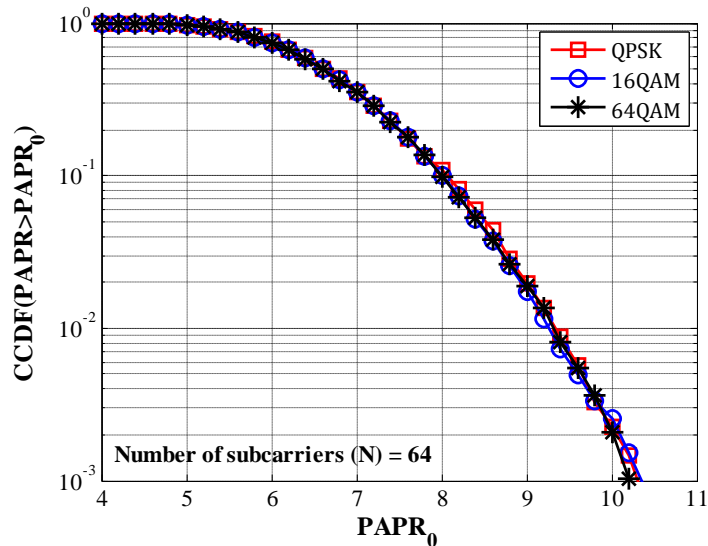
Figure 1.4: PAPR performance when changing modulation technique.

Figure 1.4 shows the example calculation results of PAPR performance for the conventional OFDM signal when changing the modulation technique. The modulation technique is taken by QPSK, 16QAM, and 64QAM, respectively. Form the Figure, it can be observed that all modulation techniques show the same PAPR performance. This means that the modulation technique does not affect the PAPR performance for the OFDM signal.

From (1.1), the OFDM complex baseband signal for N subcarriers can be rewritten as,

$$x_k = \sum_{n=1}^{N}\left\{a_n \cdot \cos\left(\omega_n k\right) + j \cdot b_n \cdot \sin\left(\omega_n k\right)\right\} \tag{1.5}$$

where a_n and b_n are the in-phase and quadrature modulating symbols. If each subcarrier has amplitude A, the maximum PAPR of the signal can be calculated the following as,

$$\max\left(PAPR\left(x_k\right)\right) = \frac{\left(N \cdot A\right)^2}{N \cdot \dfrac{A^2}{2}} = 2N \tag{1.6}$$

From (1.6), the maximum PAPR of OFDM signal will be higher when the number of subcarriers (N) becomes larger. Figure 1.5 shows the PAPR performance of conventional OFDM signal when changing the number of subcarriers. The number of subcarriers is taken by 64, 256 and 1028 subcarriers, respectively. From the Figure, it can be seen that the PAPR performance is increasing when increasing the number of subcarriers.
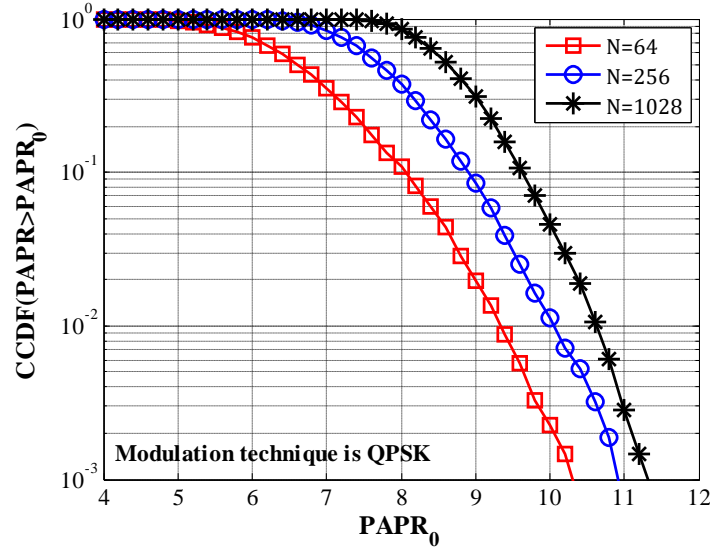
Figure 1.5: PAPR performance when changing the number of subcarriers.

1.1.4 Solutions for PAPR Problem

To solve the PAPR problem in OFDM systems, various PAPR reduction methods have been proposed up to today including such as partial transmit sequence method (PTS) [7][8], selected mapping method (SLM) [9][10], and etc.

1.1.4.1 Partial Transmit Sequence Method (PTS)

Figure 1.6 shows the block diagram of PTS method. In the PTS method, the data information in the frequency domain X_n is partitioned into V clusters as $X_n^{(v)} (1 \leq v \leq V)$. All subcarriers for each cluster are multiplied by the weighting factor, $b_k^{(v)} = e^{j\phi_k^{(v)}}$ in order to reduce the PAPR performance. Here the phase value which is considered in each cluster will be given by the following equation,

$$\phi_k^{(v)} \in \left\{ \frac{2\pi w}{W} \right\}, \ 0 \leq w \leq W-1 \tag{1.7}$$

where W is the number of predetermined discrete phase. After multiplying the weighting factor for each cluster, the subcarrier vector is given by,

$$y_k = \sum_{v=1}^{V} \left(b_k^{(v)} \cdot IFFT\left\{ X_n^{(v)} \right\} \right) = \sum_{v=1}^{V} \left(b_k^{(v)} \cdot x_k^{(v)} \right) \tag{1.8}$$

From (1.8), the optimized PAPR performance can be given by,

$$\tilde{V} \triangleq \min_{0 \leq w \leq W-1} \left\{ \max_{0 \leq l \leq L-1} \left[\left| \sum_{v=1}^{V} \left(b_k^{(v)} \cdot x_k^{(v)} \right) \right| \right] \right\} \tag{1.9}$$

where $\tilde{V}$ is optimized argument that can reduce to the lowest PAPR performance. L is the number of OFDM symbols in one frame. The information about the selected phase factor is sent to the receiver as Side Information so as to be used for recovering the original data block. Here, it should be noted that the amount of PAPR reduction of PTS method depends on the number of subblocks (N/V) and the number of allowed phase factors (W).
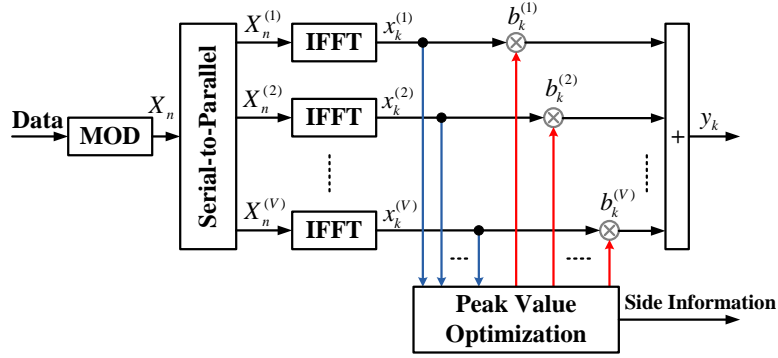
Figure 1.6: Block diagram of PTS method.

1.1.4.2 Selected Mapping Method (SLM)

Figure 1.7 shows the block diagram of SLM method. In the SLM method, the data information in the frequency domain X_n is modified to be U data blocks as $X_n^{(u)}$ ($1 \le u \le U$). All U data blocks are multiplied by U different phase sequences, $B_n^{(U)}$ which is defined so that $\left| B_n^{(U)} \right| = 1$ where $|\cdot|$ denotes the modulus operator, in order to reduce the PAPR performance. Each resulting $B_n^{(u)} \cdot X_n^{(u)}$ after performed by IFFT processing can be given by,

$$x_k^{(u)} = \frac{1}{\sqrt{N}} \cdot \sum_{n=1}^{N} \left(B_n^{(u)} \cdot X_n^{(u)} \right) \cdot e^{j\frac{2\pi(n-1)(k-1)}{N}}, 1 \le k \le N \tag{1.10}$$

All of the modified data blocks after IFFT processing, $x_k^{(u)}$ ($u=1,2,…,U$) are calculated the PAPR which is given by (1.2) then the one with the lowest PAPR performance is selected for transmission. Similarly to the PTS method, the original data block at the receiver can be recovered by using the side information sent from the transmitter. Here, it should be noted that the amount of PAPR reduction of SLM method depends on the number of phase sequences U and the design of the phase sequences.
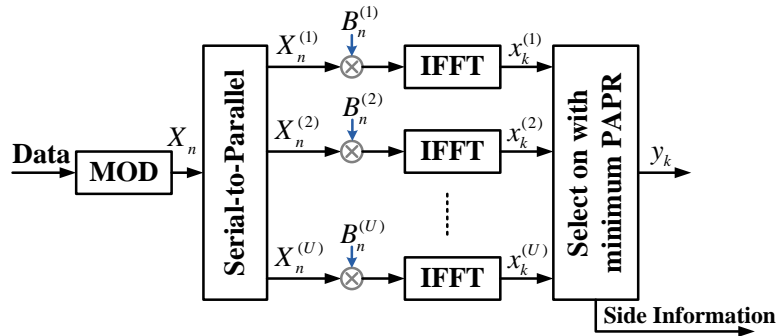
Figure 1.7: Block diagram of SLM method.

1.1.4.3 Other Solutions

Beside two above methods, it also has the other methods such as Clipping and Filtering [11][12] method which reduces the PAPR by setting the threshold value for clipping the amplitude of any subcarriers and Filtering the signal to bring out a lower PAPR performance, Dummy Sequence Insertion (DSI) [13][14] which reduces the PAPR by increasing the average power of the signal and etc. However, it's not given the detail in this thesis.

1.2 Overview of MIMO-OFDM System

One of the radio communication technologies is Multiple Input Multiple Output (MIMO) technique which the communication system transmits and receives by using multiple antennas on both transmit and receive sides. Up to today, MIMO technique is still developing extensively because of its potential capability to increase the link capacity and spectral efficiency with keeping higher signal quality. The two main formats for MIMO technique are the spatial diversity and spatial multiplexing. Firstly, the spatial diversity can be divided into two methodologies: transmit and receive diversities which can improve the reliability of the system. Another, the spatial multiplexing can be used to provide additional data capacity by utilizing the different paths to carry additional traffic. From the mentioned above, it can be concluded that the MIMO technique has a capability to achieve the spatial diversity gains for improving the transmission quality and to realize the spatial multiplexing for improving the transmission rate.

1.2.1 MIMO-OFDM System

Figure 1.8 shows the structure of MIMO-OFDM system. At the transmitter, the information data input is modulated and separated by N subcarriers into each transmit antenna. Then converted into the time domain signal by N points IFFT at each transmit antenna. The time domain signal x_k^i at the k-th time sample transmitted from the T_i transmit antenna ($1 \leq i \leq N_T$) can be expressed as,

$$x_k^i = \frac{1}{\sqrt{N}} \sum_{n=1}^{N} X_n^i \cdot e^{j\frac{2\pi(k-1)(n-1)}{N}}, 1 \leq k \leq N \tag{1.11}$$

The channel impulse response (CIR) of multipath fading between the i-th transmit and the j-th receive antennas can be expressed by,

$$h_k^{i,j} = \sum_{q(i,j)=1}^{N_P} \rho_{q(i,j)}^{i,j} \cdot \delta\left(k - q(i,j)\right), 1 \leq k \leq N \tag{1.12}$$

where N_P is the number of delay paths and $\rho_{q(i,j)}^{i,j}$ represents the complex amplitude of CIR for the $q(i,j)$-th delay path occurred in the channel between the i-th transmit and j-th receive antennas. At the j-th receive antenna, the superimposed received signal r_k^j sent from all transmit antennas after adding the guard interval (GI) to avoid the inter symbol interference (ISI) can be given by,

$$r_k^j = \sum_{i=1}^{N_T} \left\{ x_k^i \otimes h_k^{i,j} \right\} + z_k^j = \sum_{i=1}^{N_T} \sum_{q(i,j)=1}^{N_P} \left\{ \rho_{q(i,j)}^{i,j} \cdot x_{k-q(i,j)}^i \right\} + z_k^j, \quad \left(1 \leq j \leq N_R\right) \tag{1.13}$$

where z_k^j is the additive white Gaussian noise (AWGN) at the k-th time sample of the j-th receive antenna and $\otimes$ represents the convolution operator.

By performing FFT to (1.13), the received frequency domain $\tilde{X}_n^j$ at the n-th subcarrier is given by,

$$\tilde{X}_n^j = X_n^i \cdot \sum_{q(i,j)=1}^{N_P} \rho_{q(i,j)}^{i,j} \cdot e^{-j\frac{2\pi(q(i,j)-1)}{N}(n-1)} + Z_n^j = X_n^i \cdot H_n^{i,j} + Z_n^j \tag{1.14}$$

where $H_n^{i,j}$ and Z_n^j are the channel frequency response (CFR) at the n-th subcarrier between the i-th transmit and j-th receive antennas and AWGN at the j-th receive antenna both is the frequency domain. Finally, the information data can be demodulated precisely by the MIMO detection including the equalization and data detection of using the CFR matrix.

From (1.14), it can be seen that the CFR $H_n^{i,j}$ needs to be estimated at the receiver to be employed in the frequency domain equalization in order to enable the demodulation of information data precisely.
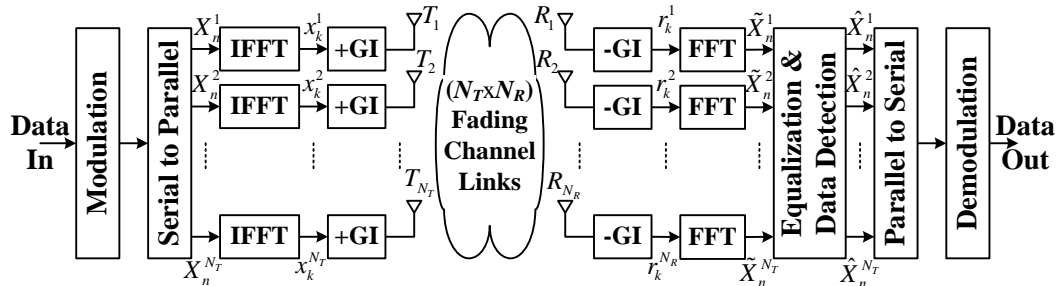
Figure 1.8: Overview of MIMO-OFDM system.

1.2.2   STBC and SFBC MIMO-OFDM System

Space-Time Block Coding (STBC) is widely a lot of attention for wireless communication by using multiple antennas due to its potential capability of high diversity gain which can provide high signal quality. Although, the transmission efficiency of MIMO-OFDM by using STBC technique becomes decreased twice as the conventional MIMO-OFDM, the bit error rate performance would be improved a lot. In STBC technique, two consecutive OFDM symbols in the time axis are encoded so as to obtain the frequency diversity gain in the multipath fading channel. Another technique which is similar technique to STBC technique is Space-Frequency Block Coding (SFBC). In SFBC technique, two consecutive data subcarriers in the frequency axis in OFDM symbol are encoded. Furthermore, the SFBC technique has a potential capability of self cancellation for the inter carrier interference (ICI) occurring in higher time-varying fading channel [15][16].

1.2.3   Standards of MIMO-OFDM System

Up to today, the MIMO based OFDM signal is used to several standards in wireless communication [17] such as;
- The next generation for Wireless LAN or IEEE 802.11n
- The new metropolitan area networks standard or IEEE802.16e
- The next generation mobile communication network or LTE

1.3   Overview of Uplink OFDMA System

One of promising wireless access techniques to enable accommodation of multiple users for flexibly and efficiently is Orthogonal Frequency Division Multiple Access (OFDMA). The OFDMA is considered by using the concept of the OFDM technique. In OFDMA communication system, it can be divided into 2 parts of communication such as uplink OFDMA system which is the communication between users and Base Station (BS), and downlink OFDMA system which is the communication between BS and end Users. However, the uplink OFDMA system is only described in this section, in part of downlink OFDMA system is not given the detail in this thesis.

1.3.1   Uplink OFDMA System

Figure 1.9 shows the simple model of transceiver for uplink OFDMA system. The information data input of each user is modulated to obtain X_n^u ($1 \leq u \leq U$) modulated signal at the n-th subcarrier for user-u. Then it is converted into the time domain signal by IFFT processing before adding the guard interval (GI) and is sent to the BS which can be given by,

$$x_k^u = \frac{1}{\sqrt{N}} \sum_{n=1}^{N} X_n^{iu} \cdot e^{j\frac{2\pi(k-1)(n-1)}{N}}, 1 \leq k \leq N \tag{1.15}$$

where x_k^u is the time domain signal at the k-th time sample for user-u within N subcarriers. The received time domain signal r_k after removing the GI at the BS can be given by,

$$r_k = \sum_{u=1}^{U} \left\{ x_k^u \otimes h_k^u \right\} + z_k = \sum_{u=1}^{U} \sum_{l_u=1}^{N_P} \left\{ \rho_{l_u}^u \cdot x_{k-l_u}^u \right\} + z_k \tag{1.16}$$

where $\otimes$ represents the convolution operator, h_k^u is the channel impulse response (CIR) in time domain occurred in channel between user-u and BS link and z_k is the additive white Gaussian noise (AWGN) in time domain at the BS. The CIR h_k^u is given by,

$$h_k^u = \sum_{l_u=1}^{N_P} \rho_{l_u}^u \cdot \delta\left(k - l_u\right) \tag{1.17}$$

where N_P is the number of channel delay paths and $\rho_{l_u}^u$ represents the complex amplitude of CIR for the l_u-th delay path occurred in channel between user-u and BS link. By performing FFT to (1.16), the frequency domain received signal R_n is given by,

$$R_n = \frac{1}{\sqrt{N}} \sum_{k=1}^{N} r_k \cdot e^{-j\frac{2\pi(n-1)(k-1)}{N}}, \ 1 \leq n \leq N \tag{1.18}$$

From (1.18), the frequency domain signal for the user-u is given by,

$$R_n^u = X_n^u \cdot \underbrace{\sum_{l_u=1}^{N_P} \rho_{l_u}^u \cdot e^{-j\frac{2\pi(l_u-1)}{N}(n-1)}}_{H_n^u} + Z_n \quad = X_n^u \cdot H_n^u + Z_n \tag{1.19}$$

where H_n^u is the CFR for channel between user-u and BS link and Z_n is the AWGN.

From (1.19), it can be seen that the CFR H_n^u needs to be estimated at the BS to be employed in the frequency domain equalization in order to enable the demodulation of information data sent from each user precisely.
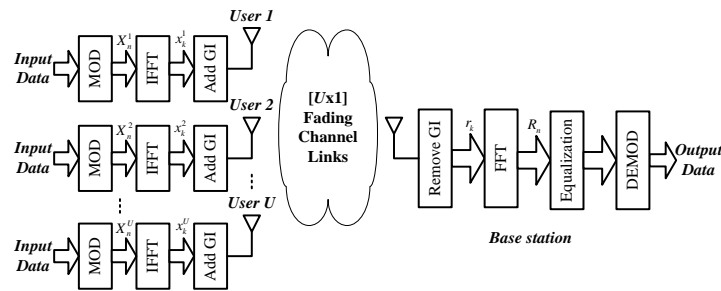
Figure 1.9: Overview of transceiver for uplink OFDMA system.

1.3.2   Transmission Data Pattern for uplink OFDMA System

For the data transmission in the uplink OFDMA system, there are two popular assignments which have proposed [18]; Localized and Distributed as shown in Figure 1.10. If the information data for each user are assigned by using a set of N/U consecutive subcarriers where N is the number of subcarriers and U is the number of users, this method is called "Localized subcarrier" as shown in Figure 1.10(a). Another method, each user assigns the information data by using a set of interleaved subcarrier among N subcarriers with the interval of subcarrier in frequency axis; this method is called "Distributed subcarrier" as shown in Figure 1.10(b). The uplink information data for each user can be assigned in one of two assignments; Localized or Distributed which can be defined as,

Localized OFDMA:

$$D_n^u = \begin{cases} Data, & (u-1)\frac{N}{U} \le n \le (u)\frac{N}{U}-1 \\ 0, & otherwise \end{cases}, 1 \le u \le U \tag{1.20}$$

Distributed OFDMA:

$$D_n^u = \begin{cases} Data, & n = (u-1)+sI_d \\ 0, & otherwise \end{cases}, \left(0 \le s \le \frac{N}{U}-1\right) \tag{1.21}$$

where D_n^u is the modulation data at the n-th subcarrier of user-u and I_d is the interval of users' data subcarrier in the frequency axis.

(a) Localized subcarrier

(b) Distributed subcarrier
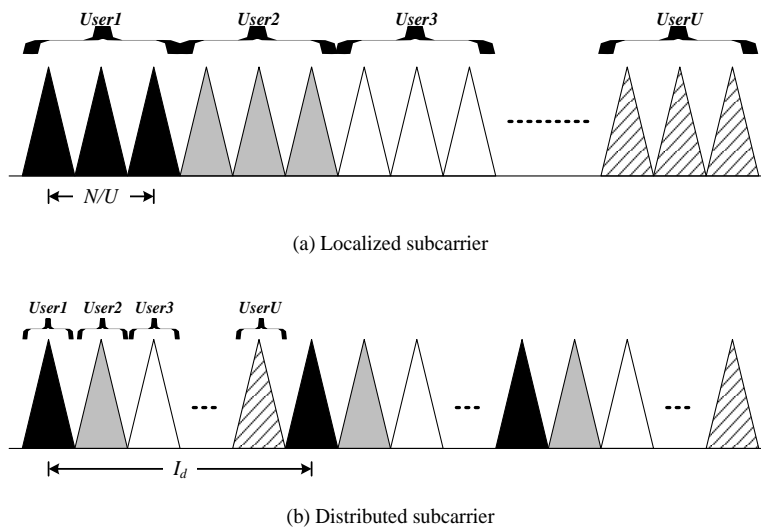
Figure 1.10: Transmission of information data in uplink OFDMA system.

1.4 Overview of ANC-OFDM System

1.4.1 ANC Benefits

ANC (Analog Network Coding) technique is one of communication techniques which utilizes the interference signals to pick the sender so as to increase the channel capacity and transmission efficiency for network in order to satisfy the demand for broadband wireless services which is rapidly increasing for providing multimedia services such as Multicasting, Video on demand, Video conference, Mobile internet services etc.. The ANC technique can be described easily as using two-way relay communication including two user terminals (UT) and one relay station (RS). In the two-way relay communication based ANC-OFDM system, each UT can send his information data to another UT through RS by using two timeslots.

However, the two-way relay communication based ANC-OFDM system can be divided into two kinds of system: Relay feedback and without Relay feedback. The two-way relay communication based ANC-OFDM system with relay feedback needs to estimate the channel response at RS to obtain the channel state information (CSI) in 1st timeslot then the CSI will be sent to the end user terminal, the end user terminal employs the CSI in the frequency domain equalization with removing its self information in 2nd timeslot. The two-way relay communication based ANC-OFDM system without relay feedback does not need to estimate the channel response at RS and inform the CSI from the RS which the channel response is estimated only at end user terminal at 2nd timeslot.

From these two kinds of two-way relay communication based ANC-OFDM system as mentioned above, it can be observed that the two-way relay communication based ANC-OFDM system with relay feedback can provide good system performance because end user terminal can use the separate estimated channel response in both 1st and 2nd timeslot links. However the system has more complicated due to the estimation processing at RS. For the two-way relay communication based ANC-OFDM system without relay feedback, although the system performance would be degraded due to the combined channel response estimated at end user terminal, the complicated of system would be reduced because the RS does not any estimation of channel response, the RS only amplifies the information data sent from each user terminal in 1st timeslot and rebroadcast it to end user terminals in 2nd timeslot, respectively.

From the above paragraph, it can be concluded that the quality of system performance depends on the accurate estimation of channel response in the multipath fading channel which is employed in the frequency domain equalization with removing its self information at end user terminal.

1.4.2 ANC-OFDM System

Figure 1.11 shows the network model of two-way relay communication based ANC-OFDM system including two user terminals (UT) and one relay station (RS) which both UTs can exchange their information data through the RS by using two timeslots for communication. In the 1st timeslot, the information data $A_1(m,n)$ and $A_2(m,n)$ are sent simultaneously from UT_1 and UT_2 at the n-th subcarrier of the m-th symbol to the RS. The superimposed received signal at the RS after performing by using FFT processing $R(m,n)$ can be expressed by,

$$R(m,n) = A_1(m,n) \cdot H_{1R}(m,n) + A_2(m,n) \cdot H_{2R}(m,n) + Z_{RS}(m,n) \tag{1.22}$$

where $H_{1R}(m,n)$ and $H_{2R}(m,n)$ are the channel frequency responses (CFRs) between UT_1 to RS and UT_2 to RS, respectively. $Z_{RS}(m,n)$ is the additive white Gaussian noise (AWGN) added at the RS. In the 2nd timeslot, the RS amplifies the received signal $R(m,n)$ and rebroadcasts it to both end UTs. The received signal after performing by using FFT processing $R_{Ti}(m,n)$ at end UT_i can be given by,

$$R_{T_i}(m,n) = R(m,n) \cdot H_{R_i}(m,n) + Z_{T_i}(m,n) \tag{1.23}$$

where $H_{\text{R}i}(m,n)$ is the CFR between the RS to UT$_i$ and $Z_{\text{T}i}(m,n)$ is the AWGN at the UT$_i$. By using (1.22) and (1.23), the frequency domain received signal $R_{\text{T}i}(m,n)$ at the UT$_i$ can be expressed by,

$$R_{T_i}(m,n) = A_i(m,n) \cdot H_{iR}(m,n) \cdot H_{R_i}(m,n) + A_j(m,n) \cdot H_{jR}(m,n) \cdot H_{R_i}(m,n) + Z'_{T_i}(m,n) \tag{1.24}$$

where $Z'_{Ti}(m,n) = Z_{RS}(m,n) \cdot H_{Ri}(m,n) + Z_{Ti}(m,n)$ denotes the composite noise.

From (1.24), the other user terminal's information data $\hat{A}_j(m,n)$ sent from UT$_j$ can be demodulated at UT$_i$ by removing the self-information data with the frequency domain equalization which is given by,

$$\hat{A}_j(m,n) = \frac{R_{T_i}(m,n) - A_i(m,n) \cdot \left\{ H_{iR}(m,n) \cdot H_{R_i}(m,n) \right\}}{\left\{ H_{jR}(m,n) \cdot H_{R_i}(m,n) \right\}} \tag{1.25}$$

From (1.25), it can be seen that the combined CFRs $H_{iR}(m,n) \cdot H_{R_i}(m,n)$ and $H_{jR}(m,n) \cdot H_{R_i}(m,n)$ need to be estimated at the UT$_i$ to be employed in the removal the self-information with frequency domain equalization.

(a) 1st timeslot

(b) 2nd timeslot
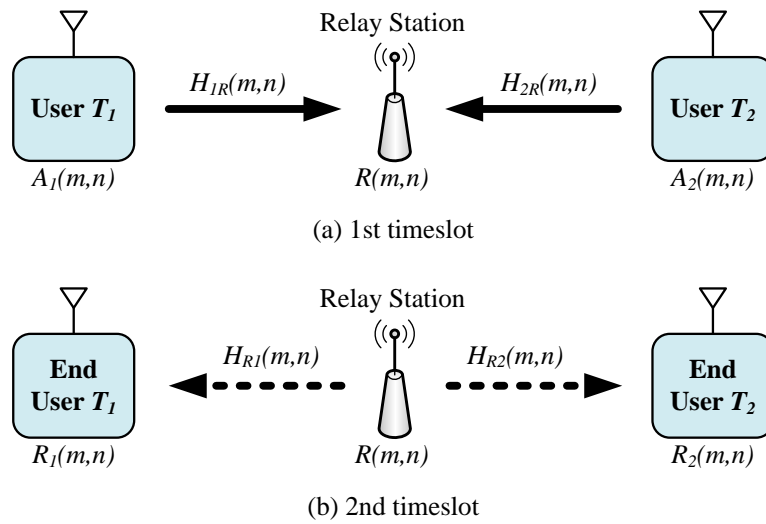
Figure 1.11: Model of two-way relay communication based ANC-OFDM system.

1.5 Sampling of Signal

1.5.1 Nyquist Sampling Rate [19-20]

Basically, in a Band limited function in time, the sampling frequency rate (f_s) which is at least greater than twice the highest frequency contained in the signal (f_c) according to the Nyquist sampling theorem ($f_s \geq 2 \cdot f_c$) is provided to enable the reconstruction of the signal by using an ideal low pass filter. From Figure 1.12, it shows the reconstruction procedure of the repeated signal with f_c by using an ideal low pass filter. From the Figure, it can be seen that the repeated signals with f_c can be perfectly reconstructed when $f_s \geq 2 \cdot f_c$ as shown in Figure 1.12(a). In contrast with when $f_s < 2 \cdot f_c$, the aliasing of signals would be occurred which leads to the distortion of signal after reconstruction as shown in Figure 1.12(b).
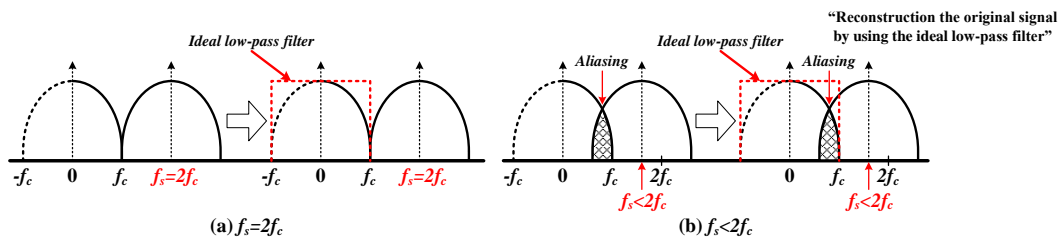
Figure 1.12: The reconstruction procedure of the signal with f_c by using an ideal low pass filter.

1.5.2 Oversampling by Zero Padding Insertion in OFDM Signal [21]

By using the concept of sampling of signal as mentioned in section 1.5.1, in the basic of wireless communication based OFDM signal, the desired OFDM signal with M data subcarriers which is converting by N points IFFT into the time domain signal is provided under the condition of the Nyquist sampling rate which the number of IFFT points (N) is equal to the number of data subcarriers (M). However, in the actual OFDM system, the null subcarrier (zero-padding) is required to insert at around the both ends of M data subcarriers before IFFT processing in order to avoid the aliasing occurring at the output signal of digital-to-analog (D/A) converter as shown in Figure 1.13. From Figure 1.13, it shows the oversampling in OFDM signal by adding zero padding, the analog filter would be located after D/A converter as shown in Figure 1.3 in order to deny the aliasing. From this reason, the number of zero-padding, which is required to add for OFDM signal, corresponds to the achievable sharpness of analog filter. It is easily to reject the aliasing when the number of zero-padding is larger but the number of IFFT points becomes larger which leads to the degradation of transmission efficiency as well.
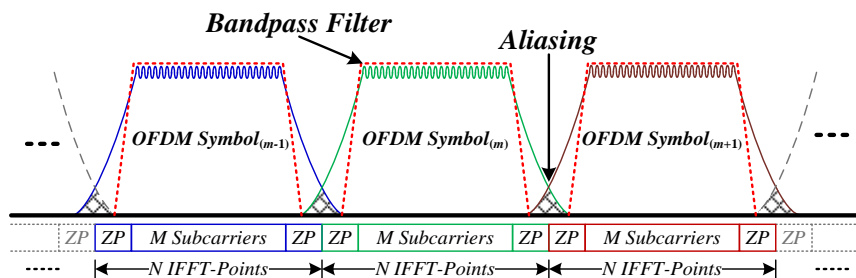
Figure 1.13: The OFDM signal at the output of D/A converter.

1.6   Research Background

The Orthogonal Frequency Division Multiplexing (OFDM) technique has been received a lot of attentions especially in the wireless communication systems because of its efficient usage of frequency bandwidth and robustness to the multi-path fading. From these advantages, OFDM technique has been already adopted in many wireless communication systems as the standard transmission technique such as the wireless LAN (WLAN) system, broadband wireless communication system, the 4th generation mobile telecommunication (4G) system and the terrestrial digital broadcasting systems including the Digital Audio Broadcasting (DAB) and the Digital Video Broadcasting (DVB). Recently, many researchers proposed the various new systems based on OFDM technique such as Multi-Input and Multi-Output (MIMO)-OFDM system which can achieve higher data transmission rate or higher signal quality, uplink OFDM Access (OFDMA) system which can accommodate multiple users flexibly and efficiently, two-way relay communication system with broadband analogue network coding (ANC) which can increase the channel capacity and transmission efficiency. To achieve the potential capability for the proposed OFDM based wireless communication systems, there are still remaining many unsolved problems. In this thesis, several practical solutions are proposed to realize the above proposed OFDM based systems which can achieve higher signal quality and higher transmission efficiency in higher time-varying fading channel.

One of the limitations of using OFDM technique is the larger peak to average power ratio (PAPR) of its time domain signal which causes the severe degradations of bit error rate (BER) performance and undesirable spectrum re-growth due to the non-linear distortion occurring at the non-linear amplifier. In the wireless communication systems especially for the user terminal, a non-linear amplifier is usually employed at the transmitter which is required for the efficient usage of transmission power because of its battery operation. To solve this problem, the Partial Transmit Sequence (PTS) method was proposed as one of promising PAPR reduction methods which can achieve better PAPR performance with reasonable computation complexity. However the PTS method is required to inform the side information (SI) to the receiver for the correct demodulation of data information by using the separate channel which leads the complexity of transceiver and inefficient usage of frequency bandwidth. To solve this problem, this thesis proposes a new PAPR reduction method based on the packet-switched transmission systems in which all the clusters within the certain number of OFDM symbols have the sequential cluster ID numbers embedded in the header of each cluster. The proposed method enables the reduction of PAPR performance by re-ordering of clusters (ROC) in the frequency domain at the transmitter and reconstructs the original ordering of clusters by using the cluster ID numbers demodulated from each cluster at the receiver which requests no side information.

Intelligent Transport Systems (ITS) have been expanding with the popularization of Electrical Toll Collection System (ETC) and Vehicle Information and Communication System (VICS). The OFDM based Road to Vehicle Communication (RVC) system has been considered as one of the promising ITS technologies which can provide the drivers for safety and comfortable driving and collection of variable information from network in the real-time. This thesis proposes a RVC system of using the STBC (Space Time Block Coding) MIMO-OFDM technique which can achieve better BER performance even in higher time-varying fading channel. To achieve the potential capability in the proposed RVC system, it is the essential to realize the accurate channel estimation method. This thesis proposes a novel channel frequency response (CFR) estimation method by using the scattered pilot subcarriers in the frequency domain. From computer simulation results, this thesis demonstrates that the STBC MIMO-OFDM based RVC system of using the proposed CFR estimation method can achieve higher channel estimation accuracy and better BER performance even in the time varying fading channel.

To achieve a potential capability of MIMO-OFDM system, it is the essential to realize an efficient and accurate channel estimation method. The conventional Discrete Fourier Transform Interpolation-based channel estimation (DFTI-CE) method of using the scattered

pilot symbol can achieve higher estimation accuracy only when the transmission OFDM signal is sampled by the Nyquist rate. However the estimation accuracy of using the conventional DFTI-CE method would be degraded relatively when null subcarriers (zero padding) are inserted at both ends of data subcarrier to reject the aliasing occurring at the output of Digital to Analogue (D/A) converter which corresponds to the non-Nyquist sampling rate. To solve this problem, the Maximum Likelihood (ML) channel estimation method was proposed for MIMO-OFDM system which can achieve better estimation accuracy than the conventional DFTI-CE method. However its estimation accuracy would be degraded at around the both ends of data subcarrier at the non-Nyquist rate especially when increasing the number of transmit antennas and zero padding. To solve the above problem, this thesis proposes the ML based time domain channel estimation (TD-CE) method for MIMO-OFDM system which can achieve higher estimation accuracy even when the non-Nyquist rate and increasing the number of transmit antennas. From computer simulation results, this thesis demonstrates the effectiveness of propose ML based TD-CE method for MIMO-OFDM system.

OFDMA technique is considered as one of promising wireless access techniques which can accommodate multiple users flexibly and efficiently. In the uplink OFDMA system, since all users transmit their information data symbols to the base station (BS) simultaneously, it is required to estimate all user's channel frequency responses all together at the BS before receiving the information data symbols. The estimation of multiple users' channels in the uplink OFDMA system is similar to that the estimation of multiple channels between the transmit antenna and the receive antenna in the MIMO-OFDM system. From computer simulation results, this thesis also demonstrates the effectiveness of above proposed ML based TD-CE method when employing in the uplink OFDMA system.

Broadband ANC of using the OFDM technique has been widely investigated to increase the capacity of two-way relay communication. In the two-way relay communication, it can be simply modeled by two user terminals (UTs) and one relay station (RS) in which each UT sends his information data to the other UT through the RS by using two timeslots. Each UT can demodulate the other user's information data by removing its self-information data with frequency domain equalization (FDE). To conduct the removal of self-information data and the FDE precisely, it is the essential to realize the accurate channel estimation method for the combined CFR in the 1st and 2nd timeslots from the superimposed received signal sent from both UTs at each UT. To solve this problem, this thesis proposes the ML based combined CFR estimation method for two-way relay communication system by using a novel scattered pilot assignment method including the null subcarriers to avoid the collision of pilot subcarriers sent from both UTs. From the various computer simulation results, this thesis demonstrates the effectiveness of proposed ML based combined CFR estimation method which can achieve higher estimation accuracy and better BER performance even in higher time-varying fading channel.

This thesis also demonstrates the effectiveness of proposed ML based combined CFR estimation method when employing the two-way communication system of using the SFBC (Space-Frequency Block Coding) MIMO-OFDM technique to improve the BER performance. The salient feature of proposed CFR estimation method is to employ the pilot subcarriers with Walsh code to differentiate the pilot subcarriers sent from both UTs. From computer simulation results, this thesis confirms that the proposed SFBC MIMO-OFDM system of using the ML based combined CFR estimation method can achieve higher CFR estimation accuracy and better BER performance with higher transmission efficiency even in higher time-varying fading channel.

From the numerous computer simulation results, it is confirmed that the proposed methods presented in this thesis can be employed as the practical solutions to realize the next generation OFDM based wireless communication systems.

1.7   Thesis Structure

The remainder of this thesis is organized as follows.

Chapter 2 presents a new PAPR reduction method without requiring the separate channel. Section 2.1 introduces the description of research backgrounds. Section 2.2 presents PAPR properties of OFDM signal. Section 2.3 presents the proposed ROC method of using the low computation complexity technique. Section 2.4 presents the various computer simulation results to verify the effectiveness of the proposed method as compared with the conventional OFDM. Section 2.5 gives the conclusions of this chapter 2.

Chapter 3 presents the proposed channel estimation method for ITS system. Section 3.1 introduces the description of research backgrounds. Section 3.2 shows the proposed STBC MIMO-OFDM system model. Section 3.3 proposes a channel estimation method for the proposed system by using the scattered pilot subcarriers assignment method. Section 3.4 presents the various computer simulation results to verify the effectiveness of the proposed method as compared with the conventional methods. Section 3.5 draws some conclusions of this chapter 3.

Chapter 4 presents the proposed time domain channel estimation method for MIMO-OFDM system. Section 4.2 presents the conventional CE methods for MIMO-OFDM systems and their problems on the estimation accuracy at the non-Nyquist rate and when increasing the number of transmit antennas. Section 4.3 proposes the TD-CE method for MIMO-OFDM systems which can solve the problems on the conventional methods. Section 4.4 presents various computer simulation results to verify the effectiveness of proposed method. Section 4.5 gives the conclusions of this chapter 4.

Chapter 5 presents the proposed time domain channel estimation method for uplink OFDMA system. Section 5.1 introduces the description of research backgrounds. Section 5.2 presents the system model for the uplink OFDMA system. Section 5.3 proposes the TD-CE method which can solve the problem on the conventional DFTI-CE method. Section 5.4 presents various computer simulation results in the time-varying fading channels to verify the effectiveness of proposed TD-CE method as comparing with the conventional DFTI-CE method. Section 5.5 draws some conclusions of this chapter 5.

Chapter 6 presents the proposed channel estimation method for ANC-OFDM based Wireless two-way relay system. Section 6.1 introduces the description of research backgrounds. Section 6.2 shows the network model. Section 6.3 proposes a channel estimation method by using the scattered pilot subcarriers. Section 6.4 presents the various computer simulation results to verify the effectiveness of the proposed method as comparing with the conventional methods. Section 6.5 gives the conclusions of this chapter 6.

Chapter 7 presents the proposed CFR estimation method for wireless two-way relay system of using SFBC MIMO-OFDM technique. Section 7.1 introduces the description of research backgrounds. Section 7.2 shows a model of MIMO-OFDM based two-way relay communication system. Section 7.3 proposes the two-way relay communication system of using the SFBC MIMO-OFDM technique. Section 7.4 proposes a CFR estimation method of using the scattered pilot subcarrier with Walsh code for SFBC MIMO-OFDM system. Section 7.5 presents the various computer simulation results to demonstrate the effectiveness of proposed method. Section 7.6 draws some conclusions of this chapter 7.

Finally, the overall conclusion of this thesis is given in Chapter 8.

CHAPTER 2

PROPOSAL OF PAPR REDUCTION METHOD FOR OFDM SIGNAL BY RE-ORDERING OF CLUSTERS IN FREQUENCY DOMAIN

One of the limitations of using OFDM technique is the larger peak to average power ratio (PAPR) of its time domain signal which causes the severe degradations of bit error rate (BER) performance and undesirable spectrum re-growth due to the non-linear distortion occurring at the non-linear amplifier. In the wireless communication systems especially for the user terminal, a non-linear amplifier is usually employed at the transmitter which is required for the efficient usage of transmission power because of its battery operation. To solve this problem, the Partial Transmit Sequence (PTS) method was proposed as one of promising PAPR reduction methods which can achieve better PAPR performance with reasonable computation complexity. However the PTS method is required to inform the side information (SI) to the receiver for the correct demodulation of data information by using the separate channel which leads the complexity of transceiver and inefficient usage of frequency bandwidth. To solve this problem, this chapter proposes a new PAPR reduction method based on the packet-switched transmission systems in which all the clusters within the certain number of OFDM symbols have the sequential cluster ID numbers embedded in the header of each cluster. The proposed method enables the reduction of PAPR performance by re-ordering of clusters (ROC) in the frequency domain at the transmitter and reconstructs the original ordering of clusters by using the cluster ID numbers demodulated from each cluster at the receiver which requests no side information.

2.1   Introduction

OFDM (Orthogonal Frequency Division Multiplexing) technique has been received a lot of attentions especially in the field of wireless communications because of its efficient usage of frequency bandwidth and robustness to the multi-path fading. From these advantages, the OFDM technique has already been adopted as the standard transmission techniques in the wireless LAN [19], the terrestrial digital TV broadcasting [20] and the next generation of mobile communication system (LTE: Long Term Evolution) [24-25]. One of the limitations of using OFDM technique is the larger peak to average power ratio (PAPR) of its time domain signal [26-27] as compared with the single carrier transmission method. The OFDM signal with larger PAPR would lead the severe degradation of bit error rate (BER) performance and the larger adjacent channel interference due to the un-desirable spectrum re-growth which are caused by the inter-modulation noise occurring at the non-linear amplifier.

To solve the PAPR problem in OFDM systems, various PAPR reduction methods have been proposed up to today including such as the Clipping and Filtering method [28-29], Selected Mapping method (SLM) [30-31], and Partial Transmit Sequence method (PTS) [32-33]. One of the promising methods among these methods is the PTS method which can achieve the better PAPR performance with reasonable computation complexity. In the PTS method, each transmission OFDM symbol is divided into several clusters in the frequency domain and all subcarriers in each cluster are weighted by one of the predetermined phase coefficients in the time domain so as to reduce the PAPR performance. Although the PTS method can achieve the better PAPR performance with reasonable computation complexity, this method is required to inform the phase coefficients of PTS to the receiver as the side information through the data or separate channels. To simplify the transceiver of OFDM system with the PTS method, the phase coefficients of PTS obtained after the PTS processing are usually embedded in the data information separately. However since the phase coefficients of PTS are obtained after the PTS processing only for the data information, the PTS method is unable to reduce the PAPR performance both for the data information and phase coefficients of PTS simultaneously. From this fact, the PAPR performance after embedding the information of phase coefficients into the data information would be degraded from the original PAPR performance.

To solve the problem of conventional PTS method as mentioned above, this chapter proposes a new PAPR reduction method for the OFDM signal based on the packet-switched transmission systems. In the proposed OFDM system, one packet is composed from all the clusters over the certain number of OFDM symbols in which each cluster has the sequential cluster ID number embedded in the header of each cluster. The reduction of PAPR performance is performed for each packet by Re-Ordering of Clusters (ROC) in the frequency domain. The proposed ROC method can reduce the PAPR performance over the certain number of OFDM symbols simultaneously which include both the data information and the cluster ID numbers. At the receiver, the proposed ROC method enables the correct demodulation of data information for each cluster independently, because the ROC method only changes the locations of clusters in the frequency domain over the certain number of OFDM symbols at the transmitter. From this fact, the cluster ID number embedded in the header of each cluster can be identified from the demodulated data information for each cluster. By using the demodulated cluster ID number for each cluster, the original ordering of clusters over the certain number of OFDM symbols can be reconstructed correctly at the receiver. The proposed ROC method is completely different from the PTS method which is required to inform the phase coefficients of PTS as the side information to the receiver separately. This chapter also proposes a low computation complexity technique for the ROC method which enables the re-ordering of clusters in the time domain by using the feature of IFFT algorithm.

2.1 Introduction

In this chapter, Section 2.2 presents PAPR properties of OFDM signal. Section 2.3 presents the proposed ROC method of using the low computation complexity technique. Section 2.4 presents the various computer simulation results to verify the effectiveness of the proposed method as compared with the conventional OFDM, and finally Section 2.5 concludes this chapter.

2.2 PAPR Properties of OFDM Signal

Let $\{X_n\}_{n=0}^{N-1}$ denotes the frequency domain OFDM signal, where N is the number of FFT/IFFT points and n is the frequency index. The discrete time domain OFDM signal is obtained by taking the N-point Inverse Discrete Fourier Transform (IDFT) for X_n as given by the following equation,

$$x_k = \frac{1}{\sqrt{N}} \sum_{n=0}^{N-1} X_n \cdot W_N^{-nk} \tag{2.1}$$

where k is the discrete time index, $W_N = e^{-j2\pi/N}$ (known as the twiddle factor of IFFT), and $j^2 = -1$. From (2.1) it can be seen that the time domain signal is generated by summation of complex independent random information data of X_n. From this fact, the distribution of time domain signal has the property of Gaussian which has larger peak amplitude as compared with the single carrier transmission signal. To evaluate the envelop variations of OFDM time domain signal, the peak to average power ratio (PAPR) is usually employed as given by,

$$PAPR = 10\log_{10}\left(\frac{\displaystyle\max_{0\leq k\leq N-1}\left[|x_k|^2\right]}{\dfrac{1}{N}\displaystyle\sum_{k=0}^{N-1}|x_k|^2}\right) \tag{2.2}$$

Here it should be noted that the discrete time PAPR can be evaluated precisely by taking more than four times oversampling ratio for the OFDM signal [34].

2.3 Proposal of Re-Ordering of Clusters (ROC) Method

This section proposes the ROC method [35] which can improve the PAPR performance with low computation complexity.

2.3.1 Re-Ordering of Clusters

Figure 2.1 shows the structure of OFDM symbol in the frequency domain to be used in the proposed ROC method. The OFDM symbol consists of M data subcarriers and $(N-M)/2$ null subcarriers (zero padding) inserted at the both ends of M data subcarriers. M data subcarriers are divided into V clusters in which each cluster has M/V subcarriers.
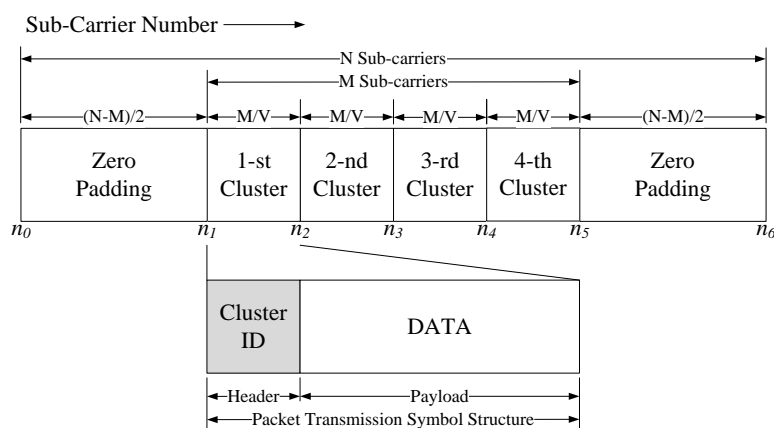
Figure 2.1: Structure of frequency domain OFDM symbol for the proposed ROC method.

In the proposed ROC method, one packet is constructed by all the clusters within the certain number of OFDM symbols which have the sequential cluster ID numbers based on the packet-switched transmission systems. The cluster ID number for assigning each cluster is ordered sequentially from the 1st to the $(P \cdot V)$-th when the number of clusters in one OFDM symbol is V and the re-ordering of clusters is performed over P OFDM symbols. In the ROC method, the processing for the reduction of PAPR performance is conducted over the consecutive P OFDM symbols by changing the order of clusters in the frequency domain. Figure 2.2 shows an example of the proposed ROC method when $V=4$ and $P=2$. In this example for the proposed ROC method, the locations of 8 clusters are changed over two OFDM symbols in the frequency domain so as to achieve the better PAPR performance at the transmitter. From Figures 2.1 and 2.2, it can be observed that the proposed ROC method can reduce the PAPR performance both for the data information and cluster ID numbers simultaneously. This is completely different from the conventional PTS method which can reduce the PAPR performance only for the data information and the obtained phase coefficients of PTS is required to inform the receiver separately.
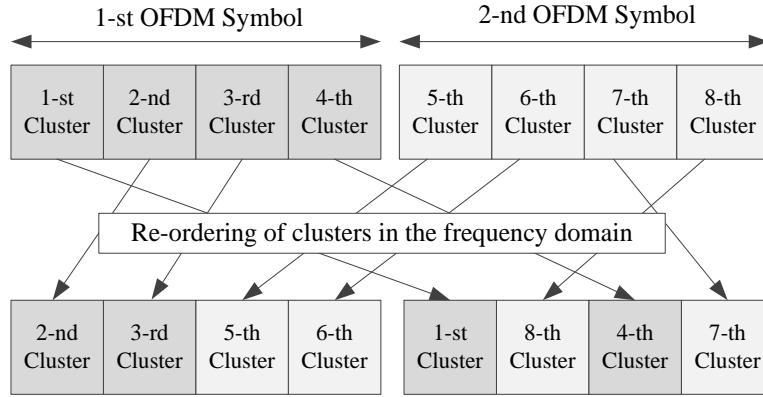
Figure 2.2: An example of ROC method when *V*=4 and *P*=2.

2.3.2 Low Computation Complexity Technique for ROC Method

In the proposed ROC method, the re-ordering of clusters is conducted in the frequency domain as mentioned above. However, when employing the frequency domain approach, the IFFT processing is required for each re-ordering of clusters in the frequency domain because the PAPR performance is required to evaluate in the time domain. This means that the computation complexity for the proposed ROC method becomes larger to achieve the better PAPR performance, because the computation complexity increases proportionally to the required number of IFFT processing. To solve this problem, this chapter proposes a low computation complexity technique for the ROC method which can perform the re-ordering of clusters in the time domain by using the feature of IFFT algorithm.

When the number of clusters in one OFDM symbol is 4 (*V*=4) and the re-ordering of clusters is performed over two symbols (*P*=2) as shown in Figures 2.1 and 2.2, the data information including the cluster ID number for each cluster in the frequency domain is given by the following equation,

$$X_{\ell,n}^{(v)} = \begin{cases} X_{\ell,n}^{(1)} & n_1 \le n \le n_2 -1 \\ X_{\ell,n}^{(2)} & n_2 \le n \le n_3 -1 \\ X_{\ell,n}^{(3)} & n_3 \le n \le n_4 -1 \\ X_{\ell,n}^{(4)} & n_4 \le n \le n_5 -1 \\ 0 & others\,(zero\,padding) \end{cases} \tag{2.3}$$

where $X_{\ell,n}^{(v)}$ is the data information at the *n*-th subcarrier of the ℓ-th symbol ($1\le \ell \le 2$) for the *v*-th cluster ($1\le v \le 4$). In the proposed method, the time domain signal for each cluster is firstly calculated by the following equation,

$$\tilde{x}_{\ell,k}^{(v)} = \frac{1}{\sqrt{N}} \sum_{n=0}^{M/V-1} X_{\ell,n+n_v}^{(v)} \cdot e^{j\frac{2\pi nk}{N}} \quad (0 \le k \le N-1) \tag{2.4}$$

where n_v ($1\le v \le 4$) is the first subcarrier number for the cluster *v* as given in (2.3). The time domain signal given in (2.4) corresponds to that the data information for the cluster *v* is located from the subcarrier number 0 to *M/V*-1 in the frequency domain. By using (2.4), the time domain signal for all clusters ($1\le v \le 4$) over two symbols ($1\le \ell \le 2$) can be obtained. By using these time domain signals, the re-ordering of clusters can be conducted in the time domain. When the *i*-th cluster is changed to the *j*-th cluster in the frequency domain, its time domain signal can be given by the following equation,

$$x_{\ell,k}^{(j)} = \frac{1}{\sqrt{N}} \sum_{n=0}^{M/V-1} X_{\ell,n+n_i}^{(i)} \cdot e^{j\frac{2\pi(n+n_j)k}{N}}$$

$$= e^{j\frac{2\pi n_j k}{N}} \cdot \frac{1}{\sqrt{N}} \sum_{n=0}^{M/V-1} X_{\ell,n+n_i}^{(i)} \cdot e^{j\frac{2\pi nk}{N}} \qquad (2.5)$$

$$= O_{n_j,k} \cdot \tilde{x}_{\ell,k}^{(i)} \qquad (0 \le k \le N-1)$$

where $\tilde{x}_{\ell,k}^{(i)}$ is the time domain signal for the *i*-th cluster given in (2.4) and $O_{n_j,k}$ is the time domain coefficient for changing the location of cluster to the *j-th* cluster which is given by the following equation,

$$O_{n_j,k} = e^{j\frac{2\pi n_j k}{N}} \qquad (2.6)$$

From (2.5), it is concluded that the re-ordering of clusters in the frequency domain can be conducted in the time domain by using (2.6). The required number of computation processing for the proposed method is N times multiplications as shown in (2.5) which is smaller computation complexity than $N \cdot log_2 N$ when using the IFFT processing. This means that the proposed method can reduce the computation complexity by $log_2 N$ times as compared with that for using the IFFT processing.

As mentioned above, the proposed ROC method can reduce the PAPR performance by using the time domain signal obtained after IFFT processing for each cluster as given in (2.4). From this fact, the computation complexity required in the proposed ROC method would increase as increasing the number of clusters V. To solve the above problem, this chapter employs the sprit-radix DIF-IFFT technique [36] for the ROC method to reduce the computation complexity required in the IFFT processing.

Table 2.1 shows the computation complexity for the processing of IFFT when using the various radix techniques [36]. From the table, it can be observed that the split-radix IFFT which is combined by the radix-2 and radix-4 IFFTs can reduce the computation complexity by 33.3% as compared with the conventional IFFT. From these results, this chapter employs the split-radix IFFT for the proposed ROC method to reduce the computation complexity of IFFT processing.

Table 2.1: Comparison of computation complexity for various Radix IFFT techniques.

Techniques	Computation complexity	multiplications (N=256)
Conventional	$N \cdot log_2 N$	100
Radix-2	$(N/2)\, log_2 N$	50%
Radix-4	$(3N/8) \cdot log_2 N$	37.5%
Split-radix	$(N/3) \cdot log_2 N$	$\cong$33.3%

Figure 2.3 shows the block diagram of the proposed ROC method with the reduction of computation complexity technique when $V=4$ and $P=2$. In the proposed method, the time domain signals for all clusters which are re-ordered in the frequency domain, are calculated over two OFDM symbols by using (2.5) with small computation complexity. And the time domain signals for the 1st and 2nd symbols after re-ordering of clusters over two OFDM symbol can be obtained by the summation of time domain signals over 4 clusters which is given by the following equation,

$$x_{\ell,k}^t = \sum_{v_\ell=1}^{V} x_{\ell,k}^{(v_\ell)}, \quad (0 \le k \le N-1) \qquad (2.7)$$

where $x_{\ell,k}^t$ is the aggregate time domain signal of 4 clusters for the ℓ-th symbol and v_ℓ is the cluster number in the ℓ-th symbol after re-ordering of clusters over two OFDM symbols.

In the proposed ROC method, the maximum number of iterations (MAX_{ite}) for changing the re-ordering of clusters and the threshold level of PAPR (TH_{PAPR}) are pre-determined to reduce the computation complexity.
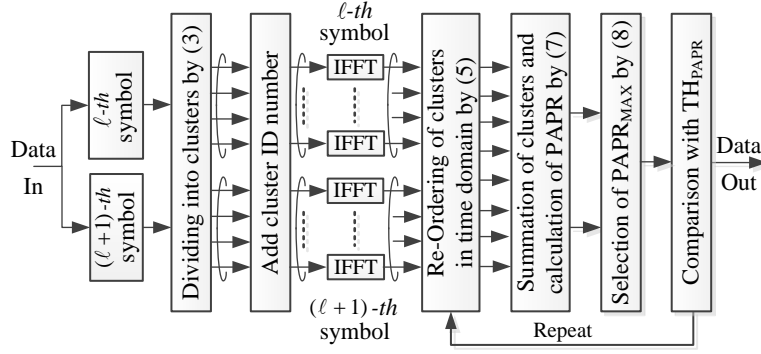
Figure 2.3: Block diagram of the proposed ROC method.

Figure 2.4 shows the flow chart for the proposed ROC method when employing MAX_{ite} and TH_{PAPR}. Firstly, all the sequence patterns for re-ordering of clusters are generated of which the number of sequences is the same as the maximum number of iterations MAX_{ite}. The sequence patterns are generated by changing the order of clusters over two symbols randomly. By using the time domain signal given by (2.7) for each sequence pattern, the $PAPR_1$ and $PAPR_2$ are calculated for the 1st and 2nd symbols, respectively. The maximum $PMAX_{ite}$ at the *ite*-th iteration is selected by,

$$PMAX_{ite} = Max\left[PAPR_1, \ PAPR_2\right] \tag{2.8}$$

Then the $PMAX_{ite}$ is compared with the given threshold level of TH_{PAPR}. If the $PMAX_{ite}$ is smaller than the TH_{PAPR}, the iteration is stopped and the time domain signals both for the 1st and 2nd symbols are transmitted to the channel. If not the iteration is continued by using the next sequence pattern for the re-ordering of clusters. The above procedures are performed up to either the $PMAX_{ite}$ is smaller than the TH_{PAPR} or the iteration number is reached to the MAX_{ite}. If the iteration number is reached to the MAX_{ite}, the time domain signals corresponding to the minimum $PMAX_{ite}$ obtained among all iterations are transmitted to the channel.

By following the above procedures, the average number of iterations to satisfy the TH_{PAPR} would become relatively smaller than the MAX_{ite} and consequently the computation complexity which can achieve the better PAPR performance would become smaller.
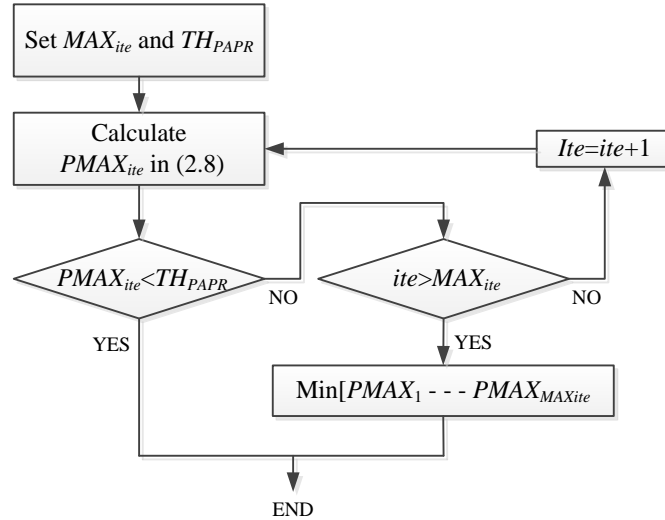
Figure 2.4: Flow chart for the low computation complexity technique for the proposed ROC method.

2.3.3 Demodulation of Data Information for ROC Method

At the receiver the received time domain signal is converted to the frequency domain signal by FFT which is given by the following equation,

$$R_{\ell,n} = H_{\ell,n} \cdot X_{\ell,n}^{(v_\ell)} + W_{\ell,n} \tag{2.9}$$

where $R_{\ell,n}$ is the received signal, $X_{\ell,n}^{(v_\ell)}$ is the data information given in (2.3), $H_{\ell,n}$ is the channel frequency response, $W_{\ell,n}$ is the *AWGN* at the n-th subcarrier of the ℓ-th symbol, and v_l is the cluster number within the ℓ-th symbol after re-ordering of clusters at the transmitter. After the frequency domain equalization for (2.9), all the subcarriers within each cluster can be demodulated correctly, because the proposed method changes only the location of clusters in the frequency domain at the transmitter. Therefore the cluster ID number embedded in the header of each cluster as shown in Figure 2.1 can be demodulated without any side information. By using the obtained cluster ID numbers, the original order of clusters over two OFDM symbols can be reconstructed and the data information over two symbols can be demodulated correctly.

2.4 Performance Evaluations of Proposed ROC Method

This section presents the various computer simulation results to verify the effectiveness of the proposed ROC method as compared with the conventional PTS method. Table 2.2 shows the list of simulation parameters to be used in the following evaluations.

Table 2.2: Simulation parameters.

Information	Parameter
Modulation for data symbol	16QAM
Demodulation	Coherent
OFDM occupied bandwidth	10MHz
Number of IFFT-points ($N=Z+M$)	256
Number of zero-padding (Z)	192
Number of data subcarriers (M)	64
Number of samples in Guird interval (N_g)	25
Symbol duration (T_s)	6.4 us
Guard interval duration (T_g)	0.625 us
Number of clusters per symbol (V)	4
Number of phase coefficients for PTS (W)	4
Number of symbols for ROC (P)	2

The computation complexity both for the conventional PTS and proposed ROC methods when employing the predetermined PAPR threshold level TH_{PAPR} and the maximum number of iterations MAX_{ite} can be given by the following equations,

$$P_{PTS} = N \cdot (V-1) \cdot (W + AVE_{ite}) + V \cdot N/3 \cdot \log_2 N \tag{2.10}$$

$$P_{ROC} = N \cdot (V-1) \cdot (V + AVE_{ite}) + V \cdot N/3 \cdot \log_2 N \tag{2.11}$$

where the computation complexity of the ROC method is evaluated per one OFDM symbol. In (2.10) and (2.11) both for the PTS and ROC methods, the first term of the right hand is the required number of multiplication processing. In (2.10), W is the number of predetermined phase coefficients for the PTS. The second term and the third term both for (2.10) and (2.11) are the required number of addition processing and the required processing load when using the sprit-radix IFFT technique as shown in Table 2.1, respectively. From (2.10) and (2.11), it can be seen that when the number of phase coefficients W for the PTS method is the same as the number of clusters V both for the PTS and proposed ROC methods, the computation complexities both for the PTS and ROC become the same.

Table 2.3 shows the computation complexity for achieving the PAPR performance of 7dB at $CCDF=10^{-2}$ for the proposed ROC and the conventional PTS methods when using the conventional IFFT and the sprit-radix IFFT techniques. The computation complexity is evaluated based on the averaged iteration numbers (AVE_{ite}) which is required to satisfy the predetermined threshold level of PAPR (TH_{PAPR}). In Table 2.3, "Improvement from PTS" shows the percentage of reduction in the computation complexity as compared with the PTS method with the conventional IFFT technique when all possible combinations of phase coefficients over V clusters ($MAX_{ite}=64$) are performed which can achieve the best PAPR performance. From the table, it can be observed that the AVE_{ite} for the proposed ROC method would be increasing as decreasing the TH_{PAPR}. This is the reason that the required number of iterations to satisfy the lower TH_{PAPR} becomes larger. The proposed ROC method with TH_{PAPR} =6.5dB and the conventional PTS method with TH_{PAPR}=6.1dB can reduce the computation complexity by 48% from the conventional PTS method with the conventional IFFT technique.

Table 2.3: Comparison of computation complexity for the proposed ROC and conventional PTS methods.

Methods	TH$_{PAPR}$	AVE$_{ite}$	Complexity in (2.10)&(2.11)	Improvement from PTS (%)
Conventional PTS w/o Split-Radix	N/A	64	60,416	100
	6.1 dB	$\cong 30$	$\cong 34,304$	$\cong 57$
Conventional PTS w/ Split-Radix	N/A	64	54,955	91
	6.1 dB	$\cong 30$	$\cong 28,843$	$\cong 48$
Proposed ROC w/o Split-Radix	6.5 dB	$\cong 30$	$\cong 34,304$	$\cong 57$
	6.4 dB	$\cong 40$	$\cong 41,984$	$\cong 69$
	6.3 dB	$\cong 60$	$\cong 57,344$	$\cong 95$
Proposed ROC w/ Split-Radix	6.5 dB	$\cong 30$	$\cong 28,843$	$\cong 48$
	6.4 dB	$\cong 40$	$\cong 36,523$	$\cong 60$
	6.3 dB	$\cong 60$	$\cong 51,883$	$\cong 86$

Figure 2.5 shows the PAPR performance for the proposed ROC method with the proposed low computation complexity and the split-radix IFFT techniques. In the Figure, the conventional OFDM and the PTS methods with the sprit-radix IFFT techniques are also shown. The modulation technique is 16QAM, the number of IFFT-points N is 256, the number of data subcarriers M is 64 and the number of zero padding Z is 192. The over sampling ratio is taken by 4 to evaluate the PAPR performance precisely. The PAPR performances for the proposed ROC method are evaluated when the MAX_{ite} is 256 and the TH_{PAPR} are 6.3, 6.4, and 6.5dB, respectively. In the Figure, the PAPR performance is evaluated by using the Complementary Cumulative Distribution Function (CCDF). From the Figure, it can be observed that the proposed ROC method with TH_{PAPR}=6.5dB shows better PAPR performance than the conventional OFDM by 2.8dB at $CCDF$=10^{-2} and almost the same PAPR performance as the conventional PTS method with TH_{PAPR}=6.1dB. From Table 2.3 and Figure 2.5, it can be concluded that the proposed ROC method with the low computation complexity technique can achieve almost the same PAPR performance with the same computation complexity as that for the conventional PTS method. The advantage of proposed ROC method is to reduce the PAPR performance both for the data information and cluster ID numbers simultaneously which is completely different from the conventional PTS method. In the conventional PTS method, the phase coefficients of PTS are obtained after the PTS processing only for the data information at each OFDM symbol which leads the difficulty to embed the phase coefficients of PTS into the data information separately without degradation of PAPR performance.
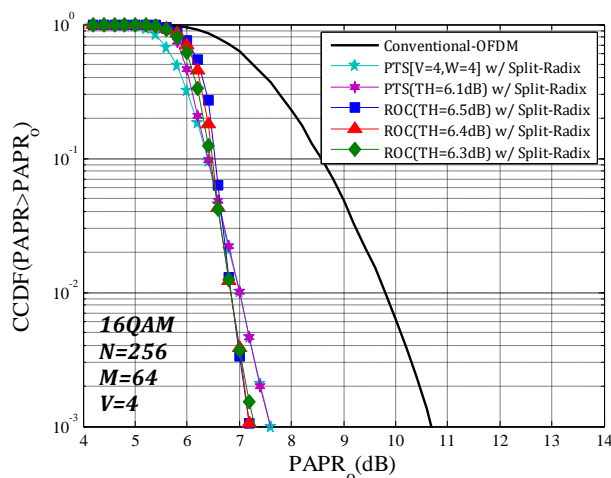
Figure 2.5: PAPR Performance for the proposed ROC method with sprit-radix IFFT technique.

2.5   Conclusions

This chapter proposed the new PAPR reduction method based on the packet-switched transmission systems in which all the clusters within the certain number of OFDM symbols have the sequential cluster ID numbers embedded in the header of each cluster. The salient features of the proposed method is to improve the PAPR performance both for the data information and cluster ID numbers simultaneously by re-ordering of clusters in the frequency domain at the transmitter and to reconstruct the original order of clusters by using the cluster ID number embedded in the data information at the receiver. This Chapter also proposed the computation complexity reduction technique for the ROC method by using the feature of IFFT processing. The proposed ROC method is completely different from the PTS method which is required to inform the phase coefficients obtained after the PTS processing as the side information to the receiver separately. From this fact, The PTS method has a difficulty to embed the phase coefficients of PTS into the data information separately without the degradation of PAPR performance.

From the computer simulation results, it is concluded that the proposed ROC method can achieve almost the same PAPR performance and the computation complexity as those for the conventional PTS method. The advantage of proposed ROC method is to reduce the PAPR performance both for the data information and cluster ID numbers simultaneously which enables the realization of transmitter and receiver much simpler than that for the PTS method.

CHAPTER 3

PROPOSAL OF CHANNEL ESTIMATION METHOD FOR ITS SYSTEMS BY USING STBC MIMO-OFDM

Intelligent Transport Systems (ITS) have been expanding with the popularization of Electrical Toll Collection System (ETC) and Vehicle Information and Communication System (VICS). The OFDM based Road to Vehicle Communication (RVC) system has been considered as one of the promising ITS technologies which can provide the drivers for safety and comfortable driving and collection of variable information from network in the real-time. This chapter proposes a RVC system of using the STBC (Space Time Block Coding) MIMO-OFDM technique which can achieve better BER performance even in higher time-varying fading channel. To achieve the potential capability in the proposed RVC system, it is the essential to realize the accurate channel estimation method. This chapter proposes a novel channel frequency response (CFR) estimation method by using the scattered pilot subcarriers in the frequency domain. From computer simulation results, this chapter demonstrates that the STBC MIMO-OFDM based RVC system of using the proposed CFR estimation method can achieve higher channel estimation accuracy and better BER performance even in the time varying fading channel.

3.1   Introduction

Intelligent Transport Systems (ITS) have been expanding with the popularization of Electrical Toll Collection System (ETC) and the Vehicle Information communication Systems (VICS) which enable the drivers for the safety and comfortable driving, and collection of variable information from the network in the real-time [37-39]. Various transmission techniques for the communications systems in the ITS are currently studying in the various projects and some of them have already been standardized in the ITS systems.

From the above backgrounds, the ITS could become an advanced information network systems for the transportation infrastructures which are essential to greatly improve our social activities and the quality of our social life. The Communications systems for the ITS can be classified into the road-to-vehicle communication (RVC) and the vehicle-to-vehicle communication (VVC). The communication services through the RVC have been investigated to provide various kinds of information to the users on vehicles. In the RVC, the received signal power at the vehicle decreases as increasing the distance from the base stations located along the road. The received signal is also fluctuated in the short time period due to the time varying multipath fading when the vehicles are moving at high speed. These conditions cause the fatal degradation of bit error rate (BER) performance in the RVC. From this fact, the achievable transmission data rate in the current RVC is insufficient to provide the mobile multimedia communications services to the users on the vehicles.

The IEEE 802.11p is adopted as the standard specifications for the VVC and RVC in the ITS [40]. The IEEE 802.11p employs the Orthogonal Frequency Division Multiplexing (OFDM) as the transmission technique in the 5GHz band used by the IEEE 802.11a. Although the OFDM technique can achieve high signal quality in the multipath fading channel, this standard is insufficient to achieve the higher transmission data rate with the higher signal quality especially in the higher time varying fading channels which are typical operation environments in the ITS.

To solve the above problems, this chapter proposes a new RVC system by using the STBC (Space Time Block Coding) MIMO (Multiple Input Multiple Output)-OFDM [41-42] technique for the future ITS which can provide the mobile multimedia communications services to the users on the vehicle. To realize the proposed STBC MIMO-OFDM systems, the channel estimation method is required as the key technique which enables the accurate channel estimation at every symbol in the higher time varying fading channels. This chapter proposes a channel estimation method by using the scattered pilot and null subcarrier which enables the demodulation of multiplexed signal encoded with the STBC. The proposed STBC MIMO-OFDM system in conjunction with the proposed channel estimation method can achieve higher transmission data rate with keeping the higher signal quality even in the time varying fading channels.

This chapter is organized as follows. Section 3.2 shows the proposed STBC MIMO-OFDM system model, and Section 3.3 proposes a channel estimation method for the proposed system by using the scattered pilot subcarrier assignment method. Section 3.4 presents the various computer simulation results to verify the effectiveness of the proposed method as compared with the conventional methods. Finally Section 3.5 draws some conclusions.

3.2   Proposed System Model

Figure 3.1 shows the proposed STBC MIMO-OFDM system model to be used in this chapter. The vehicle (MS) with two receiving antennas receives the OFDM signals with STBC encoded by Alamounti scheme [41] from both base stations (BS#1 and BS#2) located along the road. The communication channel is modeled by the Rician fading including one direct path and several reflected paths which follows the Rayleigh fading. In Figure 3.1, *PL* represents the propagation loss between the BS and MS, θ is the signal arrival angle from the BS to the MS, and *DD*1 and *DD*2 are the distances from the BS#1 and BS#2 to MS, respectively.
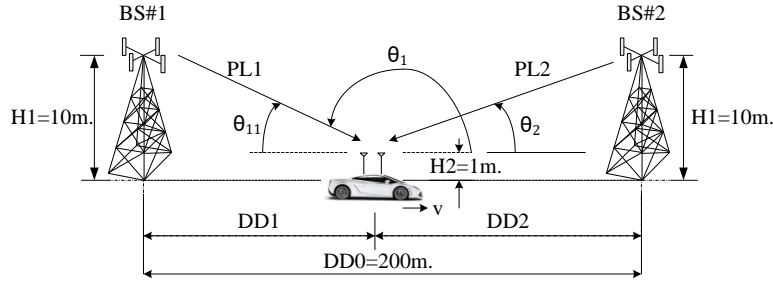
Figure 3.1: Overview of proposed system model.

Figure 3.2 shows the block diagram of proposed STBC MIMO-OFDM transceiver. In Figure 3.2, $D(m,n)$ is the modulated information signal at the *n*-th subcarrier of the *m*-th symbol in the frequency domain, $X(m,n)$ is the modulated signal after insertion of scattered pilot signals, and $S_1(m,n)$ and $S_2(m,n)$ are transmission signals from BS#1 and BS#2 which are encoded by STBC. The STBC encoded signals $S_1(m,n)$ and $S_2(m,n)$ are converted to the time domain signal by using IFFT, and the guard interval (GI) is added to avoid the inter-symbol-interference (ISI). The time domain signal is transmitted to the MS receiver through the Rician fading channel with having the time impulse response $h_{ij}(m,k)$ at the *k*-th time sampling of the *m*-th symbol. At the receiver, $r_1(m,k)$ and $r_2(m,k)$ including the additive white Gaussian noise $w(m,k)$ are received at the MS receiving antenna MS#1 and MS#2, respectively. The received time domain signals are converted to the frequency domain signal $R_1(m,n)$ and $R_2(m,n)$ by FFT after removing the GI. The received frequency domain signal inputs to the channel estimator to estimate the channel frequency response (CFR) for $\hat{H}_{ij}(m,n)$ which represents the channel response from BS#*i* to MS#*j* link at the *n*-th subcarrier of the *m*-th symbol. The received signal also inputs to the combiner to detect the modulated signals $\hat{X}(m,n)$ and $\hat{X}(m+1,n)$ at the *n*-th subcarrier of the *m*-th and (*m*+1)-th symbols, respectively.

In the STBC MIMO-OFDM system with the Alamounti coding, the modulated information data $X(m,n)$ is encoded into two signals S_1 and S_2 as given by the following equation,

$$
\begin{aligned}
S_1(m,n) &= X(m,n), \\
S_1(m+1,n) &= -X^*(m+1,n), \\
S_2(m,n) &= X(m+1,n), \\
S_2(m+1,n) &= X^*(m,n).
\end{aligned}
\tag{3.1}
$$

To easily understand the process at the receiver, we divide the processes into 4 parts as follows,
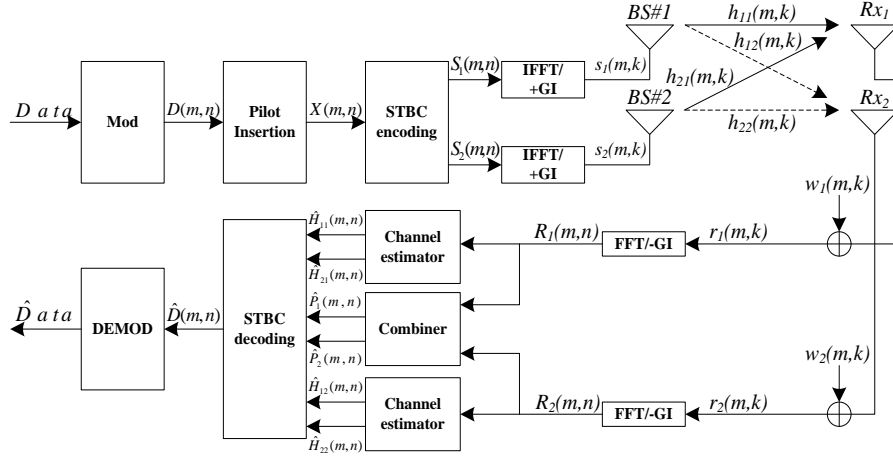
Figure 3.2: Block diagram of proposed STBC MIMO-OFDM transceiver.

PART 1: Received Signal

The frequency domain received signal $R_1(m,n)$ and $R_2(m,n)$ at MS#1 and MS#2 can be given by,

At MS#1,

$$R_1(m,n) = H_{11}(m,n) \cdot S_1(m,n) + H_{21}(m,n) \cdot S_2(m,n)$$
$$R_1(m+1,n) = H_{11}(m+1,n) \cdot S_1(m+1,n) + H_{21}(m+1,n) \cdot S_2(m+1,n)$$

(3.2)

At MS#2,

$$R_2(m,n) = H_{12}(m,n) \cdot S_1(m,n) + H_{22}(m,n) \cdot S_2(m,n)$$
$$R_2(m+1,n) = H_{12}(m+1,n) \cdot S_1(m+1,n) + H_{22}(m+1,n) \cdot S_2(m+1,n)$$

(3.3)

Substituting (3.1) into (3.2) and (3.3), they can be rewritten by the following equation,

At MS#1,

$$R_1(m,n) = \quad H_{11}(m,n) \cdot X(m,n) + H_{21}(m,n) \cdot X(m+1,n)$$
$$R_1(m+1,n) = -H_{11}(m+1,n) \cdot X^*(m+1,n) + H_{21}(m+1,n) \cdot X^*(m,n)$$

(3.4)

At MS#2,

$$R_2(m,n) = \quad H_{12}(m,n) \cdot X(m,n) + H_{22}(m,n) \cdot X(m+1,n)$$
$$R_2(m+1,n) = -H_{12}(m+1,n) \cdot X^*(m+1,n) + H_{22}(m+1,n) \cdot X^*(m,n)$$

(3.5)

PART 2: Channel Estimator

The details of the CFR estimation method is proposed in Section 3.3.

PART 3: Combining Scheme

From (3.4) and (3.5), $X(m,n)$ can be rewritten into the following equations by using the CFR $H_{ij}(m,n)$ estimated in Part 2,

At MS#1,

$$X_{MS\#1}(m,n) = \hat{H}_{11}^*(m,n) \cdot R_1(m,n) + \hat{H}_{21}(m+1,n) \cdot R_1^*(m+1,n)$$
$$X_{MS\#1}(m+1,n) = \hat{H}_{21}^*(m,n) \cdot R_1(m,n) - \hat{H}_{11}(m+1,n) \cdot R_1^*(m+1,n)$$

(3.6)

At MS#2,

$$X_{MS\#2}(m,n) = \hat{H}_{12}^*(m,n) \cdot R_2(m,n) + \hat{H}_{22}(m+1,n) \cdot R_2^*(m+1,n)$$
$$X_{MS\#2}(m+1,n) = \hat{H}_{22}^*(m,n) \cdot R_2(m,n) - \hat{H}_{12}(m+1,n) \cdot R_2^*(m+1,n)$$

(3.7)

From (3.6) and (3.7), we obtain the combined received signals as follows,

At MS#1,

$$\hat{X}(m,n) = \hat{H}_{11}^*(m,n) \cdot R_1(m,n) + \hat{H}_{21}(m+1,n) \cdot R_1^*(m+1,n)$$
$$+ \hat{H}_{12}^*(m,n) \cdot R_2(m,n) + \hat{H}_{22}(m+1,n) \cdot R_2^*(m+1,n)$$

(3.8)

3.2. Proposed System Model

At MS#2,

$$
\begin{aligned}
\hat{X}(m+1,n) = \; &\hat{H}_{21}^{*}(m,n)\cdot R_{1}(m,n) - \hat{H}_{11}(m+1,n)\cdot R_{1}^{*}(m+1,n) \\
&+ \hat{H}_{22}^{*}(m,n)\cdot R_{2}(m,n) - \hat{H}_{12}(m+1,n)\cdot R_{2}^{*}(m+1,n)
\end{aligned}
\tag{3.9}
$$

PART 4: STBC decoding

   The information data after the STBC decoding can be given by,

$$
\hat{D}(m,n) = \frac{d(m,n)\cdot \hat{X}(m,n) - b(m,n)\cdot \hat{X}(m+1,n)}{a(m,n)\cdot d(m,n) - b(m,n)\cdot c(m,n)}
$$

$$
\hat{D}(m+1,n) = \frac{a(m,n)\cdot \hat{X}(m+1,n) - c(m,n)\cdot \hat{X}(m,n)}{a(m,n)\cdot d(m,n) - b(m,n)\cdot c(m,n)}
\tag{3.10}
$$

where

$$
\begin{aligned}
a(m,n) &= A_{i}(m,n) + A_{i+1}(m,n) \\
b(m,n) &= B_{i}(m,n) + B_{i+1}(m,n) \\
c(m,n) &= C_{i}(m,n) + C_{i+1}(m,n) \\
d(m,n) &= D_{i}(m,n) + D_{i+1}(m,n) \\
A_{i}(m,n) &= \left|\hat{H}_{1i}(m,n)\right|^{2} + \left|\hat{H}_{2i}(m+1,n)\right|^{2} \\
B_{i}(m,n) &= \hat{H}_{1i}^{*}(m,n)\cdot \hat{H}_{2i}(m,n) - \hat{H}_{1i}^{*}(m+1,n)\cdot \hat{H}_{2i}(m+1,n) \\
C_{i}(m,n) &= \hat{H}_{1i}(m,n)\cdot \hat{H}_{2i}^{*}(m,n) - \hat{H}_{1i}(m+1,n)\cdot \hat{H}_{2i}^{*}(m+1,n) \\
D_{i}(m,n) &= \left|\hat{H}_{1i}(m+1,n)\right|^{2} + \left|\hat{H}_{2i}(m,n)\right|^{2}
\end{aligned}
$$

3.3   Proposal of Channel Estimation Method

In this section, we propose the channel estimation method for the proposed STBC MIMO-OFDM system. Firstly, we define the Rician fading channel which consists of one direct path and several reflected paths which follows the Rayleigh distribution. Secondly, we propose the scattered pilot and null subcarrier assignment method both in the frequency and time axes which enables the estimation of CFR for the multiplexed signal with STBC coding transmitted from both BSs. Finally, we propose the CFR estimation method by using the Maximum Likelihood (ML) method in the frequency axis and the cubic spline interpolation method which enables the demodulation of received signal with the STBC coding.

3.3.1   Fading Channel Model

The channel impulse responses $h_{tr}(m,k)$ in the Rician Fading Channel between the t-th transmitting antenna at the BS#t and the r-th receiving antenna at the MS#r can be given by,

$$h_{tr}(m,k) = \sum_{l=1}^{NP} \rho_{tr}^{(l)}(m) \cdot \delta(k-l)$$

$$\rho_{tr}^{(l)}(m) = \sum_{s=1}^{C_l} \mu_{ls} \cdot e^{j2\pi f_D \cos(\varphi_{ts})m}$$

(3.11)

where $t(=1,2)$ and $r(=1,2)$ represent the Tx antenna and Rx antenna numbers, $\rho_{tr}^{(l)}$ is the channel impulse response in the time domain between the t-th transmitting antenna and the r-th receiving antenna for the l-th delay path, NP is the number of delay paths, μ_{ls} is the coefficient of scattered path for the s-th arrival angle of the l-th delay path, C_l is the number of scattered paths for the delay path l, and f_D is the maximum Doppler frequency spread at the speed of the vehicle v (km/hr) in the radio frequency (f_c).

By using (3.11), the time domain received signal $r_1(m,k)$ and $r_2(m,k)$ at each receiving antenna at the MS can be given by,
At MS#1,

$$r_1(m,k) = \left\{ h_{11}(m,k) \otimes s_1(m,k) \right\} \cdot PL1 + \left\{ h_{21}(m,k) \otimes s_2(m,k) \right\} \cdot PL2 + w_1(m,k) \quad (3.12)$$

At MS#2,

$$r_2(m,k) = \left\{ h_{12}(m,k) \otimes s_1(m,k) \right\} \cdot PL1 + \left\{ h_{22}(m,k) \otimes s_2(m,k) \right\} \cdot PL2 + w_2(m,k) \quad (3.13)$$

where $\otimes$ denotes the convolution operation. Here, the channel frequency response $H_{tr}(m,n)$ can be obtained by converting the channel impulse response given in (3.11) to the frequency domain by FFT which is given by,

$$H_{tr}(m,n) = \sum_{l=1}^{NP} \rho_{tr}^{(l)}(m) \cdot e^{-\frac{j2\pi(l-1)(n-1)}{N}}$$

(3.14)

3.3.2   Scattered Pilot Subcarrier Assignment Method

From (3.14), it can be seen that the channel frequency response under the high mobile environments is required to estimate at every symbol for the frequency domain equalization of received signal. From this fact, this chapter proposes pilot subcarrier assignment methods to be used in the estimation of channel frequency response. Figure 3.3 shows the pilot subcarrier assignment method. In the Figure, I_f and I_t represent the interval of subcarrier in the frequency axis and interval of pilot symbols including the pilot subcarrier in the time axis.

In Figure 3.3, the consecutive two pilot symbols including the pilot and null subcarrier assignment method with the interval of I_f in which the locations of all pilot subcarrier for the BS#1 are assigned by the null subcarrier for the BS#2 so as to avoid the collision of pilot

subcarrier between the received signals at the MS from BS#1 and BS#2, are inserted into the data symbols with the interval of I_t in order to improve the CFR estimation accuracy. From this assignment method, it is possible to use the estimated CFR over the consecutive two pilot symbols for improving the CFR estimation accuracy.
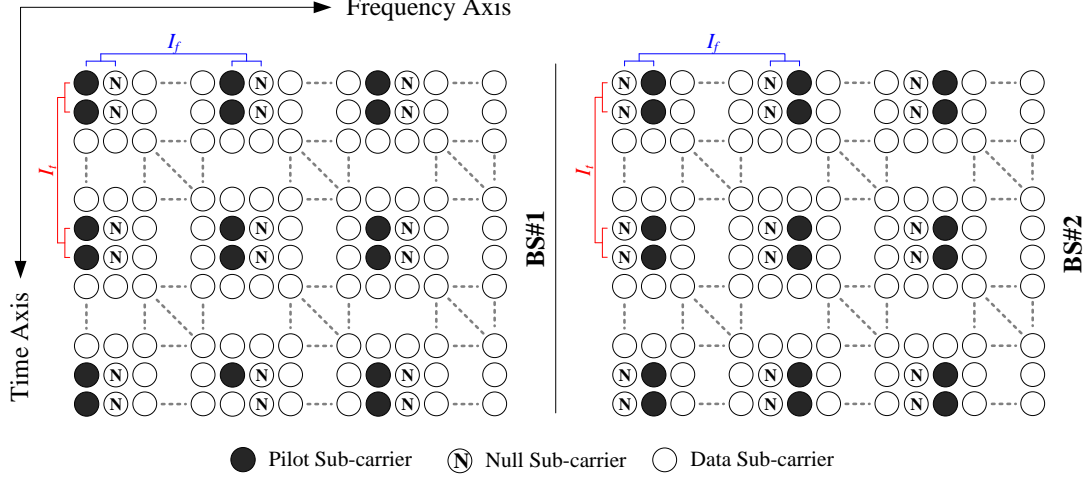
Figure 3.3: Proposed scattered pilot subcarriers assignment method.

3.3.3 Channel Estimation Method

In the previous section, we propose the scattered pilot subcarrier assignment method. In this section, we propose the channel estimation (CE) method by using the scattered pilot subcarrier for the STBC MIMO-OFDM system. The CFR can be estimated in both the frequency and time axes separately. For the frequency axis, the CFR over the OFDM frequency bandwidth can be estimated by applying the Maximum Likelihood (ML) method [43-45] for the estimated CFR at the pilot subcarrier. For the time axis including the data symbols, the CFR over one frame can be estimated by applying the cubic spline interpolation method for the estimated CFR over the OFDM frequency bandwidth at the pilot symbols. In this section, the ML method for the frequency axis and interpolation method for the time axis are presented.

The time domain signals given in (3.12) and (3.13) are converted to the frequency domain signals $R_1(m,n)$ and $R_2(m,n)$ by FFT which can be expressed by the following,

At MS#1,

$$R_1(m,n) = \{H_{11}(m,n) \cdot S_1(m,n)\} \cdot PL1 + \{H_{21}(m,n) \cdot S_2(m,n)\} \cdot PL2 + W_1(m,n) \qquad (3.15)$$

At MS#2,

$$R_2(m,n) = \{H_{12}(m,n) \cdot S_1(m,n)\} \cdot PL1 + \{H_{22}(m,n) \cdot S_2(m,n)\} \cdot PL2 + W_2(m,n) \qquad (3.16)$$

By dividing (3.15) and (3.16) by the known pilot subcarrier data, the CFRs $S_{P1}(mp(k),np_1(i))$ and $S_{P2}(mp(k),np_2(i))$ at the location of pilot subcarrier can be estimated as follows,

At MS#1,

$$\hat{H}_{11}(mp(k),np_1(i)) = \frac{R_1(mp(k),np_1(i))}{S_{P1}(mp(k),np_1(i))} - \frac{W_1(mp(k),np_1(i))}{S_{P1}(mp(k),np_1(i))},$$

$$\hat{H}_{21}(mp(k),np_2(i)) = \frac{R_1(mp(k),np_2(i))}{S_{P2}(mp(k),np_2(i))} - \frac{W_1(mp(k),np_2(i))}{S_{P2}(mp(k),np_2(i))}$$

$$(3.17)$$

At MS#2,

3.3. Proposal of Channel Estimation Method

$$\hat{H}_{12}(mp(k),np_1(i)) = \frac{R_2(mp(k),np_1(i))}{S_{P1}(mp(k),np_1(i))} - \frac{W_2(mp(k),np_1(i))}{S_{P1}(mp(k),np_1(i))},$$

$$\hat{H}_{22}(mp(k),np_2(i)) = \frac{R_2(mp(k),np_2(i))}{S_{P2}(mp(k),np_2(i))} - \frac{W_2(mp(k),np_2(i))}{S_{P2}(mp(k),np_2(i))}$$

(3.18)

where the pilot symbol number $mp(k)$ and pilot subcarrier number $np_1(i)$ for the BS#1 and $np_1(i)$ for the BS#2 are given by,

$$mp(k) = (k-1)\cdot I_t + 1 \ \ if \ \ k = 1 \sim L/I_t + 1,$$

$$\left. \begin{array}{l} np_1(i) = (i-1)\cdot I_f + 1 \\ np_2(i) = (i-1)\cdot I_f + 2 \end{array} \right\} if \ \ i = 1 \sim N/I_f$$

Since W_1 and W_2 are uncorrelated Gaussian variable in (3.17) and (3.18), the ML solution of both equations comes into the minimum square error (MSE) optimization problem. To estimate the CFR precisely, the number of guard interval length (Ng) must be taken by larger than NPi. The unknown parameters for the channel impulse response (CIR) $\hat{\rho}_{xr}^{(l)}(mp(k))$, where x is BS#1 or BS#2, can be obtained by,

$$L_{ML}(\hat{\rho}_{xr}^{(l)}(mp(k))) = \min_{\hat{\rho}_{xr}^{(l)}(mp(k))} \left[\sum_{i=1}^{NPi} \left| H_{xr}(mp(k),np_x(i)) - \sum_{l=1}^{Ng} \hat{\rho}_{xr}^{(l)}(mp(k)) \cdot e^{\frac{-j2\pi(l-1)(np_x(i)-1)}{N}} \right|^2 \right]$$

(3.19)

$$where \ \ \hat{\rho}_{xr}^{(l)}(mp(k)) = \left[\hat{\rho}_{xr}^{(1)}(mp(k)),....,\hat{\rho}_{xr}^{(Ng)}(mp(k)) \right]$$

Taking $\partial(3.19) \Big/ \partial \rho_{xr}^{*(l)}(mp(k)) = 0$, where (*) denotes conjugate, (3.19) can be expressed by the following,

$$\sum_{i=1}^{NPi} \left[\left\{ H_{xr}(mp(k),np_x(i)) - \sum_{l=1}^{Ng} \hat{\rho}_{xr}^{(l)}(mp(k)) \cdot e^{\frac{-j2\pi(l-1)(np_x(i)-1)}{N}} \right\} \cdot \sum_{ll=1}^{Ng} e^{\frac{j2\pi(ll-1)(np_x(i)-1)}{N}} \right] = 0$$

(3.20)

From (3.20), it can be rewritten as following,

$$\sum_{i=1}^{NPi} \sum_{ll=1}^{Ng} H_{fromBS\#x}(mp(k),np_x(i)) \cdot e^{j\frac{2\pi(np_x(i)-1)(ll-1)}{N}} = \sum_{i=1}^{NPi} \sum_{l=1}^{Ng} \sum_{ll=1}^{Ng} \hat{\rho}_{xr}^{(l)}(mp(k)) \cdot e^{-j\frac{2\pi(np_x(i)-1)(l-ll)}{N}}$$

(3.21)

From (3.21), since the dependence from optimization parameters $\hat{\rho}_{xr}^{(l)}(mp(k))$ is linear in (3.21), its solution can be realized by the Moore-Penrose generalized matrix inversion which can be given by,

$$\left[\hat{\rho}_{xr}^{(l)}(mp(k)) \right] = \dagger[D] \bullet [B(mp(k),np_x(i))]$$

(3.22)

where $\left[\hat{\rho}_{xr}^{(l)}(mp(k)) \right]$ is the ($Ng \times 1$) matrix of $\hat{\rho}_{xr}^{(l)}(mp(k))$, $[B(mp(k),np_x(i))]$ is ($Ng \times 1$) matrix of $R_r(mp(k),np_x(i))/S_{Px}(mp(k),np_x(i))$, $[D]$ is ($Ng \times N$) matrix of $exp(-j2\pi(np_x(i)-1)(l-ll)/N)$. $\dagger$ denotes the Moore-Penrose inverse and $\bullet$ denotes matrix multiplication. Because the matrix $[D]$ depends on the locations of pilot subcarrier and they are known at the receiver, the Moore-Penrose inverse matrix can be calculated in advance at the receiver. From this fact, the computation complexity for the estimation of CFR can be reduced relatively. The frequency channel response over the OFDM frequency bandwidth can be obtained by converting the CIR given in (3.22) to the frequency domain by FFT.

As for the estimation of CFR in the time axis, the cubic spline interpolation method is applied to the estimated CFR which is given by using ML method as mentioned above. The CFRs of pilot symbol#1 and pilot symbol#2 with the interval of I_t are estimated by performing two interpolations separately as shown in Figure 3.4. From Figure 3.4, it can be seen that the CFR for pilot symbol#1 and pilot symbol#2 are interpolated every $mp(k)=(k-1)I_t+1$ and $mp(k)=(k-1)I_t+2$, respectively. Then $\hat{H}_{ij}^{INTP\#1}(m,n)$ and $\hat{H}_{ij}^{INTP\#2}(m,n)$ can be estimated for each interpolation. Where i and j are the index of BS and the receiving antenna, and $INTP\#1$ and $INTP\#2$ denote the interpolations #1 and #2, respectively.

3.3. Proposal of Channel Estimation Method
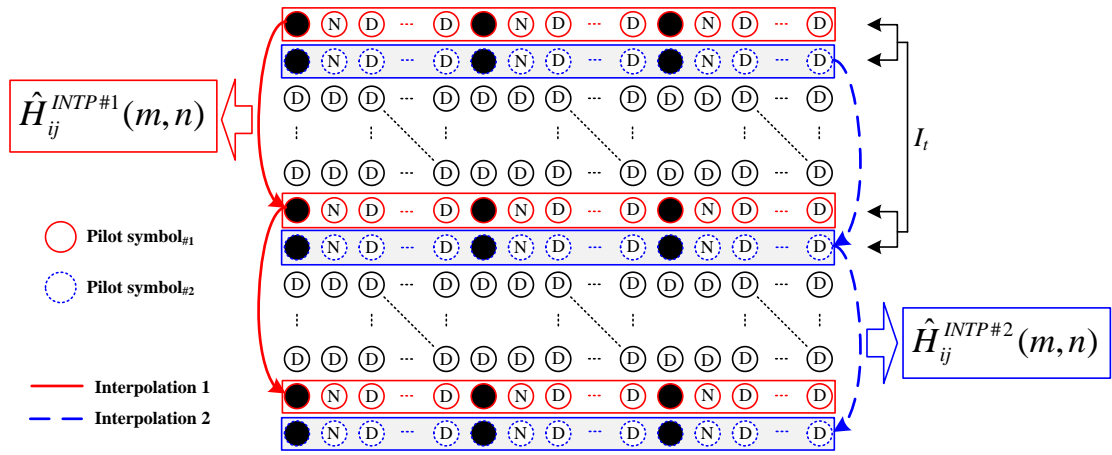
Figure 3.4: Proposed CFR estimation method.

By using two estimated CFR, the estimation accuracy of CFR can be improved by taking the average of them which is given by,

$$\hat{H}_{ij}(m,n) = mean\left[\hat{H}_{ij}^{INTP\#1}(m,n) + \hat{H}_{ij}^{INTP\#2}(m,n)\right] \qquad (3.23)$$

3.4   Performance Evaluations

This section presents the various computer simulation results to select the best pilot subcarrier assignment method and to verify the effectiveness of the proposed STBS MIMO-OFDM system in conjunction with the proposed CFR estimation method. The simulation parameters used in the following evaluations are listed in Table 3.1.

Table 3.1: Simulation parameters.

Information	Parameter
Modulation for data subcarriers	64QAM
Modulation for pilot subcarriers	QPSK
Demodulation	Coherent
Number of subcarriers (N)	128
Symbol duration (T_s)	12.8uS
Guard interval duration (T_{sg})	1.2uS
Number of sample points in GI (Ng)	12
Interval of pilot symbol (I_t)	1,4,8 and 16
Interval of pilot subcarrier (I_f)	1,4,8 and 16
OFDM occupied bandwidth (W)	10MHz
Radio frequency (f_c)	5.4GHz
Rician fading channel model	
Rice factor (K)	6dB
C/N at BS#1 and BS#2	50dB
Delay profile	Exponential
Decay constant	-1dB
Number of delay paths (NP)	4
Number of scattered paths (C_l)	20

Figure 3.5 shows the BER performance of the proposed method of using one and two receiving antennas at the MS when changing the carrier-to-noise power ratio (C/N). In the simulation, the vehicle is located at the center of two base stations (*DD*1 is 100m as shown in Figure 3.1) which corresponds to the worst condition for the road-to-vehicle communication. The operation C/N is 50dB which is defined at the right beneath of BS#1. The vehicle speed is 200km/h, and the I_f and I_t intervals are 4 and 8, respectively. The conventional-OFDM employs the Single Frequency Network technique (SFN) [46] in which both base stations transmit the same OFDM data information and the MS can demodulates the data information correctly from the multiplexed received signal when the maximum delay time deference for two received signals from the BS#1 and BS#2 is within the guard interval length *Ng*. The SFN technique is employed in the terrestrial digital TV system of using OFDM method. In the Figure, the BER performances for both conventional-OFDM with and without the Maximum Ratio Combining (MRC) [47] techniques are also shown as for the purpose of comparison with the proposed method. From the Figure, it can be observed that the proposed method with 2×2 antennas shows much better BER performance than that for the conventional OFDM of using SFN and MRC techniques.

3.4. Performance Evaluations
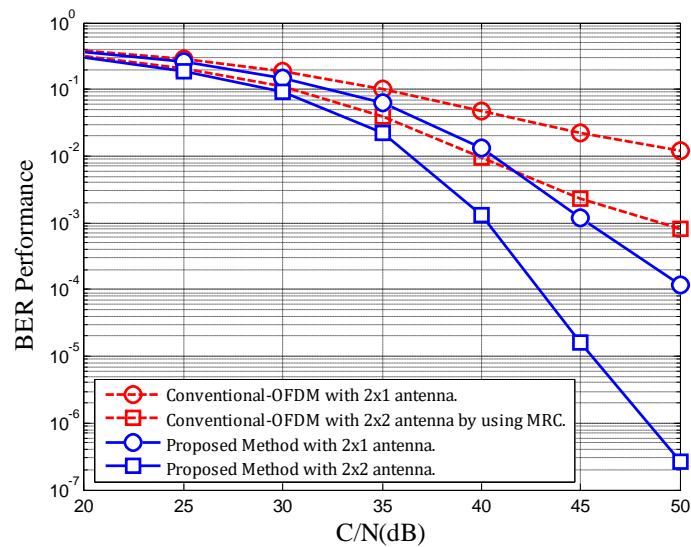
Figure 3.5: BER performances versus C/N(dB).
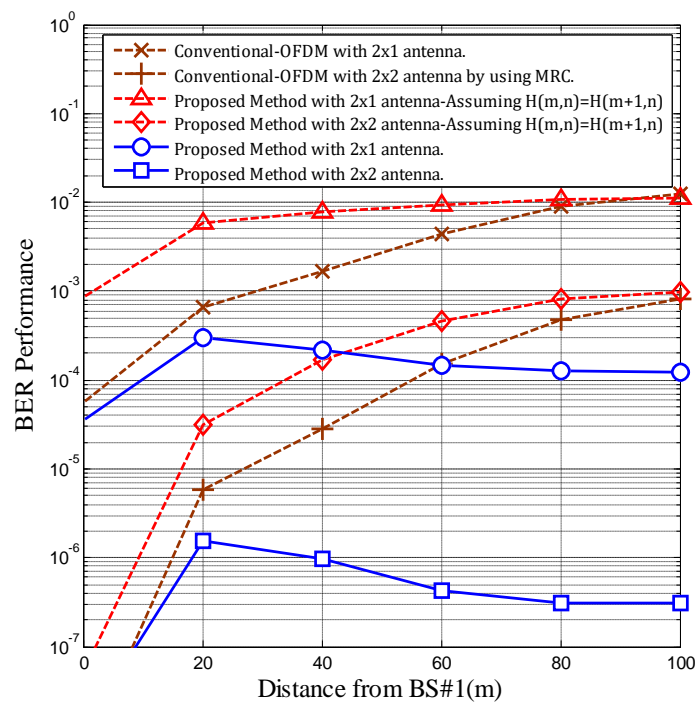
Figure 3.6: BER performances when changing the distance from BS#1 to MS.

Figure 3.6 shows the BER performance of the proposed method of using one and two receiving antennas at the MS when changing the distance from BS#1 to MS. In the simulation, the operation C/N is 50dB which is defined at the right beneath of BS#1 and the vehicle speed is 200km/h. From the Figure, it can be observed that the proposed method with two receiving antennas shows much better BER performance than the other methods especially when the vehicle is located at the center of two base stations (*DD*1 is 100m) which corresponds to the worst case in the road to vehicle communications. The BER performance of proposed method when assuming $H(m,n)=H(m+1,n)$ is worse than the conventional OFDM methods. From these results, the channel estimation is required at every symbol for the proposed STBC MIMO-OFDM system under higher mobile environments.

3.5 Conclusions

This chapter proposed the new road-to-vehicle communication system for the future ITS which can provide the mobile broadband multimedia wireless communications. The salient features of the proposed method are to employ the STBC MIMO-OFDM techniques and channel estimation method of using the scattered pilot subcarriers both for the frequency and time axes. From the various computer simulation results, this chapter demonstrated the effectiveness of the proposed STBC MIMO-OFDM system with Type III pilot subcarrier assignment method even in the higher time varying fading channel.

CHAPTER 4

PROPOSAL OF TIME DOMAIN CHANNEL ESTIMATION METHOD FOR MIMO-OFDM SYSTEMS

To achieve a potential capability of MIMO-OFDM system, it is the essential to realize an efficient and accurate channel estimation method. The conventional Discrete Fourier Transform Interpolation-based channel estimation (DFTI-CE) method of using the scattered pilot symbol can achieve higher estimation accuracy only when the transmission OFDM signal is sampled by the Nyquist rate. However the estimation accuracy of using the conventional DFTI-CE method would be degraded relatively when null subcarriers (zero padding) are inserted at both ends of data subcarrier to reject the aliasing occurring at the output of Digital to Analogue (D/A) converter which corresponds to the non-Nyquist sampling rate. To solve this problem, the Maximum Likelihood (ML) channel estimation method was proposed for MIMO-OFDM system which can achieve better estimation accuracy than the conventional DFTI-CE method. However its estimation accuracy would be degraded at around the both ends of data subcarrier at the non-Nyquist rate especially when increasing the number of transmit antennas and zero padding. To solve the above problem, this chapter proposes the ML based time domain channel estimation (TD-CE) method for MIMO-OFDM system which can achieve higher estimation accuracy even when the non-Nyquist rate and increasing the number of transmit antennas. From computer simulation results, this chapter demonstrates the effectiveness of propose ML based TD-CE method for MIMO-OFDM system.

4.1   Introduction

Orthogonal Frequency Division Multiplexing (OFDM) has been widely adopted in the current wireless communications systems as the standard transmission technique such as the Digital Audio and Video Broadcasting (DAB [48] and DVB [49]), Broadband Wireless Access (IEEE 802.16) [50] and Wireless Local Area Network (WLAN) [51] because of its efficient usage of frequency bandwidth and robustness to the multipath fading. Furthermore, the Multi Input Multi Output (MIMO) technique is employed with OFDM technique (MIMO-OFDM) [52] to achieve higher data transmission rate and higher signal quality in various wireless communication systems.

   In MIMO-OFDM systems, the receiver needs to estimate the channel frequency responses (CFR) precisely for all links between transmit and receive antennas which are used in the demodulation of information data with the MIMO detection. From this fact, the channel estimation (CE) method which can achieve higher estimation accuracy is essential in MIMO-OFDM systems to achieve higher data transmission rate with keeping higher signal quality. Up to today, many CE methods have been proposed for MIMO-OFDM systems including the Discrete Fourier Transform interpolation-channel estimation (DFTI-CE) method [53] and the Maximum Likelihood-channel estimation (ML-CE) method [54]. The DFTI-CE method can achieve higher estimation accuracy only when the sampling rate of transmission signal is the Nyquist rate *i.e.* the number of IFFT points (N) is equal to the number of data subcarriers (M). However the estimation accuracy of DFTI-CE method would be degraded relatively in the practical MIMO-OFDM systems in which the sampling rate is taken by the non-Nyquist rate. In the practical OFDM system, the null subcarriers (zero padding) are usually inserted at the both ends of M data subcarriers in every transmission OFDM symbol to reject the aliasing occurring at the output of digital to analogue (D/A) converter. From this fact, the channel estimation accuracy of using this method would be degraded especially at around the both ends of data subcarriers which are the borders between the data and null subcarriers due to the mismatching of sampling rate between the transmission signal with N samples and received signal with M samples. This phenomenon is called the border effect [55]. To solve the above problem, the ML-CE method was proposed for the MIMO-OFDM systems which can achieve higher estimation accuracy than the conventional DFTI-CE method [54]. However its estimation accuracy at the both ends of data subcarriers would be degraded when increasing the number of transmit antennas.

   To solve the above problems on the conventional CE methods, this chapter proposes a novel channel estimation method which can achieve higher estimation accuracy even when the non-Nyquist rate and increasing the number of transmit antennas in the MIMO-OFDM systems. The salient feature of proposed TD-CE method is to employ the superimposed time domain received scattered pilot preamble (SPP) symbol sent from all the transmit antennas in which pilot subcarriers sent from each transmit antenna are assigned cyclically including the both ends of transmission frequency band for data subcarriers. In the proposed method, the channel frequency responses for all links between transmit and receive antennas are estimated over the frequency band corresponding from the first to the end pilot subcarriers of which frequency band is also used in the transmission of data information.

   This chapter is organized as follows. Section 4.2 presents the conventional CE methods for MIMO-OFDM systems and their problems on the estimation accuracy at the non-Nyquist rate and when increasing the number of transmit antennas. Section 4.3 proposes the TD-CE method for MIMO-OFDM systems which can solve the problems on the conventional methods. Section 4.4 presents various computer simulation results to verify the effectiveness of proposed method and Section 4.5 draws some conclusions.

4.2 Conventional Channel Estimation Method

4.2.1 System Model for MIMO-OFDM Systems

For simplicity, we consider the MIMO-OFDM systems employing the Space Division Multiple Access (SDMA) technique with N_T transmit and N_R receive antennas which enables the transmission of separate information data from each transmit antenna.
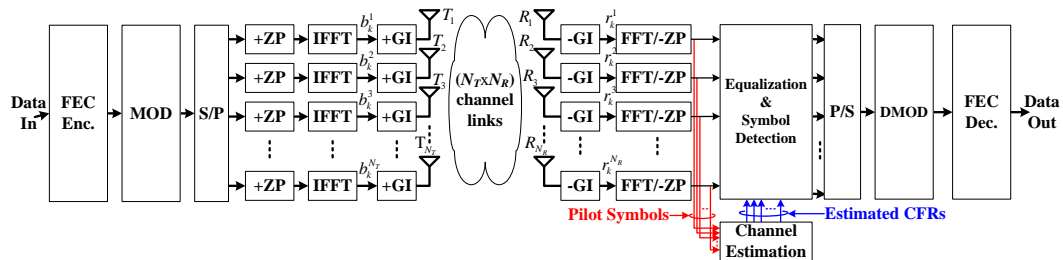
Figure 4.1: Overview of MIMO-OFDM systems.

Figure 4.1 shows a block diagram of MIMO-OFDM system with the SDMA. At the transmitter, the information data encoded by FEC is modulated and separated by M subcarriers into each transmit antenna. The zero padding are added at the both ends of M data subcarriers then converted into the time domain signal by N points IFFT at each transmit antenna. The time domain signal b_k^i at the k-th time sample ($0 \leq k \leq N-1$) transmitted from the T_i transmit antenna ($1 \leq i \leq N_T$) is sent to the receive antenna R_j ($1 \leq j \leq N_R$) after adding the guard interval (GI) to avoid the inter symbol interference (ISI). At the receiver, the data information transmitted from N_T transmit antennas are demodulated by using the MIMO detection with the estimated channel frequency response matrix consisting of all links between transmit and receive antennas.
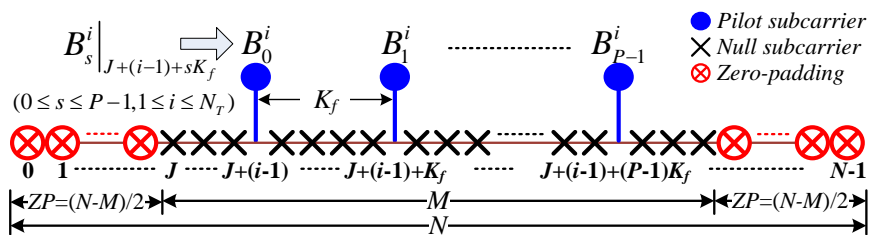
Figure 4.2: Assignment of pilot subcarrier in SPP symbol.

In the MIMO-OFDM systems, ($N_T \times N_R$) channels between transmit and receive antennas are required to estimate by using one common SPP symbol. Figure 4.2 shows an example of pilot subcarriers assignment in the SPP symbol sent from the i-th transmit antenna. In the Figure 4.2, N is the number of IFFT points, M is the number of data subcarriers, ($N-M$) represents the total number of null subcarriers (zero padding) and the half of the null subcarriers ($N-M$)/2 are inserted at both ends of M data subcarrier. Each transmit antenna can use $P(=M/K_f)$ pilot subcarriers within M subcarrier which are inserted cyclically with an interval of K_f subcarrier. J represents the first data subcarrier number ($J=(N-M)/2$) within N subcarriers including the zero padding. The pilot subcarriers for the i-th transmit antenna are assigned from $J+(i-1)$ to $J+(i-1)+sK_f$ ($0 \leq s \leq P-1$) with the interval of K_f subcarriers. Here it should be noted that the pilot subcarriers sent from each transmit antenna are assigned

cyclically so as to avoid a collision among the pilot subcarriers sent from all transmit antennas. The time domain SPP symbol b_k^i transmitted from the i-th transmit antenna is given by,

$$b_k^i = \frac{1}{N} \cdot \sum_{s=0}^{P-1} B_s^i \cdot e^{j\frac{2\pi k}{N}(J+(i-1)+sK_f)}, \quad (0 \le k \le N-1) \tag{4.1}$$

where B_s^i is the s-th pilot data for the i-th transmit antenna of which subcarrier number is $J+(i-1)+sK_f$ within N subcarriers. The channel impulse response (CIR) of multipath fading between the i-th transmit and the j-th receive antennas can be expressed by,

$$h_k^{i,j} = \sum_{q(i,j)=0}^{N_P-1} \rho_{q(i,j)}^{i,j} \cdot \delta(k-q(i,j)) \tag{4.2}$$

where N_P is the number of delay paths and $\rho_{q(i,j)}^{i,j}$ represents the complex amplitude of CIR for the $q(i,j)$-th delay path occurred in the channel between the i-th transmit and the j-th receive antennas. At the j-th receive antenna, the superimposed received SPP signal r_k^j sent from all transmit antennas after removing the GI can be given by,

$$r_k^j = \sum_{i=1}^{N_T} \left\{ b_k^i \otimes h_k^{i,j} \right\} + z_k^j = \sum_{i=1}^{N_T} \sum_{q(i,j)=0}^{N_P-1} \left\{ \rho_{q(i,j)}^{i,j} \cdot b_{k-q(i,j)}^i \right\} + z_k^j, \quad (1 \le j \le N_R) \tag{4.3}$$

where z_k^j is the additive white Gaussian noise (AWGN) at the k-th time sample of the j-th receive antenna and $\otimes$ represents the convolution. The CFR at the pilot subcarriers between the i-th transmit and the j-th receive antennas can be estimated independently by using the superimposed frequency domain received SPP symbol which is converted from the time domain signal in (4.3), because the pilot subcarriers sent from all transmit antennas are assigned without a collision as described above. By performing FFT to (4.3), the received frequency domain SPP symbol at the $J+(i-1)+sK_f$-th pilot subcarrier is given by,

$$R_{J+(i-1)+sK_f}^j = B_s^i \sum_{q(i,j)=0}^{N_P-1} \rho_{q(i,j)}^{i,j} \cdot e^{-j\frac{2\pi q(i,j)}{N}(J+(i-1)+sK_f)} + Z_{J+(i-1)+sK_f}^j = B_s^i \cdot H_{J+(i-1)+sK_f}^{i,j} + Z_{J+(i-1)+sK_f}^j \tag{4.4}$$

where $H_{J+(i-1)+sK_f}^{i,j}$ and $Z_{J+(i-1)+sK_f}^j$ are the CFR at the $J+(i-1)+sK_f$-th pilot subcarrier between the i-th transmit and the j-th receive antennas and AWGN at the j-th receive antenna both in the frequency domain. From (4.4), the CFR $H_{J+(i-1)+sK_f}^{i,j}$ can be estimated by using the pilot data B_s^i known at the receiver which is given by,

$$\hat{H}_{J+(i-1)+sK_f}^{i,j} = \frac{R_{J+(i-1)+sK_f}^j}{B_s^i} = H_{J+(i-1)+sK_f}^{i,j} + \frac{Z_{J+(i-1)+sK_f}^j}{B_s^i} \tag{4.5}$$

The next section presents the conventional ML-CE method by using the estimated CFR at the pilot subcarriers given in (4.5).

4.2.2 Conventional ML-CE Method

In the ML-CE method [54], the CIR $\hat{\rho}_{q(i,j)}^{i,j}$ can be estimated by the following Maximum Likelihood (ML) equation [45],

$$L_{ML}\left\langle \hat{\rho}_{q(i,j)}^{i,j} \right\rangle = \min_{\hat{\rho}_{q(i,j)}^{i,j}} \left[\sum_{s=0}^{P-1} \left| \sum_{q(i,j)=0}^{Ng-1} \rho_{q(i,j)}^{i,j} \cdot e^{-j\frac{2\pi q(i,j)}{N}(J+(i-1)+sK_f)} - \hat{H}_{J+(i-1)+sK_f}^{i,j} \right|^2 \right] \tag{4.6}$$

The ML equation given in (4.6) can be expressed by the following simultaneous equations,

$$\left\| \hat{\rho}_{q(i,j)}^{i,j} \right\|_{Ng\times1} = \dagger \left\| D_{q(i,j),J+(i-1)+sK_f}^{i,j} \right\|_{P\times Ng} \bullet \left\| \hat{H}_{J+(i-1)+sK_f}^{i,j} \right\|_{P\times1} \tag{4.7}$$

where $\dagger$ denotes the Moore-Penrose pseudo inverse matrix, $\left\| \hat{\rho}_{q(i,j)}^{i,j} \right\|$ is the matrix of the complex amplitude of CIR with the matrix size $[Ng\times1]$, and $\left\| D_{q(i,j),J+(i-1)+sK_f}^{i,j} \right\|$ with the matrix size $[P\times Ng]$ can be given by,

$$D_{q(i,j),J+(i-1)+sK_f}^{i,j} = e^{-j\frac{2\pi q(i,j)}{N}(J+(i-1)+sK_f)}, \quad (0 \le q(i,j) \le Ng-1) \tag{4.8}$$

Since the number of actual delay paths N_P is unknown at the receiver, the length of GI (Ng) is used in the estimation of CIR in (4.6). After performing DFT to (4.7), the CFR can be estimated over M data subcarriers. Although the ML-CE method can improve the border effect and achieve higher channel estimation accuracy, its estimation accuracy at the both ends of data subcarriers would be degraded when increasing the number of transmit antennas [54]. When increasing the number of transmit antennas, the interval of pilot subcarriers K_f becomes larger and the number of subcarriers which are not covered by pilot subcarriers at the both ends of M data subcarriers are increased as shown in Figure 4.2. This is the reason that the estimation accuracy of ML-CE method obtained by (4.6) would be degraded when increasing the number of antennas.

4.3 Proposal of Time Domain Channel Estimation Method

To solve the above problems having the conventional ML-CE method, this section proposes a time domain-channel estimation (TD-CE) method by using one SPP symbol which can improve the border effect even when the non-Nyquist rate and increasing the number of transmit antennas.

4.3.1 Proposed Pilot and Data Subcarriers Assignment Method

Figure 4.3(a) shows the proposed pilot subcarriers assignment for the SSP symbol sent from the i-th transmit antenna. In the Figure 4.3, the pilot subcarriers are inserted with the interval of K_f subcarriers starting from the $J+(i-1)$-th to the $J+(i-1)+(P-1)K_f$-th subcarriers which covers the bandwidth of $M_p=M-N_T+1$. Here it should be noted that the frequency band covered by both ends of pilot subcarriers for the i-th transmit antenna is different from other transmit antennas and the data subcarriers are assigned within the same bandwidth of M_p subcarriers between the first to the end pilot subcarriers as shown in Figure 4.3(b). In the proposed pilot assignment method, the active number of data subcarriers becomes $M_p=M-N_T+1$ which is smaller number than M for the conventional method as shown in Figure 4.2. However, it can be expected that channel estimation accuracy at around the borders between the null subcarriers and data subcarriers could be better than the conventional method because the pilot subcarriers are inserted at the both ends of data subcarriers.

(a) SPP Symbol

(b) Data Symbol

$(0 \le s \le P-1), (1 \le i \le N_T), P = M_p / K_f$

● *Pilot subcarrier*   □ *Data subcarrier*
✕ *Null subcarrier*   ⊗ *Zero-padding*
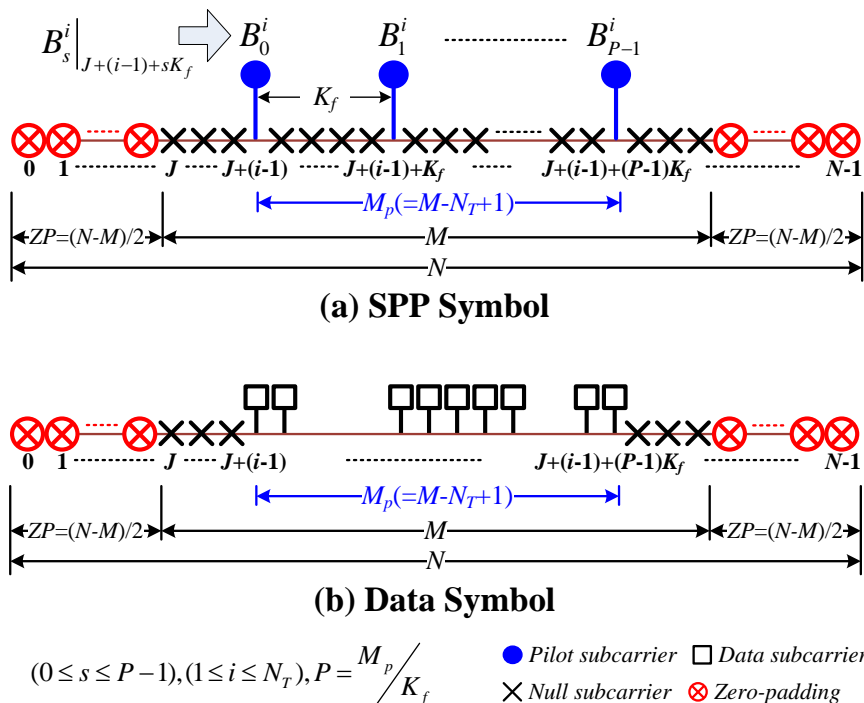
Figure 4.3: Proposed pilot and data subcarriers assignment for the i-th transmit antenna.

4.3.2 Proposed Time Domain Channel Estimation (TD-CE) Method

This section proposes the TD-CE method by using the proposed pilot and data assignment method as shown in Figure 4.3 which can achieve higher estimation accuracy at around the borders between the data and zero padding subcarriers even when the Non-Nyquist rate and when increasing the number of transmit antennas. Accordingly, it can be expected that the proposed TD-CE method can achieve better BER performance than those for the conventional ML-CE method.

The superimposed received SPP symbol r_k^j at the j-th receive antenna can be given by the following equation in which the received SPP symbol sent from each transmit antenna to the j-th receive antenna is expressed separately,

$$r_k^{\;j} = \underbrace{\sum_{q(1,j)=0}^{Ng-1} \rho_{q(1,j)}^{1,j} \cdot b_{k-q(1,j)}^i}_{from\ T_1\ to\ R_j} + \cdots + \underbrace{\sum_{q(N_T,j)=0}^{Ng-1} \rho_{q(N_T,j)}^{N_T,j} \cdot b_{k-q(N_T,j)}^{N_T}}_{from\ T_{N_T}\ to\ R_j} + z_k^{\;j} \tag{4.9}$$

The length of GI Ng in (4.9) is usually taken by longer than the N_P so as to avoid the Inter-symbol interference (ISI). By using the matrix multiplication, (4.9) can be rewritten by,

$$\mathbf{r}_j = \underbrace{\begin{bmatrix} b_0^1 & b_{-1}^1 & \cdots & b_{1-Ng}^1 \\ b_1^1 & b_0^1 & \cdots & b_{2-Ng}^1 \\ \vdots & \vdots & \ddots & \vdots \\ b_N^1 & b_{N-1}^1 & \cdots & b_{N-Ng}^1 \end{bmatrix}}_{\mathbf{b}_1} \bullet \underbrace{\begin{bmatrix} \rho_0^{1,j} \\ \rho_1^{1,j} \\ \vdots \\ \rho_{Ng-1}^{1,j} \end{bmatrix}}_{\mathbf{c}_{1,j}} + ... + \underbrace{\begin{bmatrix} b_0^{N_T} & b_{-1}^{N_T} & \cdots & b_{1-Ng}^{N_T} \\ b_1^{N_T} & b_0^{N_T} & \cdots & b_{2-Ng}^{N_T} \\ \vdots & \vdots & \ddots & \vdots \\ b_N^{N_T} & b_{N-1}^{N_T} & \cdots & b_{N-Ng}^{N_T} \end{bmatrix}}_{\mathbf{b}_{N_T}} \bullet \underbrace{\begin{bmatrix} \rho_0^{N_T,j} \\ \rho_1^{N_T,j} \\ \vdots \\ \rho_{Ng-1}^{N_T,j} \end{bmatrix}}_{\mathbf{c}_{N_T,j}} + \mathbf{z}_j \tag{4.10}$$

where $\mathbf{r}_j$ is the matrix of received signal r_k^j with the matrix size $[N\times1]$, $\mathbf{b}_i$ and $\mathbf{c}_{i,j}$ are the matrix of time domain SPP symbol b_k^i with the matrix size $[N\times Ng]$ and the matrix of complex amplitude of CIR $h_k^{i,j}$ with the matrix size $[Ng\times1]$ and $\mathbf{z}_j$ is the matrix of AWGN z_k^j with the matrix size $[N\times1]$. The matrix operation of (4.10) at the j-th receive antenna is rewritten by,

$$\mathbf{r}_j = \underbrace{\mathbf{b}_1 \bullet \mathbf{c}_{1,j}}_{from\ T_1\ to\ R_j} + \cdots + \underbrace{\mathbf{b}_{N_T} \bullet \mathbf{c}_{N_T,j}}_{from\ T_{N_T}\ to\ R_j} + \mathbf{z}_j = \underbrace{\begin{bmatrix} \mathbf{b}_1 \cdots \mathbf{b}_{N_T} \end{bmatrix}}_{\mathbf{B}} \bullet \underbrace{\begin{bmatrix} \mathbf{c}_{1,j} \cdots \mathbf{c}_{N_T,j} \end{bmatrix}^T}_{\mathbf{G}_j} + \mathbf{z}_j = \mathbf{B} \bullet \mathbf{G}_j + \mathbf{z}_j \tag{4.11}$$

where $[\ ]^T$ is the transpose matrix operation. $\mathbf{B}$ is the matrix of time domain SPP symbol $\mathbf{b}_i$ sent from all transmit antennas with the matrix size $[N_R\times N_T Ng]$ and $\mathbf{G}_j$ is the matrix of CIR $\mathbf{c}_{i,j}$ for all links from all transmit antennas to the j-th receive antenna with the matrix size $[N_T Ng\times1]$. From (4.11), the CIRs in matrix $\mathbf{G}_j$ can be estimated by using the Moore-Penrose pseudo inverse $\mathbf{B}^\dagger$ which can be given by,

$$\hat{\mathbf{G}}_j = \mathbf{B}^\dagger \bullet \mathbf{r}_j = \mathbf{G}_j + \mathbf{B}^\dagger \bullet \mathbf{z}_j \tag{4.12}$$

All CIRs can be estimated together by using (4.12) in the time domain at the j-th receive antenna. Since all the time domain SPP symbols sent from all transmit antennas are known at the receiver, $\mathbf{B}^\dagger$ can be calculated in advance at the receiver. From this fact, the estimation of CIRs for all links can be estimated by simple matrix multiplication as given in (4.12) which leads the considerable reduction of computational complexity in the proposed TD-CE method. In the time varying fading channels, the SPP symbols are inserted with the interval of K_t symbols in one frame and the CIRs over one frame can be estimated by applying the cubic interpolation method to the CIRs estimated at the SPP symbols with the interval of K_t symbols by (4.12). The CFRs for all links over one frame can be obtained by performing DFT to the estimated CIRs. Finally, the information data in one OFDM frame can be demodulated precisely by the MIMO detection of using the estimated CFR matrix even in higher time-varying fading channel.

4.4   Performance Evaluations

This section presents various computer simulation results to verify the effectiveness of proposed TD-CE method in the time-varying fading channel. Table 4.1 shows the simulation parameters used in the following evaluations.

Table 4.1: Simulation parameters.

Information	Parameter
Modulation for data subcarriers	16QAM
Modulation for pilot subcarriers	QPSK
Demodulation	Coherent
Number of FFT-points (N)	128
Number of data subcarriers in conventional methods (M)	96
Number of data subcarriers in proposed method (M_P)	M-N_T+1
Length of GI (Ng)	11
OFDM frame length (L-Symbols)	17
Interval of pilot in frequency (K_f) and in time (K_t) axes	K_f=N_T and K_t=4
Number of transmit and receive antennas ($N_T \times N_R$)	4×4 and 8×8
OFDM occupied bandwidth (BW)	5 MHz
Radio frequency (f_c)	2 GHz
Forward Error Correction (FEC) Code	
- Encoding	Convolution (R=1/2,K=7)
- Decoding	Hard-decision with Viterbi
- Interleave	Matrix with one frame (L)
- Packet length (information bits/packet)	512 bits
Number of delay paths (NP)	4
Multipath Rayleigh fading channel model	
- Delay profile	Exponential
- Decay constant	-1 dB
- Number of delay paths (N_P) in all links	10
- Number of scattered rays	20

Figure 4.4 shows the normalized mean square error (NMSE) performances of estimated CFR evaluated at each subcarrier for the proposed TD-CE and Conv.ML-CE methods when the sampling rate are taken by the Nyquist rate (N=M) and non-Nyquist (N≠M) rate. The number of transmit (N_T) and receive (N_R) antennas are 8×8. From the Figure, it can be seen that there is no border effect in the NMSE performances for all CE methods when the sampling rate is the Nyquist rate. When the sampling rate is the non-Nyquist rate, the proposed TD-CE methods has no border effects while the Conv.ML-CE methods have the border effects at around the both ends of data subcarriers. From these results, it can be concluded that the proposed TD-CE method can achieve higher estimation accuracy even when the non-Nyquist rate and the larger number of transmit antennas.

Figure 4.5 shows the NMSE performance of estimated CFR when changing the carrier to noise power ratio (C/N) for the proposed TD-CE and Conv.ML-CE methods at the non-Nyquist rate. In the evaluation, the number of transmit and receive antennas ($N_T \times N_R$)=4×4 and 8×8, and the normalized Doppler frequency (f_dT_s) is 10^{-2} where f_d is the maximum Doppler frequency and T_s is the OFDM symbol duration including the GI. From the Figure, it can be seen that the NMSE performance for the Conv.ML-CE method is degraded when increasing

the number of transmit antennas. The proposed TD-CE method shows higher estimation accuracy regardless of the number of transmit antennas than that for the Conv.ML-CE method.

Figure 4.6 shows the BER performances when changing C/N at $f_dT_s=10^{-2}$ for the Conv.ML-CE and proposed TD-CE methods at the non-Nyquist rate. From the Figure, it can be seen that both 4×4 and 8×8 MIMO-OFDM systems with the proposed TD-CE method shows better BER performance than those for the Conv.ML-CE method especially when the number of transmit antennas is 8. The degradation of BER performance for the Conv.ML-CE method as compared with the proposed TD-CE method is come from the degradation of channel estimation accuracy as shown in Figure 4.5.
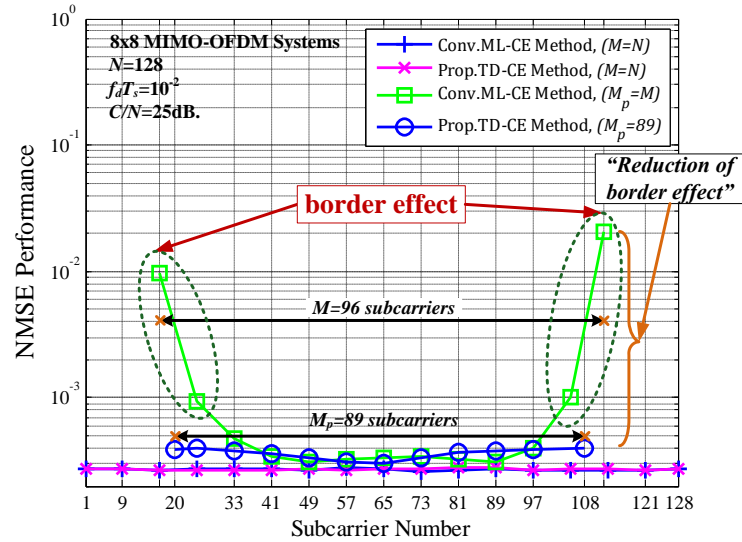
Figure 4.4: CFR estimation accuracy for proposed method at each subcarrier.
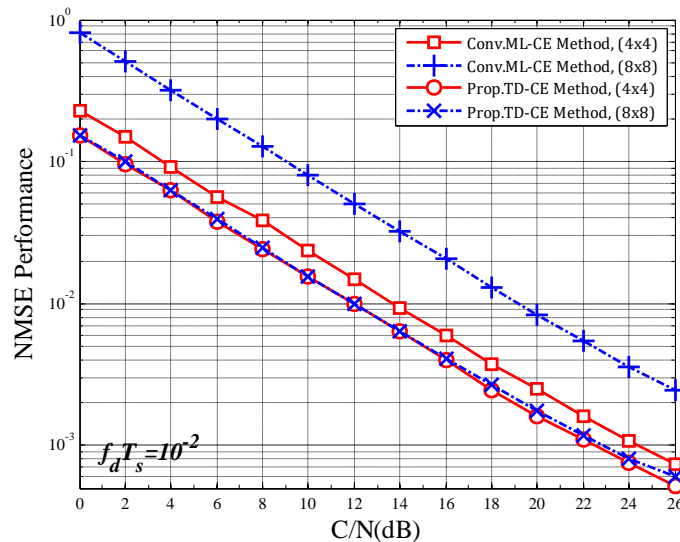
Figure 4.5: CFR estimation accuracy for proposed method vs. C/N(dB).
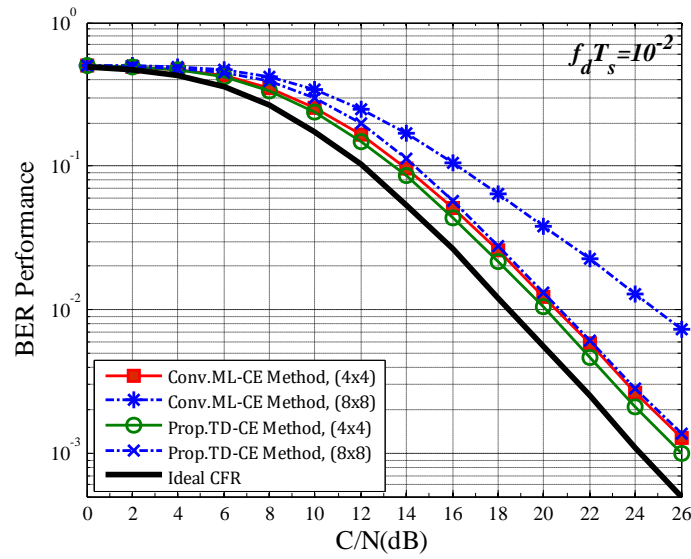
Figure 4.6: BER performance for proposed method vs. C/N(dB) at $f_d T_s = 10^{-2}$.

Table 4.2: Comparison of computational complexity for channel estimation methods.

Channel Estimation Methods	Computational complexity required in one channel estimation (N_T=8)	
Conventional ML-CE	$N \cdot log_2 N + P + P^2 + M \cdot Ng$	2,108
Proposed TD-CE ($M_P = M - N_T + 1$)	$N \cdot Ng + M_P \cdot Ng$	2,387

Table 4.2 shows the comparison of computation complexity required in one CFR estimation for the proposed and conventional methods when $(N_T \times N_R) = 8 \times 8$. From Table 4.2, it can be observed that the computation complexity for the proposed TD-CE method is slightly larger than the Conv.ML-CE methods. From Table 4.2 and Figures 4.5 and 4.6, it can be concluded that the proposed TD-CE method can achieve higher estimation accuracy and accordingly better BER performance than the conventional ML-CE methods with keeping almost the same computational complexity.

4.5   Conclusions

This chapter proposed the time domain channel estimation (TD-CE) method for the MIMO-OFDM systems. The salient feature of proposed TD-CE method is to employ the scattered pilot preamble symbol in which pilot subcarriers sent from each transmit antenna are assigned cyclically including the both ends of transmission frequency band for data subcarriers. In the proposed method, the channel frequency responses for all links between transmit and receive antennas are estimated over the frequency band between the first to the end pilot subcarriers assigned for each transmit antenna. The same frequency band assigned for pilot subcarriers in each transmit antenna is also used in the transmission of data information. From the computer simulation results, it was confirmed that the MIMO-OFDM systems with the proposed TD-CE method can achieve higher throughput performance in higher time-varying fading channel with keeping almost the same computational complexity as comparing with the conventional methods even when the non-Nyquist rate and the larger number of transmit antennas.

CHAPTER 5

TIME DOMAIN CHANNEL ESTIMATION METHOD FOR UPLINK OFDMA SYSTEM

OFDMA technique is considered as one of promising wireless access techniques which can accommodate multiple users flexibly and efficiently. In the uplink OFDMA system, since all users transmit their information data symbols to the base station (BS) simultaneously, it is required to estimate all user's channel frequency responses all together at the BS before receiving the information data symbols. The estimation of multiple users' channels in the uplink OFDMA system is similar to that the estimation of multiple channels between the transmit antenna and the receive antenna in the MIMO-OFDM system. From computer simulation results, this chapter also demonstrates the effectiveness of above proposed ML based TD-CE method when employing in the uplink OFDMA system.

5.1   Introduction

Recently Orthogonal Frequency Division Multiple Access (OFDMA) has been received a lot of attentions in wireless communication systems because of its flexibility in the accommodation of multiple users with keeping higher transmission efficiency and its robustness against the multipath fading [57-58]. In the uplink OFDMA system, since all users transmit their information data symbols to the base station (BS) simultaneously, it is required to estimate all users' channel frequency responses (CFRs) all together at the BS before receiving the information data symbols. The estimated CFR for each user is used in the frequency domain equalization to compensate the amplitude and phase distortions caused by the multipath fading.

To solve the above problem, many papers have proposed the channel estimation method for uplink OFDMA system including the Discrete Fourier Transform interpolation based channel estimation (DFTI-CE) method [59-62]. In the DFTI-CE method, all users transmit one scattered pilot (SP) symbol at the same time to the BS before the transmission of data symbols [62]. The deployment of pilot subcarriers in the SP-symbol is different for each user to avoid the collision of pilot subcarriers in the superimposed received SP-symbol sent from all users. The DFTI-CE method can achieve higher estimation accuracy for the CFR only when the number of FFT points (N) is equal to the number of data subcarriers (M) which corresponds to the Nyquist rate [61]. However the estimation accuracy for the DFTI-CE method would be degraded relatively in the real OFDM system. Because null subcarriers (zero padding) are added at both ends of OFDM allocated bandwidth to reject the aliasing occurring at the output of digital to analogue (D/A) converter of which sampling is the non-Nyquist rate. When the sampling is the non-Nyquist rate, the transmitted time domain signal with N samples is affected by channel impulse response (CIR) which corresponds to the bandwidth with N subcarriers including the zero padding. However the CIR is estimated at the BS by using the scattered pilot subcarriers inserted within the OFDM allocated bandwidth with M subcarriers. From this fact, the estimation accuracy for the DFTI-CE method would be degraded especially at around the both ends of data subcarriers which are the borders between the data and null subcarriers. This phenomenon is called the border effect [55].

To solve the above problem, this chapter proposes a time domain channel estimation (TD-CE) method for the uplink OFDMA system. The salient feature of proposed TD-CE method is to enable higher estimation accuracy for all users' CIRs by using the received time domain SP-symbol even at the non-Nyquist rate.

This chapter is organized as follows. Section 5.2 presents the system model for the uplink OFDMA system and Section 5.3 proposes the TD-CE method which can solve the problem on the conventional DFTI-CE method. Section 5.4 presents various computer simulation results in the time-varying fading channels to verify the effectiveness of proposed TD-CE method as comparing with the conventional DFTI-CE method and Section 5.5 draws some conclusions.

5.2 System Model

Figure 5.1 shows a block diagram of uplink OFDMA system to be considered in this chapter. The information data input is modulated at the pre-assigned data subcarriers for each user. All data subcarriers within one OFDM symbol are shared by all users in the uplink. Then null subcarriers are added over the whole subcarriers except the pre-assigned data subcarriers and converted into the time domain signal by IFFT. The time domain signal after adding the guard interval (GI) is sent to the Base Station (BS) from each user terminal at the same time.

At the BS, the superimposed received signal sent from all users is converted into the frequency domain by FFT after removing the GI. The information data can be demodulated at the pre-assigned data subcarriers for each user. Before the demodulation of received signal sent from each user, the received signal must be equalized in the frequency domain by using the estimated CFR to compensate the fading distortions suffered in each user link. From this fact, the CFR for all users' links are required to be estimated all together before receiving the data information. The details of channel estimation methods both for the conventional and proposed methods are presented in the next section.
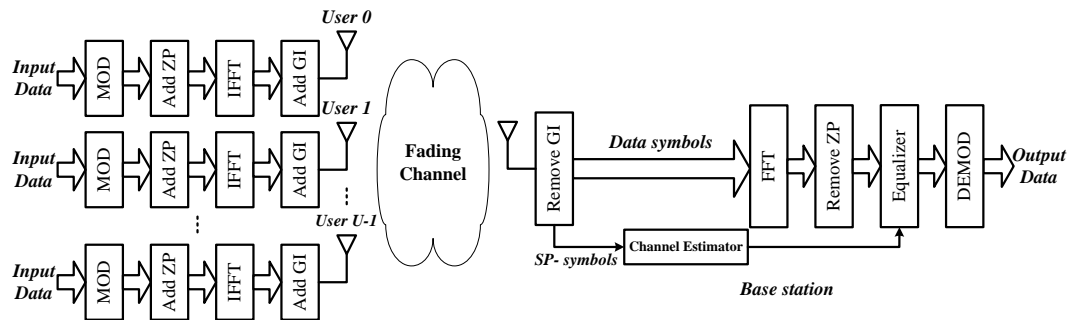
Figure 5.1: Block diagram of transceiver for uplink OFDMA system.

5.3   Channel Estimation Method

5.3.1   Channel Estimation by Using Scattered Pilot Symbol

In the uplink OFDMA system, the scattered pilot (SP) symbol is usually employed for the estimation of CFR in which scattered pilot subcarriers are uniquely assigned for each user. In the time-varying fading channel, the SP-symbol will be inserted with a certain interval of data symbols in the time axis. The CFRs for data symbols between the SP-symbol in the time axis can be estimated by using the cubic spline interpolation method.
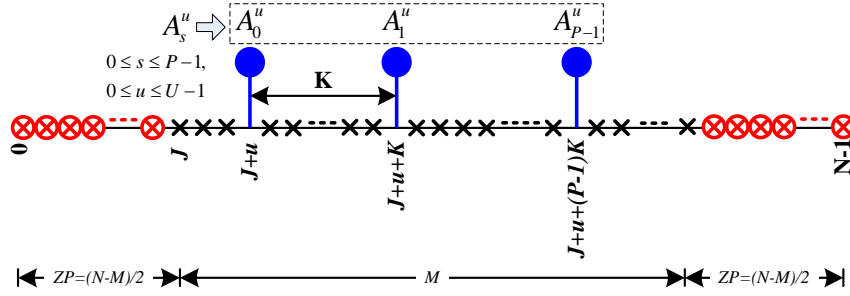
Figure 5.2: Assignment of scattered pilot symbol for user-u.

    Figure 5.2 shows an example of SP assignment in the pilot symbol for the user-u ($0 \leq u \leq U-1$). In the Figure, N is the number of FFT points, M is the number of data subcarriers shared by all users U and (N-M) represents the total number of null subcarriers (zero padding). The half of the null subcarriers (N-M)/2 are inserted at both ends of M data subcarriers. Each user can use $P(=M/K)$ pilot subcarriers within M subcarriers which are inserted periodically with an interval of K subcarriers. Here, J represents the first data subcarrier number within N subcarriers including zero padding. The pilot subcarriers for the user-u are inserted from $J+u$ to $J+u+(P$-$1)K$ with the interval of K subcarriers as shown in Figure 5.2. When the pilot subcarriers for each user are inserted at every K subcarriers, the CFRs for K different users ($=U$) can be estimated independently in the uplink OFDMA system.

    The SP-symbol b_k^u ($0 \leq k \leq N$-1) in the time domain for the user-u can be given by,

$$b_k^u = \frac{1}{\sqrt{N}} \cdot \sum_{s=0}^{P-1} A_s^u \cdot e^{j\frac{2\pi k}{N}(J+u+sK)}, \quad (0 \leq k \leq N-1) \tag{5.1}$$

where A_s^u is the s-th pilot data for the user-u at the subcarrier number of ($J+u+sK$) within N subcarriers. The time domain received signal r_k after removing the GI at the BS, which is superimposed over all user SP-symbol, can be given by,

$$r_k = \sum_{u=0}^{U-1} \left\{ b_k^u \otimes h_k^u \right\} + z_k = \sum_{u=0}^{U-1} \sum_{l_u=0}^{NP-1} \left\{ \rho_{l_u}^u \cdot b_{k-l_u}^u \right\} + z_k \tag{5.2}$$

where h_k^u is the time domain channel impulse response (CIR) occurred in the user-u channel and z_k is the additive white Gaussian noise (AWGN) at the BS. The CIR h_k^u is given by,

$$h_k^u = \sum_{l_u=0}^{NP-1} \rho_{l_u}^u \cdot \delta(k - l_u) \tag{5.3}$$

where NP is the number of CIRs (delay paths) and $\rho_{l_u}^u$ represents the complex amplitude of CIR for the l_u-th delay path occurred in the user-u channel. By performing FFT to (5.2), the frequency domain received signal, which is the summation of all user SP-symbol, is given by,

$$R_m = \frac{1}{\sqrt{N}} \sum_{k=0}^{N-1} r_k \cdot e^{-j\frac{2\pi mk}{N}}, \quad (0 \leq m \leq N-1) \tag{5.4}$$

From (5.4), the frequency domain signal at the pre-assigned pilot subcarriers for the user-u is given by,

$$R^u_{J+u+sK} = A^u_s \cdot \underbrace{\sum_{l_u=0}^{NP-1} \rho^u_{l_u} \cdot e^{-j\frac{2\pi l_u}{N}(J+u+sK)}}_{H^u_{J+u+sK}} + Z_{J+u+sK} \quad = A^u_s \cdot H^u_{J+u+sK} + Z_{J+u+sK}, \quad (0 \le s \le P-1) \tag{5.5}$$

where Z_{J+u+sK} and H^u_{J+u+sK} are the AWGN and the CFR both at the $(J+u+sK)$-th subcarrier. Since all pilot data A^u_s ($0 \le s \le P$-1) for the user-u are known at the receiver, the CFR at the pilot subcarriers inserted at every K subcarriers can be estimated by,

$$\hat{H}^u_{J+u+sK} = \frac{R^u_{J+u+sK}}{A^u_s} = H^u_{J+u+sK} + \frac{Z_{J+u+sK}}{A^u_s}, (0 \le s \le P-1) \tag{5.6}$$

By using the estimated CFR at the pilot subcarriers, the CFR over M data subcarriers can be estimated by using the DFT interpolation method.

5.3.2 Conventional DFT Interpolation based-Channel Estimation Method

The conventional DFT interpolation based channel estimation (DFTI-CE) method has been proposed in [62] which enables the estimation of all user CFRs in the uplink OFDMA system by using one SP-symbol. The time domain CIR $\hat{g}^u_q$ at the q-th time sampling point for the user-u can be obtained by performing IDFT to the estimated CFR at the pilot subcarriers in (5.6) which is given by,

$$\hat{g}^u_q = \frac{1}{\sqrt{P}} \sum_{s=0}^{P-1} \hat{H}^u_{J+u+sK} \cdot e^{j\frac{2\pi sq}{P}} = g^u_q + w^u_q, \quad (0 \le q \le P-1) \tag{5.7}$$

where w^u_q is the noise component at the q-th time sampling point and g^u_q is the ideal CIR obtained from the ideal CFR H^u_{J+u+sK} given in (5.6). By using (5.5), g^u_q can be given by,

$$g^u_q = \frac{1}{\sqrt{P}} \sum_{l_u=0}^{NP-1} \rho^u_{l_u} \cdot e^{-j\frac{2\pi l_u}{N}(J+u)} \cdot \sum_{s=0}^{P-1} e^{-j\frac{2\pi s}{P}(\frac{PK}{N}l_u-q)} \tag{5.8}$$

When N is equal to $PK(=M)$ which corresponds to the Nyquist rate ($N=M$), the second summation of (5.8) can be given by [63],

$$\sum_{s=0}^{P-1} e^{-j\frac{2\pi s}{P}(\frac{PK}{N}l_u-q)} = \sum_{s=0}^{P-1} e^{-j\frac{2\pi s}{P}(l_u-q)} = \begin{cases} P, & l_u = q \\ 0, & l_u \ne q \end{cases} \tag{5.9}$$

By using (5.9), the ideal CIR g^u_q in (5.8) can be given by,

$$\sum_{s=0}^{P-1} e^{-j\frac{2\pi s}{P}(\frac{PK_f}{N}q(i,j)-u)} = \frac{1 - e^{-j2\pi(\frac{PK_f}{N}q(i,j)-u)}}{1 - e^{-j\frac{2\pi}{P}(\frac{PK_f}{N}q(i,j)-u)}} \tag{5.10}$$

From (5.10), it can be seen that the ideal CIR g^u_q exists only at the sampling points from $q=0$ to NP-1 while the noise component exists over all sampling points. Since the number of delay paths NP occurred in the actual channel is unknown at the receiver, the length of GI (N_g) is taken by longer than NP to avoid the inter-symbol interference (ISI). From this fact, the noise components from $q=N_g$ to P-1 can be reduced from the estimated CIR in (5.7). The CFRs over M data subcarriers can be obtained by performing the DFT interpolation to $\hat{g}^u_q$ with the values of CIR from $q=0$ to N_g-1 in (5.7) and adding zeros from $q=N_g$ to M-1 which is given by,

$$\hat{H}^u_{J+n} = \sum_{q=0}^{N_g-1} \hat{g}^u_q \cdot e^{-j\frac{2\pi q}{N}(J+n)}, \quad (0 \le n \le M-1) \tag{5.11}$$

From (5.7) to (5.11), it can be concluded that the conventional DFTI-CE method can achieve higher estimation accuracy of CIR when the transmitted time domain signal is sampled at the Nyquist rate. However the estimation accuracy for the DFTI-CE method in the real OFDM system would be degraded relatively because the null subcarriers are added at the

both ends of data subcarriers which correspond to the non-Nyquist rate. When N is not equal to M, the second summation of (5.8) is represented by,

$$\sum_{s=0}^{P-1} e^{-j\frac{2\pi s}{P}(\frac{PK}{N}l_u-q)} = \frac{1-e^{-j2\pi(\frac{PK}{N}l_u-q)}}{1-e^{-j\frac{2\pi}{P}(\frac{PK}{N}l_u-q)}}, \ 0 \leq q \leq P-1 \tag{5.12}$$

From (5.12), it can be seen that the CIR exists at all sampling points from $q=0$ to $P-1$ which is completely different from (5.9) at the Nyquist rate. From this fact, it is impossible to reduce the noise component and consequently it is very hard to use the DFT interpolation method. This is the reason that the transmitted time domain signal with N samples is affected by the channel impulse responses which corresponds to the N subcarriers bandwidth including the zero padding in the frequency domain. However the CIR is estimated by using the pilot subcarriers inserted only within the OFDM allocated bandwidth (M subcarriers). From this fact, the CFR estimated by the DFT interpolation method, in which (M-P) zeros will be added at the center of estimated CIR in (5.12), has the larger estimation error especially at the both ends of data subcarriers which is called the border effect. This phenomenon leads the fatal degradation of bit error rate (BER) performance.

5.3.3 Proposal of Time Domain Channel Estimation Method

As mentioned above, the conventional DFTI-CE method has a serious problem when the transmitted time domain signal is sampled at the non-Nyquist rate. Because the transmitted time domain signal is up-sampled from M to N and its up-sampled signal is affected by the CIR in the fading channel. However the CIR is estimated by using the down-sampled signal at the receiver. This mismatching of sampling rate at the non-Nyquist rate leads the fatal degradation of CIR estimation accuracy in the conventional DFTI-CE method. To solve this problem, this chapter proposes the time domain channel estimation (TD-CE) method which can achieve higher estimation accuracy even at the non-Nyquist rate. The feature of proposed method is to employ the up-sampled time domain received SP-symbol in the estimation of CIR for each user. In the proposed TD-CE method, each user transmits SP-symbol as shown in Figure 5.2 which is the same as the conventional DFTI-CE method. By considering the received signal for each user separately, the time domain received SP-symbol r_k given in (5.2) can be rewritten by,

$$r_k = \underbrace{\sum_{l_0=0}^{Ng-1} \left\{\rho_{l_0}^0 \cdot b_{k-l_0}^0\right\}}_{User\,0\,to\,BS\,link} + \cdots + \underbrace{\sum_{l_{U-1}=0}^{Ng-1} \left\{\rho_{l_{U-1}}^{U-1} \cdot b_{k-l_{U-1}}^{U-1}\right\}}_{User\,U-1\,to\,BS\,link} + z_k, \ \left(0 \leq k \leq N-1\right) \tag{5.13}$$

In (5.13), the GI-length (Ng) is used instead of NP in (5.2) because the actual number of delay paths (NP) occurred in each user channel is unknown at the receiver and Ng is taken by longer than the NP to avoid the ISI. By using the matrix multiplication, (5.13) can be rewritten by,

$$\mathbf{r} = \underbrace{\mathbf{b}_0\boldsymbol{\rho}_0}_{User\,0\,to\,BS\,link} + \underbrace{\mathbf{b}_1\boldsymbol{\rho}_1}_{User\,1\,to\,BS\,link} + \ldots + \underbrace{\mathbf{b}_{U-1}\boldsymbol{\rho}_{U-1}}_{User\,U-1\,to\,BS\,link} + \mathbf{z} \tag{5.14}$$

where $\mathbf{r}$ is $[r_0 r_1 \cdots r_{N-1}]^T$ with the size of [$N\times1$], $\mathbf{b}_u$ and $\boldsymbol{\rho}_u$ are the matrix of b_k^u in (5.1) with the size of [$N\times Ng$] and the matrix of CIR h_k^u with the size of [$Ng\times1$] which can be given by,

$$\mathbf{b}_u = \begin{bmatrix} b_0^u & b_{-1}^u & b_{-2}^u & \cdots & b_{1-Ng}^u \\ b_1^u & b_0^u & b_{-1}^u & \cdots & b_{2-Ng}^u \\ b_2^u & b_1^u & b_0^u & \cdots & b_{3-Ng}^u \\ \vdots & \vdots & \vdots & \ddots & \vdots \\ b_N^u & b_{N-1}^u & b_{N-2}^u & \cdots & b_{N-Ng}^u \end{bmatrix} \text{ and } \boldsymbol{\rho}_u = \begin{bmatrix} \rho_0^u \\ \rho_1^u \\ \rho_2^u \\ \vdots \\ \rho_{Ng-1}^u \end{bmatrix} \tag{5.15}$$

From (5.14), it can be rewritten in a matrix form,

5.3 Channel Estimation Method

$$\mathbf{r} = \underbrace{\begin{bmatrix} \mathbf{b}_0 & \mathbf{b}_1 & \cdots & \mathbf{b}_{U-1} \end{bmatrix}}_{\mathbf{B}} \cdot \underbrace{\begin{bmatrix} \boldsymbol{\rho}_0 & \boldsymbol{\rho}_1 & \cdots & \boldsymbol{\rho}_{U-1} \end{bmatrix}^T}_{\mathbf{G}} + \mathbf{z} = \mathbf{B} \cdot \mathbf{G} + \mathbf{z} \tag{5.16}$$

where $\mathbf{B}$ and $\mathbf{G}$ denote the matrix of time domain SP-symbol $\mathbf{b}_u$ for all users with the size of $[N \times UNg]$ and the matrix of CIR $\boldsymbol{\rho}_u$ for all users with the size of $[UNg \times 1]$. $\mathbf{z}$ represents the matrix of noise component with the size of $[N \times 1]$. From (5.16), the CIR $\mathbf{G}$ can be estimated by the following equation,

$$\hat{\mathbf{G}} = \mathbf{B}^\dagger \cdot \mathbf{r} = \mathbf{G} + \mathbf{B}^\dagger \cdot \mathbf{z} \tag{5.17}$$

where $\mathbf{B}^\dagger$ denotes the Moore-Penrose pseudo inverse matrix of $\mathbf{B}$ [64]. By using (5.17), all users' CIRs can be estimated all together at the BS. Then the CFR for each user can be obtained by performing FFT to (5.17). Here, it should be noted that since the data patterns of SP-symbol for all users in the time domain are known at the receiver, the Moore-Penrose pseudo inverse matrix $\mathbf{B}^\dagger$ can be calculated in advance at the receiver. From this fact, the computational complexity for the estimation of CIR in the proposed TD-CE method can be reduced relatively.

In the time-varying fading channel, each user transmits the SP-symbol periodically in the time axis with an interval of I_t symbol. The interval of I_t will be decided according to the maximum Doppler frequency spread among all user links. At the BS, the CIR for each user is estimated at the SP-symbol with the interval of I_t symbol. By using these estimated CIRs, the CIR at data symbols between the SP-symbol over one frame can be estimated by using the cubic spline interpolation method. By using the estimated CFR in the frequency domain equalization, the data symbols for each user can be demodulated with higher signal quality even in higher time-varying fading channel.

5.4   Performance Evaluations

In this section, various computer simulations in the time-varying fading channels are conducted to verify the effectiveness of proposed TD-CE method as comparing with the conventional DFTI-CE method. Table 5.1 shows the list of parameters used in the following performance evaluations.

Table 5.1: Simulation parameters.

Information	Parameter
Modulation for data subcarriers	16QAM
Modulation for pilot subcarriers	QPSK
Demodulation	Coherent
Number of FFT-points (N)	256
Number of subcarriers (M)	192
Length of guard interval (Ng)	16
Number of active users (U)	8
Interval of pilot subcarriers (K)	8($K=U$)
Interval of pilot symbols (I_t)	4
OFDM occupied bandwidth (BW)	5 MHz
Radio frequency (f_c)	2 GHz
Multipath Rayleigh fading channel model	
- Delay profile	Exponential
- Decay constant	-1dB
- Number of delay paths (N_P) in all links	14
- Number of scattered rays	20
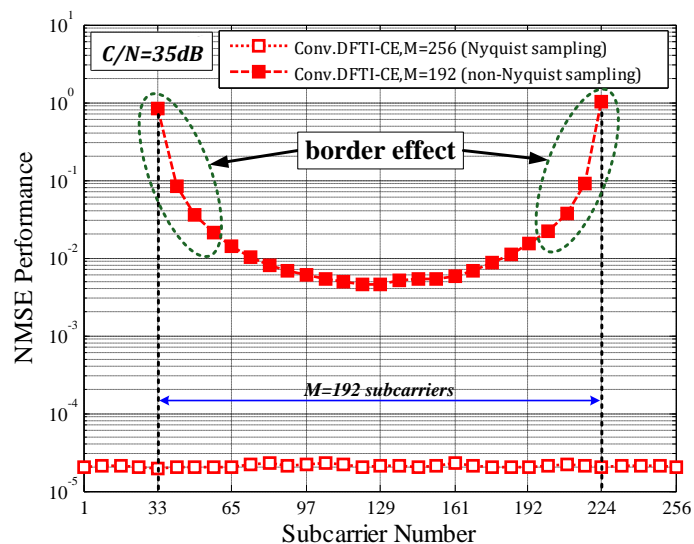
Figure 5.3: CFR estimation accuracy for conventional DFTI-CE method.

Figure 5.3 shows the estimation accuracy at each data subcarrier for the conventional DFTI-CE method when changing the number of zero padding. The estimation accuracy is evaluated by the normalized mean square error (NMSE) at each subcarrier. From the Figure, it can be seen that the conventional DFTI-CE method can achieve higher estimation accuracy over all subcarriers without the occurrence of border effect at the Nyquist rate ($N=M=256$). When the transmission of time domain signal is sampled at the non-Nyquist rate ($N=256$, $M=192$), the estimation accuracy for the DFTI-CE method is much worse over M subcarriers

as compared with that for the Nyquist rate and the border effect is occurred at around the both ends of data subcarriers.

Figure 5.4 shows the normalized mean square error (NMSE) performance of estimated CFR at each subcarrier for the conventional DFTI-CE and proposed TD-CE methods at the Nyquist rate ($N=M$) and non-Nyquist rate ($N\neq M$). From the Figure, it can be seen that there is no border effect in the NMSE performances both for the conventional and proposed methods at the Nyquist rate. On the contrary, although there is the border effect for both methods at around the both ends of data subcarriers, the proposed TD-CE method can achieve much higher estimation accuracy than the conventional DFTI-CE method when the sampling is the non-Nyquist rate.
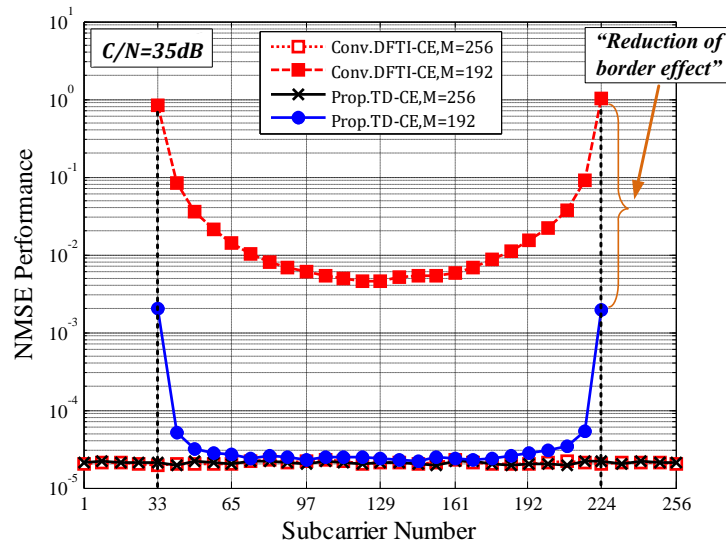
Figure 5.4: CFR estimation accuracy for proposed method at non-Nyquist rate.
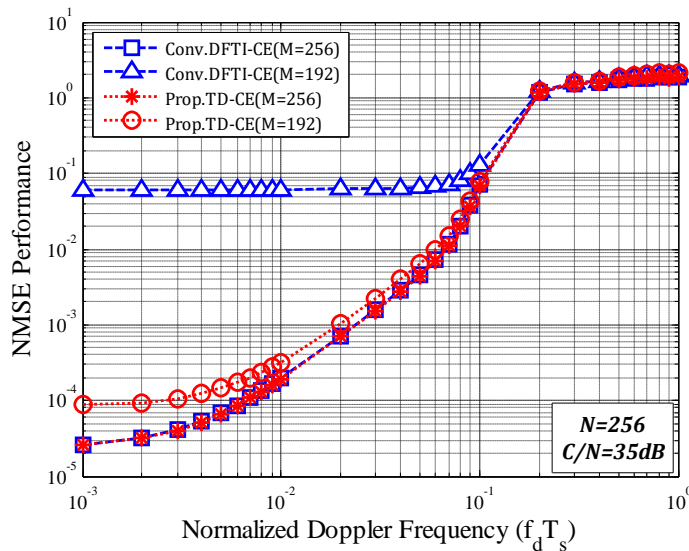
Figure 5.5: CFR estimation accuracy for proposed method vs. $f_d T_s$.

Figure 5.5 shows the CFR estimation accuracy for the conventional DFTI-CE and proposed TD-CE methods at the Nyquist and non-Nyquist rates when changing the normalized Doppler frequency ($f_d T_s$). Here f_d is the maximum Doppler frequency and T_s is the OFDM symbol time duration including the GI. From the Figure, it can be seen that both methods show almost the same higher estimation accuracy when the sampling rate is the Nyquist rate. When the sampling is the non-Nyquist rate, the proposed method shows much higher estimation accuracy than the conventional method, especially when $f_d T_s < 10^{-2}$. From the

5.4 Performance Evaluations
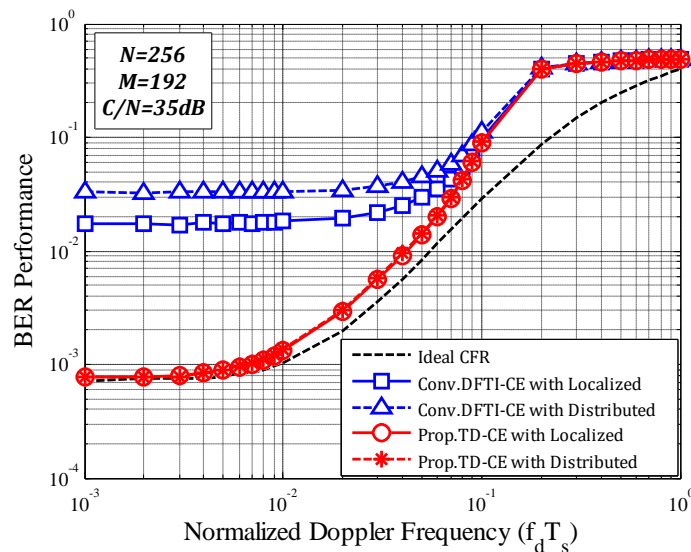
Figure 5.6: BER performance for proposed method vs. $f_d T_s$.

Figure, it can be concluded that the proposed TD-CE method can achieve higher estimation accuracy even at the non-Nyquist rate and in higher time-varying fading channel.

Figure 5.6 shows the BER performance of data symbols at the non-Nyquist rate for the uplink OFDMA system with the conventional DFTI-CE and proposed TD-CE methods when changing $f_d T_s$. In the Figure, the BER performance of using the ideal CFR is also shown as for the purpose of comparing with the proposed method. As for the data transmission in the uplink OFDMA system, the BER performances are evaluated by two assignment methods for the data subcarriers that are the Localized and Distributed methods [18]. In the Localized and Distributed data subcarrier assignment methods, each user employs a set of M/U consecutive subcarriers and M/U scattered data subcarriers with the interval of U subcarrier, respectively. The BER performance with the Localized and Distributed methods are evaluated by taking the average of BER performances for all users (U=8). From Figure 5.6, it can be observed that the proposed TD-CE method can achieve better BER performance both for the Localized and Distributed methods than the conventional DFTI-CE method when $f_d T_s$ is up to 8×10^{-2}. The BER performance of using the proposed method is very close to that of using the ideal CFR when $f_d T_s$ is lower than 5×10^{-2}.
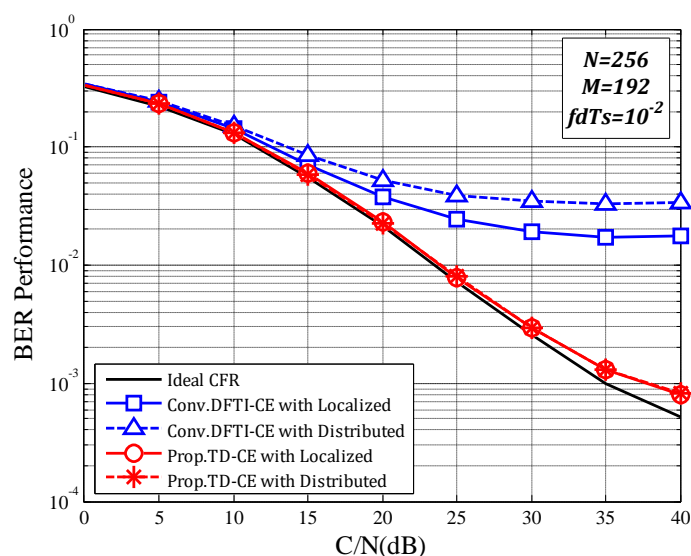
Figure 5.7: BER performance for proposed method vs. C/N(dB).

Figure 5.7 shows the BER performances of using the conventional DFTI-CE and proposed TD-CE methods at the non-Nyquist rate when changing the carrier to noise power ratio (C/N) at $f_dT_s=10^{-2}$ (corresponding to 132km/h). From the Figure, it can be seen that the proposed TD-CE method can achieve much better BER performance than the conventional DFTI-CE method and achieve almost the same BER performance as that for using the ideal CFR.

The computational complexity required in the estimation of CFR for one user when using the conventional DFTI-CE and proposed TD-CE methods can be given by,

$$L_{CONV} = N \cdot \log_2 N + P + P^2 + M \cdot P \tag{5.18}$$

$$L_{PROP} = N_g \cdot N + M \cdot N_g \tag{5.19}$$

The computational complexity for the conventional method in (5.18) includes one N point FFT, P time division, P point IDFT and M point DFT for P point non-zero values of CIR. The complexity for the proposed method given in (5.19) includes the matrix multiplication of $[N_g{\times}N]$ with $[N{\times}1]$ and one M point DFT for Ng points non-zero values of CIR. By substituting the parameters listed in Table 5.1 to (5.18) and (5.19), the computational complexity for the conventional and proposed methods can be calculated by 7,256 and 7,168, respectively.

From the computational complexity and the estimation accuracy for the conventional DFTI-CE and proposed TD-CE methods, it can be concluded that the proposed TD-CE method can achieve much higher estimation accuracy than the conventional DFTI-CE method with keeping almost the same computational complexity at the non-Nyquist rate.

5.5   Conclusions

This chapter proposed the time domain channel estimation (TD-CE) method for the uplink OFDMA system by using the scattered pilot symbols sent from all users. The salient features of proposed TD-CE method are to estimate the CIR by using the received time domain scattered pilot symbol and to enable the estimation of all user CIRs with higher accuracy even at the non-Nyquist rate. From the various computer simulation results at the non-Nyquist rate, this chapter concluded that the proposed TD-CE method can achieve higher estimation accuracy with keeping almost the same computational complexity as compared with the conventional DFTI-CE method in higher time-varying fading channel.

CHAPTER 6

PROPOSAL OF CHANNEL ESTIMATION METHOD FOR BI-DIRECTIONAL OFDM BASED ANC IN HIGHER TIME-VARYING FADING CHANNEL

Broadband ANC of using the OFDM technique has been widely investigated to increase the capacity of two-way relay communication. In the two-way relay communication, it can be simply modeled by two user terminals (UTs) and one relay station (RS) in which each UT sends his information data to the other UT through the RS by using two timeslots. Each UT can demodulate the other user's information data by removing its self-information data with frequency domain equalization (FDE). To conduct the removal of self-information data and the FDE precisely, it is the essential to realize the accurate channel estimation method for the combined CFR in the 1st and 2nd timeslots from the superimposed received signal sent from both UTs at each UT. To solve this problem, this chapter proposes the ML based combined CFR estimation method for two-way relay communication system by using a novel scattered pilot assignment method including the null subcarriers to avoid the collision of pilot subcarriers sent from both UTs. From the various computer simulation results, this chapter demonstrates the effectiveness of proposed ML based combined CFR estimation method which can achieve higher estimation accuracy and better BER performance even in higher time-varying fading channel.

6.1   Introduction

Recently demands for broadband wireless services are rapidly increasing for providing multimedia services such as multicasting, video on demand, video conference, mobile internet services etc. to wireless users located in the wider coverage area. To provide these multimedia services, it is essential to achieve higher channel network capacity and higher transmission efficiency with keeping higher signal quality in the wireless communications. Broadband analog network coding (ANC) [65-66] based on Orthogonal Frequency Division Multiplexing (OFDM) technique has been proposed as one of promising techniques to satisfy the above demands. The broadband ANC has a potential capability to increase the channel capacity and transmission efficiency by using bi-directional relay communications. In the bi-directional relay communications with ANC which is simply modeled by two user terminals (UTs) and one relay station (RS). In the ANC system, each UT can send his information data to the other UT through RS by using two timeslots.

In the bi-directional relay communications with OFDM based ANC, the accurate estimation of channel frequency response (CFR) in the multipath fading channels is required to remove the self-information data from the superimposed received signal and to demodulate the other user's information data with the frequency domain equalization. In the estimation of CFR for the bi-directional relay communications with OFDM based ANC, it is difficult to estimate the CFRs between the UT_1 to RS and UT_2 to RS separately because the received signal at the RS is the superimposed signal sent from both UTs and each signal passed through the different channel having the different CFR. Up to today, many channel estimation methods have been proposed for the OFDM based ANC. These estimation methods can be categorized into two groups. The first group [67-68] is to employ a preamble symbol with Zadoff-Chu code and the second group [69-70] is to employ the scattered pilot subcarriers with Walsh code in the estimation of CFR. Both groups enable the estimation of the CFRs for two channels separately by using the Zadoff Chu code and the Walsh code which are both orthogonal codes. Among these methods, [67] and [69] are required to estimate two channels of CFRs between UTs and RS at the RS and to feedback their estimated CFR to both UTs by using a separate channel. This feedback information is used at each UT in the removing of self-information data from the received signal. The requirement of feedback information from the RS leads the increasing of complexity for the RS transceiver and the decreasing of transmission efficiency. To solve the above problem, [68] and [70] proposed the CFR estimation method in which each UT can estimate the combined CFR for the channels between the UTs and RS without the feedback information from the RS. Although [68] and [70] can estimate the combined CFR without the feedback information, the CFR estimation accuracy would be degraded relatively in the higher time-varying fading channels.

As for the CFR estimation method employing Zadoff-Chu code proposed in [68], the CFR estimated at the preamble symbol is used in the demodulation of following all data symbols. From this fact, the BER performance would be degraded especially when the frame length is longer. Because the CFR at the last part of data symbols in a frame is much different from the CFR estimated at the preamble symbol. This means that the number of data symbols followed by the preamble symbol must be taken fewer which leads the degradation of transmission efficiency. As for the CFR estimation method employing Walsh code proposed in [70], the estimated CFR is obtained by taking the averaged value between the interval of pilot subcarriers with Walsh code. From this fact, the proposed estimation methods can achieve the higher estimation accuracy only when the changing of CFR between two pilot subcarriers has the linear or static characteristics. However these assumptions are unrealistic in the actual time-varying fading channels.

To solve the problems in the conventional methods as mentioned above, this chapter proposes a channel estimation method for the bi-directional OFDM based broadband ANC by using the scattered pilot subcarriers inserted both in the frequency and time axes. The salient

features of proposed CFR estimation method are to enable the accurate estimation of combined CFR for both channels between the UTs and RS at each UT by using scattered pilot subcarriers including the null subcarriers and to enable the demodulation of information data without feedback information from the RS even in higher time-varying fading channels.

This chapter is organized as follows. Section 6.2 shows the network model and Section 6.3 proposes a channel estimation method by using the scattered pilot subcarriers. Section 6.4 presents the various computer simulation results to verify the effectiveness of the proposed method as comparing with the conventional methods and Section 6.5 draws some conclusions.

6.2   Network Model

Figure 6.1 shows the network model to be considered in this chapter which can provide two timeslots bi-directional communications with ANC between the user terminals UT_1 and UT_2 through the relay station (RS) with amplifying and forwarding [71]. In the 1st timeslot, both user terminals UT_1 and UT_2 transmit their information data $A_1(m,n)$ and $A_2(m,n)$ at n-th subcarrier of m-th symbol to RS simultaneously. The superimposed received signal at RS in the frequency domain can be expressed by,

$$R(m,n) = A_1(m,n) \cdot H_{1R}(m,n) + A_2(m,n) \cdot H_{2R}(m,n) + Z_{RS}(m,n) \tag{6.1}$$

where $R(m,n)$ represents the superimposed received signal sent from both UTs, $H_{1R}(m,n)$ and $H_{2R}(m,n)$ are the CFR between UT_1 to RS and UT_2 to RS, respectively. $Z_{RS}(m,n)$ is the additive white Gaussian noise (AWGN) added at RS. In the 2nd timeslot, the RS amplifies and forwards $R(m,n)$ to both UTs. The frequency domain received signal at UT_i is given by,

$$R_{Ti}(m,n) = R(m,n) \cdot H_{Ri}(m,n) + Z_{Ti}(m,n) \tag{6.2}$$

where $R_{Ti}(m,n)$ represents the received signals at UT_i and $H_{Ri}(m,n)$ is the CFR between RS to UT_i and $Z_{Ti}(m,n)$ is the AWGN at UT_i. By using (6.1) and (6.2), the received signal at UT_i can be expressed by,

$$R_{Ti}(m,n) = A_i(m,n) \cdot H_{iR}(m,n) \cdot H_{Ri}(m,n) + A_j(m,n) \cdot H_{jR}(m,n) \cdot H_{Ri}(m,n)$$
$$+ \underbrace{Z_{RS}(m,n) \cdot H_{Ri}(m,n) + Z_{Ti}(m,n)}_{Z'_{Ti}(m,n)} \tag{6.3}$$

where $Z'_{Ti}(m,n)$ denotes the composite noise. From (6.3), the UT_i can demodulate the other user's information data by removing the self-information data with the frequency domain equalization which is given by,

$$\hat{A}_j(m,n) = \frac{R_{Ti}(m,n) - A_i(m,n) \cdot H_{iR}(m,n) \cdot H_{Ri}(m,n)}{H_{jR}(m,n) \cdot H_{Ri}(m,n)} \tag{6.4}$$

where $\hat{A}_j(m,n)$ is the demodulated information data sent from UT_j. From (6.4), it can be seen that the combined CFR $H_{iR}(m,n) \cdot H_{Ri}(m,n)$ and $H_{jR}(m,n) \cdot H_{Ri}(m,n)$ are required to estimate at UT_i.

In this chapter, we propose a channel estimation method for the combined CFR given in (6.4) at each UT independently by using the scattered pilot subcarriers including the null subcarriers. The salient features of proposed method are to enable the estimation of combined CFR at each user terminal without feedback information of CFR estimated at the relay station RS and to enable the accurate CFR estimation even in higher time-varying fading channels.
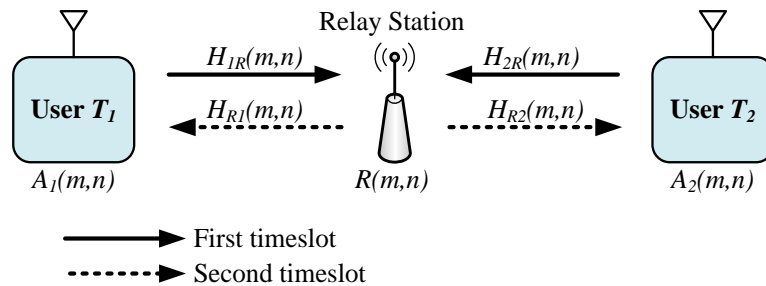
Figure 6.1: Network model of OFDM based ANC.

6.3   Proposed Channel Estimation Method

In this section, we propose a channel estimation method for two timeslots bi-directional communications with OFDM based ANC by using the scattered pilot subcarriers and pilot symbols with pilot subcarriers which are inserted periodically at the certain interval of frequency and time axes, respectively.

6.3.1   Scattered Pilot Subcarriers Assignment
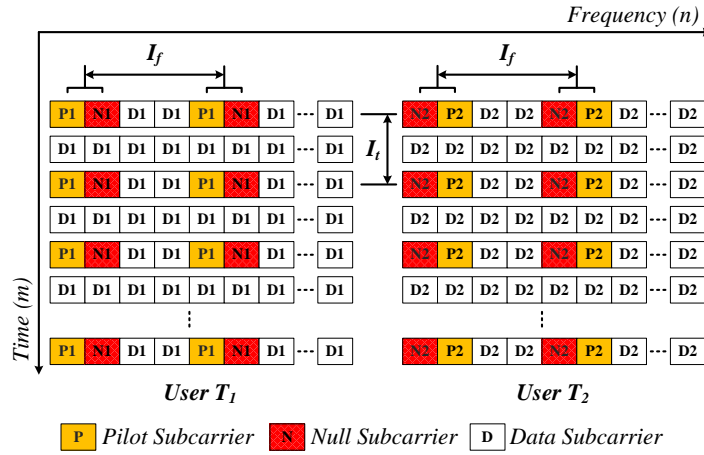
Figure 6.2: Proposed scattered pilot subcarriers assignment method.

Figure 6.2 shows the proposed scattered pilot subcarriers assignment method for the user terminals UT_1 and UT_2. In the proposed pilot subcarriers assignment method, pilot subcarriers and null subcarriers are inserted into the data subcarriers periodically at the interval of I_f in the frequency axis and pilot symbols including data and pilot subcarriers are inserted into data symbols at the interval of I_t in the time axis. In the Figure, $P1$ and $P2$ show the pilot subcarriers for the UT_1 and UT_2 of which data patterns are known at the receiver, $N1$ and $N2$ are the null subcarriers and D_1 and D_2 are the information data for the UT_1 and UT_2, respectively. All these pilot, null and data subcarriers for the UT_1 and UT_2 are transmitted at the predetermined fixed locations of subcarriers and data symbols with the interval of I_t and I_f in the frequency and time axes, respectively. Here the transmission signal $A_i(m,n)$ from UT_i (i=1 or 2) can be given by the following equation,

$$A_i(m,n) = \begin{cases} Pilot \ when \ m = m(s) \ and \ n = n(k_{fi}) \\ Null \ when \ m = m(s) \ and \ n = n(k_{ni}) \\ Data \ when \ m = m(s) \ and \ n \neq n(k_{fi}), n \neq n(k_{ni}) \\ Data \ when \ m \neq m(s) \ and \ n = all \end{cases} \tag{6.5}$$

where $m(s)$, $n(k_{fi})$ and $n(k_{ni})$ represent the locations of pilot symbol in the time axis and the locations of pilot and null subcarriers at UT_i in the frequency axis, all of which locations are given by the following equations,

$$m(s) = (s-1)I_t + 1, \ \ 1 \leq s \leq (L-1)/I_t + 1$$

$$n(k_{fi}) = \begin{cases} (k_{fi}-1)I_f & when \ i = 1 \\ (k_{fi}-1)I_f + 1 & when \ i = 2 \end{cases}, \ \ 1 \leq k_{fi} \leq N/I_f$$

$$n(k_{ni}) = \begin{cases} (k_{fi}-1)I_f + 1 & when \ i = 1 \\ (k_{fi}-1)I_f & when \ i = 2 \end{cases}, \ \ 1 \leq k_{fi} \leq N/I_f \tag{6.6}$$

where N is the number of subcarriers in one OFDM symbol and L is the number of symbols in one frame in which pilot symbols are inserted at both ends of frame to improve the estimation accuracy for the interpolation method in the time axis. From (6.6), it can be seen that the location of null subcarriers for the UT_1 and UT_2 are used as the location of pilot subcarriers for the UT_2 and UT_1, respectively. By using these assignments for the pilot and null subcarriers, it is possible to estimate the CFR independently at the UT_1 and UT_2 without the collision of pilot subcarriers.

6.3.2   Proposed Channel Estimation Method [45][72]

Since the locations of pilot and null subcarriers at the UT_1 and UT_2 which are $A_1(m(s),n(k_{f1}))$ and $A_2(m(s),n(k_{f2}))$, are known at UT_1, the combined CFR at UT_1 can be estimated by the following equations,

$$\hat{H}_{1R,R1}(m(s),n(k_{f1})) = \frac{R_{T1}(m(s),n(k_{f1}))}{A_1(m(s),n(k_{f1}))} = H_{1R}(m(s),n(k_{f1})) \cdot H_{R1}(m(s),n(k_{f1})) - \frac{Z'_{T1}(m(s),n(k_{f1}))}{A_1(m(s),n(k_{f1}))} \quad (6.7)$$

$$\hat{H}_{2R,R1}(m(s),n(k_{f2})) = \frac{R_{T1}(m(s),n(k_{f2}))}{A_2(m(s),n(k_{f2}))} = H_{2R}(m(s),n(k_{f2})) \cdot H_{R1}(m(s),n(k_{f2})) - \frac{Z'_{T2}(m(s),n(k_{f2}))}{A_2(m(s),n(k_{f2}))} \quad (6.8)$$

where $\hat{H}_{1R,R1}(m(s),n(k_{f1}))$ and $\hat{H}_{2R,R1}(m(s),n(k_{f2}))$ represent the combined CFR.

The CFR over all data subcarriers in the frequency axis can be estimated by applying the Maximum Likelihood (ML) method to the estimated CFR at the pilot subcarriers given in (6.7) and (6.8). The combined time domain channel impulse response (CIR) $\hat{\rho}_{1R,R1}^{m(s)}(\ell)$ for $\hat{H}_{1R,R1}(m(s),n)$ at ℓ-th delay path can be estimated by the following equation [72],

$$L_{ML}\left\langle \hat{\rho}_{1R,R1}^{m(s)}(\ell) \right\rangle = \min_{\hat{\rho}_{1R,R1}^{m(s)}(\ell)} \left[\sum_{k_{f1}=1}^{MP} \left| H_{1R,R1}(m(s),n(k_{f1})) - \hat{H}_{1R,R1}(m(s),n(k_{f1})) \right|^2 \right] \quad (6.9)$$

In (6.9), MP is the number of pilot subcarriers in one pilot symbol at the $m(s)$ symbol which is given by N/I_f. $\hat{H}_{1R,R1}(m(s),n(k_{f1}))$ is the estimated combined CFR given in (6.7) and $H_{1R,R1}(m(s),n(k_{f1}))$ is the expected combined CFR at the pilot symbols $m(s)$ of pilot subcarriers $n(k_{f1})$ with unknown parameters of time domain CIR $\hat{\rho}_{1R,R1}^{m(s)}(\ell)$ which is given by,

$$H_{1R,R1}(m(s),n(k_{f1})) = \sum_{\ell=0}^{NP-1} \rho_{1R,R1}^{m(s)}(\ell) \cdot \exp\left(-j2\pi n(k_{f1})\ell/N\right) \quad (6.10)$$

where NP is the total number of delay paths occurred in the channels between UT_1 to RS in the first timeslot and the RS to UT_1 in the second timeslot, and $\hat{\rho}_{1R,R1}^{m(s)}(\ell)$ represents the complex amplitude of combined CIR at the ℓ-th delay path.

The ML equation given (6.9) can be represented by the following equation [45],

$$\left\| \hat{\rho}_{1R,R1}^{m(s)}(\ell) \right\|_{N_g \times 1} = \dagger \left\| D(n(k_{f1}),\ell) \right\|_{MP \times N_g} \bullet \left\| \hat{H}_{1R,R1}(m(s),n(k_{f1})) \right\|_{MP \times 1} \quad (6.11)$$

where † denotes the Moore-Penrose inverse, • denotes the matrix multiplication, $\left\| \hat{\rho}_{1R,R1}^{m(s)}(\ell) \right\|$ with the matrix size $(Ng \times 1)$ is the combined CIR to be estimated, and $\left\| D(n(k_{f1}),\ell) \right\|$ with the matrix size $(MP \times Ng)$ are given by,

$$D(n(k_{f1}),\ell) = \exp\left(-j2\pi n(k_{f1})\ell/N\right), 0 \leq \ell \leq N_g - 1 \quad (6.12)$$

In (6.11), since the actual number of delay paths is unknown at the receiver, the number of delay paths to be estimated for the combined CIR is set by the length of GI which be decided taken into account the summation of delay paths occurred in both channels. Here it should be also noted that since the elements of matrix $\left\| D(n(k_{f1}),\ell) \right\|$ given in (6.12) is the function of $n(k_{f1})$ and ℓ which are known at the receiver, its Moore-Penrose inverse matrix can be calculated in advance at the receiver. From this fact, the computation complexity for the estimation of CIR can be reduced drastically. By using the estimated combined time domain

CIR, its frequency domain combined CFR over all subcarriers within the OFDM frequency bandwidth can be obtained by FFT processing as given in (6.10).

As for the estimation of CFR for the data symbols at $m \neq m(s)$, the Cubic Spline interpolation method is employed in this chapter for the estimated CFR at the pilot symbols of $m=m(s)$. By using the ML method in the frequency domain and the interpolation method in the time axis, the combined CFR for all symbols can be estimated precisely even in higher time-varying fading channels. By using the estimated combined CFR, both UTs can demodulate the other user's information data by using the frequency domain equalization with removing the self-information data given in (6.4).

6.3.3   Required Length of GI in the Proposed Method

In the proposed estimation method for the combined CIR, it should be noted that the channel conditions in the first and second timeslots usually have the strong correlations when the Time Division Duplex (TDD) operation is employed by using the same radio frequency. In this case the CIR for both channels between the UTs and RS is assumed to be almost the same when the relative speed between the UTs and RS is low. In this chapter, however we consider that both channels between UT_1 and RS are independent channels assuming the higher time-varying fading channels. Furthermore, the proposed CFR estimation method could employ the operation of Frequency Division Duplex (FDD) between the UT to RS and RS to UT by using the different frequencies. If assuming the FDD operation, the RS can be realized as the simple relay station with the amplifying and forwarding which enables one timeslot bi-directional communications. From the above reasons, this chapter assumes that two channels between the UT to RS and the RS to UT are independent channels.

When assuming the independent channels, the CFRs for both channels can be given by,

$$H_{1R}(m(s),n(k_{f1})) = \sum_{\ell_1=0}^{NP1-1} \rho_{1R}^{m(s)}(\ell_1) \cdot \exp(-j2\pi n(k_{f1})\ell_1/N) \tag{6.13}$$

$$H_{R1}(m(s),n(k_{f1})) = \sum_{\ell_2=0}^{NP2-1} \rho_{R1}^{m(s)}(\ell_2) \cdot \exp(-j2\pi n(k_{f1})\ell_2/N) \tag{6.14}$$

where $\rho_{1R}^{m(s)}(\ell_1)$ and $\rho_{R1}^{m(s)}(\ell_2)$ are the time domain CIR for the channels between UT_1 to RS and RS to UT_1, respectively. $NP1$ and $NP2$ are the number of delay paths occurred in the both channels. From (6.13) and (6.14), the combined CFR $H_{1R,R1}(m(s),n(k_{f1}))$ can be given by,

$$H_{1R,R1}(m(s),n(k_{f1})) = \sum_{\ell_1=0}^{NP1-1}\sum_{\ell_2=0}^{NP2-1} \rho_{1R}^{m(s)}(\ell_1) \cdot \rho_{R1}^{m(s)}(\ell_2) \cdot \exp(-j2\pi n(k_{f1})(\ell_1+\ell_2)/N) \tag{6.15}$$

From (6.15), it can be observed that the number of delay paths NP for the combined time domain CIR $\hat{\rho}_{1R,R1}^{m(s)}(\ell)$ given in (6.10) becomes ($NP1+NP2$). From this fact, the length of guard interval (GI) must be taken by larger than ($NP1+NP2$) in the proposed CFR estimation method.

6.4   Performance Evaluations

This section presents the various computer simulation results to verify the performance of proposed CFR estimation method for the bi-directional communications with ANC. The simulation parameters used in the following evaluations are listed in Table 6.1.

Table 6.1: Simulation parameters.

Information	Parameter
Modulation for data subcarriers	16QAM
Modulation for pilot subcarriers	QPSK
Demodulation	Coherent
Number of FFT-points (N)	256
Length of guard interval (Ng)	24
Interval of pilot symbols in Time-axis (I_t)	4 and 8
Interval of pilot subcarriers in Frequency-axis (I_f)	4 and 8
Frame length for proposed method (L)	33 symbols
Frame length for conventional method [68]	4 and 8 symbols
Frame length for conventional method [70]	32 symbols
OFDM occupied bandwidth	10 MHz
Radio frequency	2 GHz
Relay Station	Amplify and Forward
Multipath Rayleigh fading channel model	
- Delay profile	Exponential
- Decay constant	-1dB
- Number of delay paths (N_P) in all links	10
- Number of scattered rays	20
Normalized Doppler frequency (f_dT_s)	$1\times10^{-4}\sim1\times10^{-1}$
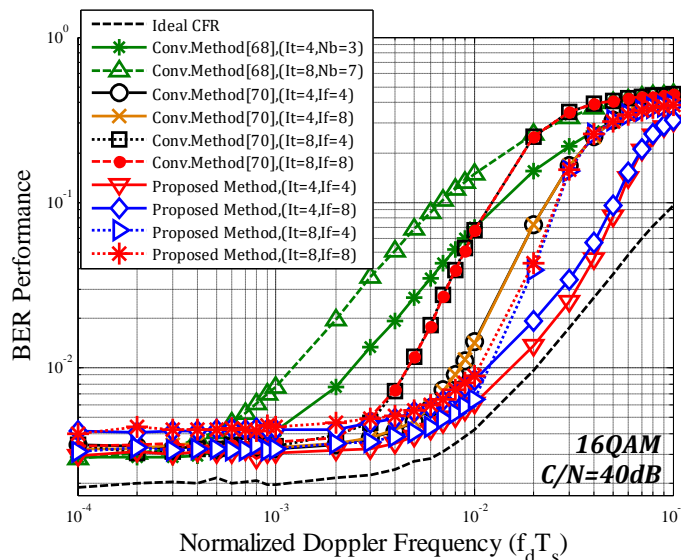
Figure 6.3: BER performances of proposed method vs. f_dT_s.

Figure 6.3 shows the BER performance of the proposed CFR estimation method when changing the f_dT_s at the Carrier-to-Noise Power Ratio (C/N) = 40dB. The guard interval length for the proposed method is taken by 24 which is decided taken into account the summation of the number of delay paths $NP1(=10)$ and $NP2(=10)$ occurred in the 1st and 2nd timeslot as mentioned in the previous section. In the Figure, the BER performance for the conventional methods [68] and [70] are also shown as for the purpose of comparison with the proposed

method. In the conventional methods [68] of using the preamble symbol, the interval of preamble symbols I_t in the time axis is taken by 4 and 8 and the number of data symbols inserted after the preamble symbols N_b is taken by 3 and 7, respectively. In the conventional method [70] of using the 2 by 2 Walsh code, I_t is 4 and 8 and the interval of pilot subcarriers I_f is 4 and 8. From the Figure, it can be observed that the proposed method with I_t=4 and 8 and I_f=4 and 8 can achieve better BER performance than both conventional methods when $f_d T_s$>6×10^{-3}. Especially, the proposed method with I_t=4 and I_f=4 can achieve much better BER performance and is almost the same BER performance as that using the ideal CFR. From these results, it can be concluded that the proposed method can achieve higher CFR estimation accuracy and better BER performance even in higher time-varying fading channel.

Figure 6.4 shows the BER performance for the proposed method when changing the C/N at the $f_d T_s$=0.02 (corresponding to 390km/h approximately). From the Figure, it can be observed that the BER performance for all conventional methods are degraded relatively especially when the interval of pilot symbols I_t is 8. This is the reason that the estimated CFR at the preamble symbol is used in the demodulation of following all data symbols in [68], and the estimated CFR in [70] is the average value between two pilot subcarriers with the Walsh code inserted with the interval of I_t. From these results, it can be concluded that the proposed method can achieve much better BER performance than the conventional methods even when the interval of pilot symbols I_t is 8.
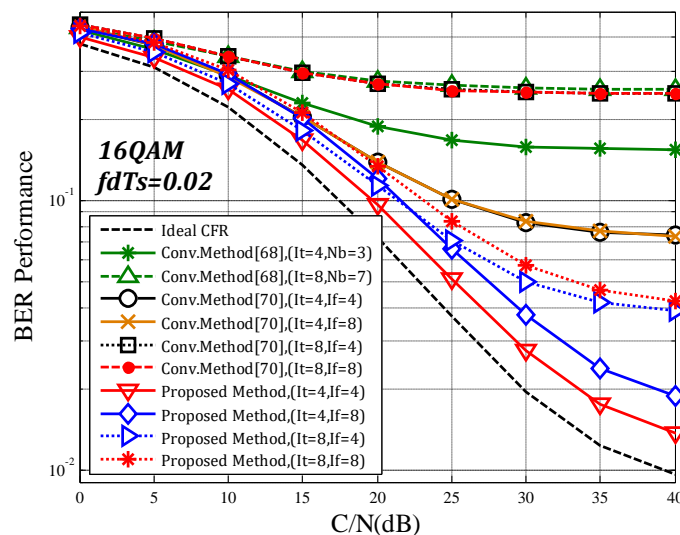
Figure 6.4: BER performances of proposed method vs. C/N(dB).

Table 6.2: Transmission efficiency of proposed method.

[I_t,I_f]	[4,4]	[4,8]	[8,4]	[8,8]
Conventional [68]	75.0% (I_t=4,N_b=3)		87.5% (I_t=8,N_b=7)	
Conventional [70]	93.8%	96.9%	96.9%	98.4%
Proposed	86.4%	93.2%	92.4%	96.2%

Table 6.2 shows the data transmission efficiency taking into account the Guard Interval (GI) length for the proposed and conventional methods [68][70] when changing the interval of pilot symbols I_t and the interval of pilot subcarriers I_f. From Table 6.2 and Figure 6.4, it can be observed that the proposed method can achieve much better BER performance and higher transmission efficiency than the conventional method of employing the preamble symbol with Zadoff Chu code [68] in higher time varying fading channels. The proposed method also shows much better BER performance than the conventional method of employing the Walsh code [70] at the cost of little degradation of transmission efficiency when comparing them under the same parameters for [I_t,I_f]=[4,8] and [I_t,I_f]=[8,8], respectively.

6.5 Conclusions

This chapter proposed the channel estimation method for the bi-directional OFDM based broadband ANC by using the scattered pilot subcarriers inserted both in the frequency and time axes. The salient features of proposed CFR estimation method are to enable the accurate estimation of combined CFR between UT to RS and RS and UT at each UT and to enable the demodulation of information data without feedback information from the RS even in higher time-varying fading channels. From the various computer simulation results, this chapter demonstrated that the proposed method can achieve much better BER performance with keeping higher transmission efficiency in higher time-varying fading channels.

CHAPTER 7

CHANNEL ESTIMATION METHOD FOR SFBC MIMO-OFDM BASED WIRELESS TWO-WAY RELAY SYSTEM IN TIME-VARYING FADING CHANNEL

This chapter also demonstrates the effectiveness of proposed ML based combined CFR estimation method when employing the two-way communication system of using the SFBC (Space-Frequency Block Coding) MIMO-OFDM technique to improve the BER performance. The salient feature of proposed CFR estimation method is to employ the pilot subcarriers with Walsh code to differentiate the pilot subcarriers sent from both UTs. From computer simulation results, this chapter confirms that the proposed SFBC MIMO-OFDM system of using the ML based combined CFR estimation method can achieve higher CFR estimation accuracy and better BER performance with higher transmission efficiency even when the transmission OFDM signal is the non-Nyquist rate in higher time-varying fading channel.

7.1   Introduction

A two-way relay communication system with OFDM (Orthogonal Frequency Division Multiplexing) based ANC (Analog Network Coding) [65-66] has been currently received a lot of attentions because of its potential capabilities for higher channel capacity with keeping higher signal quality in the wireless communications. In the two-way relay communication, it can be simply modeled by two user terminals (UTs) and one relay station (RS) of using two-timeslots. In the 1st timeslot, each UT sends his information data to another UT through the RS. Then, the RS rebroadcasts the received signal with amplifying and forwarding to both UTs in the 2nd timeslot. In the two-way relay communication, each UT removes his self-information data from its received signal and demodulates the information data sent from the other UT by using the estimated channel frequency response (CFR).

To enable the demodulation of information data with removing the self-information data at each UT, it is essential to realize the accurate channel estimation (CE) method for the two-way relay system. To meet this requirement, two leading CE methods were proposed for the OFDM based two-way relay system. One is the block-pilot frame based CE method of using the Zadoff Chu sequence [67-68]. Although the proposed CE method in [68] can estimate the combined CFR for both channels between the UT to RS in the 1st timeslot and the RS to UT in the 2nd timeslot at each UT simultaneously without the feedback information of CFR estimated at the RS, the transmission efficiency for the proposed CE method would be degraded in the higher time-varying fading channel. Because block-pilot symbols are required to add in the time axis frequently so as to achieve the precise the CFR estimation accuracy. To solve the above problem, the scattered pilot based CE method of using Walsh code was [69-70] which can achieve higher transmission efficiency even in higher time-varying fading channel.

To achieve better bit error rate (BER) performance than that for the above Single-Input and Single-Output (SISO-OFDM) systems in the two-way relay communication, [73] and [74] proposed the Space-Time Block Coding (STBC) Multi-Input and Multi-Output (MIMO) OFDM based two-way relay systems [41]. However, these systems were proposed assuming the quasi static channel and their BER performances would be degraded relatively in higher time-varying fading channel due to the occurrence of inter-channel interference (ICI). To reduce the ICI and achieve better BER performance in higher time-varying fading channel, the SISO-OFDM system with the Space-Frequency Block Coding (SFBC) was proposed in [15-16]. The SFBC SISO-OFDM method has a potential capability of self-cancelation for the ICI due to its data encoding method for the consecutive two subcarriers in the frequency axis.

From the above backgrounds, this chapter proposes a novel CE method for the SFBC MIMO-OFDM based two-way relay system which can achieve better BER performance with keeping higher transmission efficiency even in the higher time-varying fading channel. The salient features of proposed CE method are to employ the scattered pilot subcarriers with the Walsh coding in the estimation of CFR which can achieve higher transmission efficiency and to employ the SFBC for data subcarriers both in the pilot symbols and data symbols for obtaining the frequency diversity gain with self-cancellation of ICI which can achieve the better BER performance. The proposed CE method also employs the Maximum Likelihood (ML) and Cubic Spline Interpolation methods in the estimation of CFR for the frequency and time axes, respectively to improve the CFR estimation accuracy even in higher time-varying fading channel [75].

This chapter is organized as follows. Section 7.2 shows a MIMO-OFDM based two-way relay communication network model and Section 7.3 proposes the SFBC MIMO-OFDM method. Section 7.4 proposes a channel estimation method of using the scattered pilot subcarriers with Walsh coding. Section 7.5 presents the various computer simulation results to demonstrate the effectiveness of proposed method. Finally, Section 7.6 draws some conclusions.

7.2 MIMO-OFDM Two-Way Relay Network Model

Figure 7.1 shows a MIMO-OFDM system model for two-way relay system to be considered in this chapter which consists of two user terminals (UTs) and one relay station (RS). Two UTs and one RS are equipped with N_T and N_R antenna, respectively. In the two-way relay system, the data communication between two UTs is performed by using two-timeslots as shown in Fig.1. In the 1st timeslot, both user terminals UT_1 and UT_2 with N_T transmission antennas send the information data to the RS with N_R receiving antennas. In the 2nd timeslot, the RS rebroadcasts the received signal with amplifying and forwarding to both UTs.
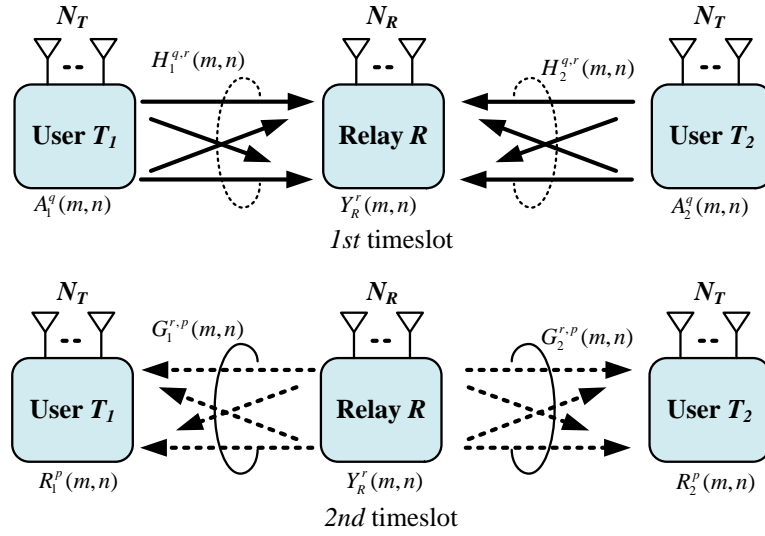
Figure 7.1: Overview of MIMO-OFDM based two-way relay system.

In the 1st timeslot, the information data $A_1^q(m,n)$ and $A_2^q(m,n)$ for the n-th subcarrier of the m-th symbol at the q-th antenna of UT_1 and UT_2 are transmitted to the RS simultaneously. The received signal at the RS can be given by,

$$Y_R^r(m,n) = \sum_{q=1}^{N_T} \sum_{j=1}^{2} \left\{ A_j^q(m,n) \cdot H_j^{q,r}(m,n) \right\} + Z_R^r(m,n) \tag{7.1}$$

where $Y_R^r(m,n)$ represents the received signal at the r-th antenna of RS, $H_j^{q,r}(m,n)$ is the CFR between the q-th antenna of UT_j and the r-th antenna of RS and $Z_R^r(m,n)$ is the Additive White Gaussian Noise (AWGN) at the r-th antenna of RS. In the 2nd timeslot, the RS rebroadcasts the received signal $Y_R^r(m,n)$ with amplifying and forwarding to both UTs. The received signal at UT_1 can be given by,

$$R_1^p(m,n) = \sum_{r=1}^{N_R} Y_R^r(m,n) \cdot G_1^{r,p}(m,n) + Z_1^p(m,n) \tag{7.2}$$

where $R_1^p(m,n)$ represents the received signal at the p-th antenna of UT_1, $G_1^{r,p}(m,n)$ is the CFR between the r-th antenna of RS and the p-th antenna of UT_1 and $Z_1^p(m,n)$ is the AWGN added at the p-th antenna of UT_1. By using (7.1) and (7.2), the received signal $R_1^p(m,n)$ can be rewritten by,

$$R_1^p(m,n) = \sum_{q=1}^{N_T} \sum_{j=1}^{2} A_j^q(m,n) \cdot \sum_{r=1}^{N_R} H_j^{q,r}(m,n) \cdot G_1^{r,p}(m,n) + \underbrace{\sum_{r=1}^{N_R} Z_R^r(m,n) \cdot G_1^{r,p}(m,n) + Z_1^p(m,n)}_{Z_1^{p'}(m,n)}. \tag{7.3}$$

where $Z_1^{p'}(m,n)$ denotes the composite noise. From (7.3), it can be seen that the combined CFR $H_j^{q,r}(m,n) \cdot G_1^{r,p}(m,n)$ is required to estimate at UT_1 which can be given by,

$$C_{1,j}^{p,q}(m,n) = \sum_{r=1}^{N_R} H_j^{q,r}(m,n) \cdot G_1^{r,p}(m,n) \tag{7.4}$$

where $C_{1,j}^{p,q}(m,n)$ is the combined *CFR* between the q-th antenna of UT_j and the p-th antenna of UT_1 though the RS. By using (7.3) and (7.4), the received signal $R_1^p(m,n)$ can be rewritten by the following equation,

$$R_1^p(m,n) = \sum_{q=1}^{N_T} \sum_{j=1}^{2} A_j^q(m,n) \cdot C_{1,j}^{p,q}(m,n) + Z_1^{p'}(m,n) \tag{7.5}$$

7.3   Proposal of SFBC MIMO-OFDM

The Space-Frequency Block Coding (SFBC) is similar technique to the Space-Time Block Coding (STBC) based on the Alamouti algorithm [41]. In the STBC technique, two consecutive OFDM symbols in the time axis are encoded so as to obtain the frequency diversity gain in the multipath fading channel. However the STBC technique has a difficulty to apply the pilot symbols including pilot subcarriers which are used for the estimation of *CFR* in the time varying fading channel. The pilot subcarriers in the pilot symbol which are inserted at a certain interval of data symbols in the time axis are unable to apply the STBC over two consecutive symbols. Because, when employing the STBC for the pilot symbol in the MIMO-OFDM based two-way relay system, the location of pilot subcarriers at the next symbol are unable to use as the data subcarriers which leads the degradation of transmission efficiency. To solve the above problem, this chapter employs the SFBC technique both for the data subcarriers in the pilot and data symbols in which two consecutive subcarriers in the frequency axis are encoded on the basis of Alamouti algorithm. Furthermore, the SFBC has a potential capability of self-cancellation for the ICI occurring in higher time-varying fading channel[15-16]. By employing the SFBC in the MIMO-OFDM based two-way relay system, the transmission efficiency can be improved with better BER performance as compared with the STBC.

When all nodes including UT_1, UT_2 and RS are equipped by 2 antennas ($N_T=N_R=2$), the transmission information data with SFBC from the antenna #1 and #2 can be given by,

$$A_j^1(m,n) = X_j(m,n), \; A_j^1(m,n+1) = -X_j^*(m,n+1)$$
$$A_j^2(m,n) = X_j(m,n+1), \;\;\; A_j^2(m,n+1) = X_j^*(m,n)$$

(7.6)

where $A_j^1(m,n)$ and $A_j^2(m,n)$ are the information data at the antenna #1 and #2 of UT_j and * denotes the complex conjugate. Substituting (7.6) into (7.5), the received signal at the *p*-th antenna of UT_1 can be rewritten by the following equation,

$$R_1^p(m,n) = X_1(m,n)\cdot C_{1,1}^{p,1}(m,n) + X_2(m,n)\cdot C_{1,2}^{p,1}(m,n)$$
$$+ X_1(m,n+1)\cdot C_{1,1}^{p,2}(m,n) + X_2(m,n+1)\cdot C_{1,2}^{p,2}(m,n)$$
$$R_1^p(m,n+1) = X_1^*(m,n)\cdot C_{1,1}^{p,2}(m,n) + X_2^*(m,n)\cdot C_{1,2}^{p,2}(m,n)$$
$$- X_1^*(m,n+1)\cdot C_{1,1}^{p,1}(m,n) - X_2^*(m,n+1)\cdot C_{1,2}^{p,1}(m,n)$$

(7.7)

By using the estimated combined CFR $\hat{C}_{1,j}^{p,q}(m,n)$ of which estimation method is proposed in Section 7.4, the data information of $\hat{X}_j(m,n)$ and $\hat{X}_j(m,n+1)$ can be given by the following equation,

$$\hat{X}_j(m,n) = \hat{C}_{1,j}^{p,1*}(m,n)\cdot R_1^p(m,n) + \hat{C}_{1,j}^{p,2}(m,n+1)\cdot R_1^{p*}(m,n+1)$$
$$\hat{X}_j(m,n+1) = \hat{C}_{1,j}^{p,2*}(m,n)\cdot R_1^p(m,n) - \hat{C}_{1,j}^{p,1}(m,n+1)\cdot R_1^{p*}(m,n+1)$$

(7.8)

From (7.7) and (7.8), each UT can demodulate the information data sent from the other UT by using the frequency domain equalization with removing the self-information data which is given by the following equations

$$\widehat{X}_j(m,n) = \frac{D_A^1(m,n)\cdot\left(B_{2,1}^{(2)}(m,n)+B_{2,2}^{(2)}(m,n)\right)-D_A^1(m,n+1)\cdot\left(A_{2,1}^{(2)}(m,n)+A_{2,2}^{(2)}(m,n)\right)}{\left(A_{2,1}^{(1)}(m,n)+A_{2,2}^{(1)}(m,n)\right)\cdot\left(B_{2,1}^{(2)}(m,n)+B_{2,2}^{(2)}(m,n)\right)-\left(A_{2,1}^{(2)}(m,n)+A_{2,2}^{(2)}(m,n)\right)\cdot\left(B_{2,1}^{(1)}(m,n)+B_{2,2}^{(1)}(m,n)\right)},$$
$$\widehat{X}_j(m,n+1) = \frac{D_A^1(m,n+1)\cdot\left(A_{2,1}^{(1)}(m,n)+A_{2,2}^{(1)}(m,n)\right)-D_A^1(m,n)\cdot\left(B_{2,1}^{(1)}(m,n)+B_{2,2}^{(1)}(m,n)\right)}{\left(A_{2,1}^{(1)}(m,n)+A_{2,2}^{(1)}(m,n)\right)\cdot\left(B_{2,1}^{(2)}(m,n)+B_{2,2}^{(2)}(m,n)\right)-\left(A_{2,1}^{(2)}(m,n)+A_{2,2}^{(2)}(m,n)\right)\cdot\left(B_{2,1}^{(1)}(m,n)+B_{2,2}^{(1)}(m,n)\right)}$$

(7.9)

7.3 Proposal of SFBC MIMO-OFDM

$$A_{i_1,i_2}^{(1)}(m,n) = \sum_{k=1}^{2}\left\{\hat{C}_{1,i_1}^{k,1}(m,n)\cdot\hat{C}_{1,i_2}^{k,1*}(m,n) + \hat{C}_{1,i_1}^{k,2*}(m,n+1)\cdot\hat{C}_{1,i_2}^{k,2}(m,n+1)\right\},$$

$$A_{i_1,i_2}^{(2)}(m,n) = \sum_{k=1}^{2}\left\{\hat{C}_{1,i_1}^{k,2}(m,n)\cdot\hat{C}_{1,i_2}^{k,1*}(m,n) - \hat{C}_{1,i_1}^{k,1*}(m,n+1)\cdot C_{1,i_2}^{k,2}(m,n+1)\right\},$$

$$B_{i_1,i_2}^{(1)}(m,n) = \sum_{k=1}^{2}\left\{\hat{C}_{1,i_1}^{k,1}(m,n)\cdot\hat{C}_{1,i_2}^{k,2*}(m,n) - \hat{C}_{1,i_1}^{k,2*}(m,n+1)\cdot\hat{C}_{1,i_2}^{k,1}(m,n+1)\right\},$$

$$B_{i_1,i_2}^{(2)}(m,n) = \sum_{k=1}^{2}\left\{\hat{C}_{1,i_1}^{k,2}(m,n)\cdot\hat{C}_{1,i_2}^{k,2*}(m,n) + \hat{C}_{1,i_1}^{k,1*}(m,n+1)\cdot\hat{C}_{1,i_2}^{k,1}(m,n+1)\right\}.$$

(7.10)

where

$$D_A^1(m,n) = \hat{X}_i(m,n) - a_1(m,n) + \hat{X}_j(m,n) - a_2(m,n),$$

$$D_A^1(m,n+1) = \hat{X}_i(m,n+1) - b_1(m,n) + \hat{X}_j(m,n+1) - b_2(m,n).$$

$$\left.\begin{array}{l} a_x(m,n) = A_i(m,n)\cdot A_{1,x}^{(1)}(m,n) + A_i(m,n+1)\cdot A_{1,x}^{(2)}(m,n) \\ b_x(m,n) = A_i(m,n)\cdot B_{1,x}^{(1)}(m,n) + A_i(m,n+1)\cdot B_{1,x}^{(2)}(m,n) \end{array}\right\} when\ x = 1\ or\ 2$$

7.4 Proposed Channel Estimation Method

In this section, we propose a channel estimation method for SFBC MIMO-OFDM based two-way relay system by using the scattered pilot subcarriers with Walsh codes.

7.4.1 Scattered Pilot Subcarriers with Walsh code

Figure 7.2 shows the proposed scattered pilot subcarriers assignment method for both UT_1 and UT_2 with two transmission antennas. In the proposed pilot subcarriers assignment method, we assign the null subcarriers inserted in the frequency axis to avoid the collision of pilot subcarriers sent from both UT_1 and UT_2. Both pilot and null subcarriers are inserted into the data subcarriers in the pilot symbols periodically with the interval of I_f in the frequency axis and the pilot symbols including information data, pilot and null subcarriers are inserted into data symbols with the interval of I_t in the time axis. All subcarriers in other symbols between two pilot symbols are data subcarriers as shown in Fig.2. All pilot subcarriers in the proposed assignment method are encoded by [2×2] Walsh code w_2 which is given by,

$$W_2^j = \begin{bmatrix} w_{1,1}^j & w_{1,2}^j \\ w_{2,1}^j & w_{2,2}^j \end{bmatrix} = \begin{bmatrix} 1 & 1 \\ 1 & -1 \end{bmatrix} \tag{7.11}$$

where first and second columns are assigned to the antenna #1 and #2, respectively both for UT_j where $j=1$ or 2. Here all data subcarriers both in the pilot and data symbols are encoded by SFBC in the frequency axis as given in (7.6). The pilot and null subcarriers in the pilot symbol and data subcarriers both in pilot and data symbols at the q-th antenna of the UT_j can be given by the following equation,

$$A_j^q(m,n) = \begin{cases} Pilot, when \ m = m(s) \ \& \ n = n_P(k_j^q) \\ Null, when \ m = m(s) \ \& \ n = n_N(k_j^q) \\ Data, \ otherwise \end{cases} \tag{7.12}$$

where the Pilot subcarriers with Walsh codes are given by,

$$A_j^q(m,n) = \begin{cases} w_{1,q}^j(m,n), when \ s \ is \ odd \ number \\ w_{2,q}^j(m,n), when \ s \ is \ even \ number \end{cases} \tag{7.13}$$

where $m(s)$, $n_P(k_j^q)$ and $n_N(k_j^q)$ represent the locations of pilot symbol in the time axis and the locations of Walsh pilot and null subcarriers in the frequency axis at the q-th antenna of UT_j, all of which locations are given by the following equation,

$$m(s) = (s-1)I_t + 1, \ \ 1 \le s \le (L-1)/I_t + 1$$

$$\left. \begin{array}{l} n_P(k_j^q) = (k_j^q - 1)I_f + j, \\ n_N(k_j^q) = (k_j^q - 1)I_f + j + 1, \end{array} \right\} \ k_j^q = 1, 2, \cdots, N/I_f \tag{7.14}$$

where N is the number of subcarriers in one OFDM symbol and L is the number of symbols in one frame in which both ends of frame are pilot symbols so as to achieve higher estimation accuracy in the interpolation method of time axis. From (7.12), it can be seen that the locations of null subcarrier for the UT_1 are used as the locations of Walsh pilot subcarrier for the UT_2. By using these assignments for the Walsh pilot and null subcarriers, it is possible to estimate the CFR independently at each UT without the collision of pilot subcarriers between UT_1 and UT_2. Although the received pilot subcarriers at the UT_j are the superimposed signal sent from antenna #1 and #2 of UT_j, the combined CFR between UT_j to RS and RS to UT_j both for the antenna #1 and #2 can be estimated separately by using the orthogonal property of Walsh codes.
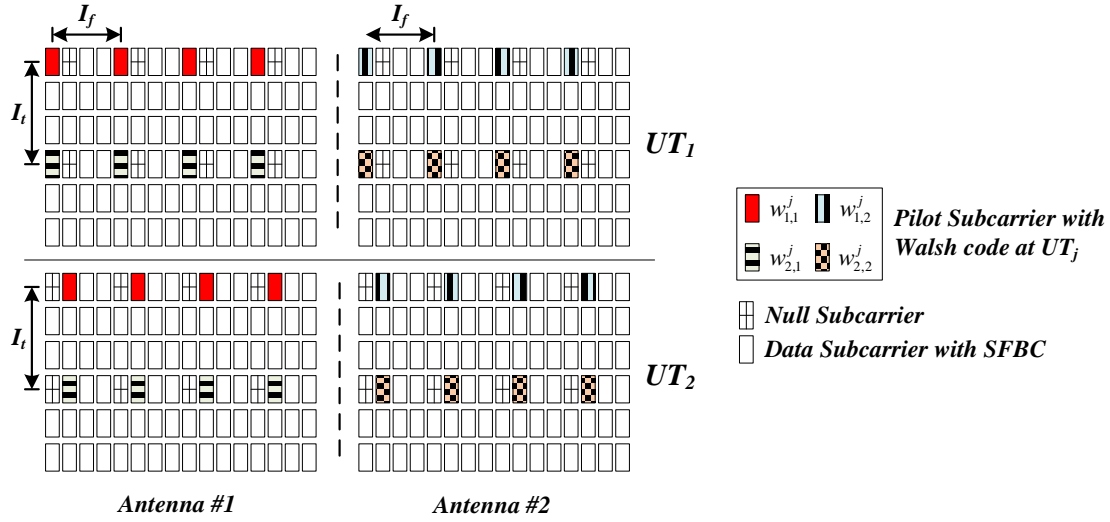
Figure 7.2: Scattered pilot subcarriers assignment.

7.4.2   Proposed Channel Estimation Method

In the scattered pilot subcarriers assignment method as mentioned in the previous section, the locations of Walsh pilot subcarriers and the null subcarriers at the q-th antenna of UT_1 and UT_2 are known at UT_1, the combined CFR $\hat{C}_{1,j}^{p,q}(m(s),n_P(k_j^q))$ at the p-th antenna of UT_1 can be estimated by the following equation [70],

$$\hat{C}_{1,j}^{p,q}(m(s),n_P(k_j^q)) = \frac{1}{4} \cdot R_1^p(m(s)-I_t,n_P(k_j^q)) \cdot A_j^q(m(s)-I_t,n_P(k_j^q))$$

$$+ \frac{1}{2} \cdot R_1^p(m(s),n_P(k_j^q)) \cdot A_j^q(m(s),n_P(k_j^q)) \qquad (7.15)$$

$$+ \frac{1}{4} \cdot R_1^p(m(s)+I_t,n_P(k_j^q)) \cdot A_j^q(m(s)+I_t,n_P(k_j^q))$$

where the combined CFR at the p-th antenna of UT_1 is denoted by $\hat{C}_{1,j}^{p,q}(m(s),n_P(k_j^q))$ where $j=1$ or 2.

The CFR in the frequency axis over all data subcarriers can be estimated by applying the Maximum Likelihood (ML) method to the estimated combined CFR at the Walsh pilot subcarriers given in (7.15) with the interval of I_f in the frequency axis. The combined time domain channel impulse response (CIR) at the p-th antenna $\hat{\rho}_{1,j}^{p,q}(m(s),l)$ for $\hat{C}_{1,j}^{p,q}(m(s),n)$ at the l-th delay path can be estimated by the following equation [75],

$$L_{ML}\left\langle \hat{\rho}_{1,j}^{p,q}(m(s),l) \right\rangle = \underset{\hat{\rho}_{1,j}^{p,q}(m(s),l)}{\arg\min} \left[\sum_{k_j^q=1}^{MP} \left| C_{1,j}^{p,q}(m(s),n_P(k_j^q)) - \hat{C}_{1,j}^{p,q}(m(s),n_P(k_j^q)) \right|^2 \right] \qquad (7.16)$$

In (7.16), *MP* is the number of pilot subcarriers in one pilot symbol which is given by N/I_f. $\hat{C}_{1,j}^{p,q}(m(s),n_P(k_j^q))$ is the estimated combined CFR at the p-th antenna given in (7.15) and $C_{1,j}^{p,q}(m(s),n_P(k_j^q))$ is the expected combined CFR at the pilot symbol $m(s)$ of Walsh pilot subcarrier $n_P(k_j^q)$ at the q-th antenna with the unknown parameter of time domain CIR $\hat{\rho}_{1,j}^{p,q}(m(s),l)$ which is given by,

$$C_{1,j}^{p,q}(m(s),n_P(k_j^q)) = \sum_{l=0}^{NP-1} \hat{\rho}_{1,j}^{p,q}(m(s),l)e^{-j2\pi n(n_P(k_j^q))l/N} \qquad (7.17)$$

where *NP* is the total number of delay paths occurred in two-timeslot channels between the q-th antenna of UT_1 to the r-th antenna of RS in the 1st timeslot and the r-th antenna of RS to the p-th antenna of UT_1 in the 2nd timeslot.

The ML equation given in (7.16) can be represented by the following equation,

7.4 Proposed Channel Estimation Method

$$\left\|\hat{\rho}_{1,j}^{p,q}(m(s),l)\right\|_{N_g \times 1} = \dagger \left\|D(n_P(k_j^q),l)\right\|_{MP \times N_g} \bullet \left\|\hat{C}_{1,j}^{p,q}(m(s),n_P(k_j^q))\right\|_{MP \times 1} \tag{7.18}$$

where $\dagger$ denotes the Moore-Penrose inverse matrix, $\bullet$ denotes the matrix multiplication, $\left\|\hat{\rho}_{1,j}^{p,q}(m(s),l)\right\|$ with the matrix size $[N_g \times 1]$ is the combined CIR to be estimated, and $\left\|D(n_P(k_j^q),l)\right\|$ with the matrix size $[MP \times N_g]$ is given by,

$$D(n_P(k_j^q),l) = e^{-j2\pi(n_P(k_j^q))l/N}, \; 0 \le l \le N_g -1 \tag{7.19}$$

In (7.18), since the actual number of delay paths is unknown at the receiver, the number of delay paths to be estimated for the combined CIR is set by the length of guard interval (GI) which be decided taken into account the summation of delay paths occurred in both channels in two-timeslots. Here it should be also noted that since the elements of matrix $\left\|D(n_P(k_j^q),l)\right\|$ given in (7.19) is the function of $n_P(k_j^q)$ and l which are known at the receiver, its Moore-Penrose inverse matrix can be calculated in advance at the receiver. From this fact, the computation complexity for the estimation of CIR can be reduced drastically. By using the estimated combined time domain CIR, its frequency domain combined CFR over all subcarriers within the OFDM frequency bandwidth can be obtained by FFT processing as given in (7.17).

As for the estimation of combined CFR for the data symbols at $m \neq m(s)$, the Cubic Spline interpolation method is employed in this chapter for the estimated combined CFR at the pilot symbols of $m = m(s)$. By using the ML method in the frequency axis and the interpolation method in the time axis, the combined CFR for all data subcarriers over the frame can be estimated precisely in higher time-varying fading channel. By using the estimated combined CFR, both UTs can demodulate the other user's information data by using SFBC decoding for all data subcarriers both in the data and pilot symbols with removing the self-information data given in (7.9).

Since this chapter proposes a channel estimation method for the combined CIR, the GI length (GI-length) is required to be decided taken into account the summation of delay paths occurred in both channels in two-timeslots. In this chapter, we assume that the channels in two-timeslots between the UT to RS and RS to UT are independent channels. Therefore, the CFRs of each link can be given by,

$$H_1^{q,r}(m(s),n_P(k_j^q)) = \sum_{l_1=0}^{NP1-1} \alpha_1^{q,r}(m(s),l_1) \cdot e^{-j2\pi(n_P(k_j^q))l_1/N}$$
$$G_1^{r,p}(m(s),n_P(k_j^q)) = \sum_{l_2=0}^{NP2-1} \beta_1^{q,r}(m(s),l_2) \cdot e^{-j2\pi(n_P(k_j^q))l_2/N} \tag{7.20}$$

where $\alpha_1^{q,r}(m(s),l_1)$ is the time domain CIR between the q-th antenna of UT$_1$ and the r-th antenna of RS in the 1st timeslot and $\beta_1^{q,r}(m(s),l_2)$ is the time domain CIR between the r-th antenna of RS and the p-th antenna of UT$_1$ in the 2nd timeslot. $NP1$ and $NP2$ are the number of delay paths occurred in the 1st and 2nd timeslot links, respectively. From (7.20), the combined CFR $C_{1,1}^{p,q}(m(s),n_P(k_1^q))$ can be given by,

$$C_{1,1}^{p,q}(m(s),n_P(k_1^q)) = \sum_{l_1=0}^{NP1-1}\sum_{l_2=0}^{NP2-1} \underbrace{\alpha_1^{q,r}(m(s),l_1) \cdot \beta_1^{q,r}(m(s),l_2)}_{\hat{\rho}_{1,1}^{p,q}(m(s),l)} e^{-j2\pi(n_P(k_1^q))(l_1+l_2)/N} \tag{7.21}$$

From (7.21), it can be observed that the number of delay paths for the combined time domain CIR $\hat{\rho}_{1,1}^{p,q}(m(s),l)$ where $j=1$ (UT$_1$) given in (7.17) becomes the summation of $NP1$ and $NP2$ ($NP1+NP2$). From this fact, the GI-length must be taken by longer than ($NP1+NP2$) in the proposed CFR estimation method so as to enable the estimation of combined CFR precisely at each UT.

7.5   Performance Evaluations

This section presents the various computer simulation results to verify the performance of proposed channel frequency response (CFR) estimation method for the SFBC MIMO-OFDM based two-way relay system. The simulation parameters used in the following evaluations are listed in Table 7.1.

Table 7.1: Simulation parameters.

Information	Parameter
Modulation method for data subcarriers	16QAM
Modulation method for pilot subcarriers	QPSK
Demodulation	Coherent
Number of sub-carriers *(N)*	256
Number of sample points in GI *(N$_g$)*	20
Interval of pilot symbols in Time-axis *(I$_t$)*	2
Interval of pilot subcarriers in Freq.-axis *(I$_f$)*	8
OFDM occupied bandwidth (*W*)	10MHz
Radio frequency (*f$_c$*)	2GHz
Relay Station (*RS*)	Amplify and forward
Multipath Fading channel model	
Fading model	*Rayleigh fading*
Delay profile	*Exponential*
Decay constant	*-1dB*
Number of delay paths *(NP)* in each channel	*8*
Number of scattered rays	*20*
Normalized Doppler frequency (*f$_d$T$_s$*)	*$10^{-4} \sim 10^{-1}$*

Figure 7.3 shows the BER performances for the SFBC MIMO-OFDM based two-way relay system with the proposed CFR estimation method when changing the normalized Doppler frequency (f_dT_s). In the simulation, the carrier-to-noise power ratio (C/N) is 30dB, the interval of pilot symbol I_t and the interval of pilot subcarrier I_f are taken by 2 and 8, respectively and all nodes including UTs and RS except the SISO-OFDM based two-way relay system are equipped with 2 antennas. In the figure, the BER performances for the SISO-OFDM and SFBC MIMO-OFDM systems with the conventional CFR estimation method [75] are also shown as for the purpose of comparison with the proposed CFR estimation method. The conventional CFR estimation method [75] employs the more pilot and null subcarriers than the proposed method to avoid the collision of pilot subcarriers between the transmission antennas and UTs because of unemployment of Walsh codes which leads the degradation of transmission efficiency. The GI-length for the proposed CFR estimation method is taken by 20 which is decided taken into account the summation of the number of delay paths $NP1(=8)$ and $NP2(=8)$ occurred in two-timeslots as mentioned in the previous section. From the figure, it can be observed that the SFBC MIMO-OFDM system with the proposed CFR estimation method can achieve better BER performance than that for the other systems. Especially, the proposed method can achieve much better BER performance than the SISO-OFDM system. The proposed method shows slightly worse BER performance than the SFBC MIMO-OFDM system with the conventional CFR estimation method [75] when f_dT_s is larger than 2×10^{-2} (Corresponds to 390km/h). This is the reason that the proposed CFR estimation method employs the pilot subcarriers with Walsh code in which the estimated CFR is obtained by taking the averaged value between the pilot subcarriers with the Walsh codes at the interval of I_t as given in (7.15). From this fact, the CFR estimation accuracy for the proposed method

would be degraded slightly in higher time-varying fading channel as compared with the conventional method of using pilot subcarriers without encoding the Walsh code.
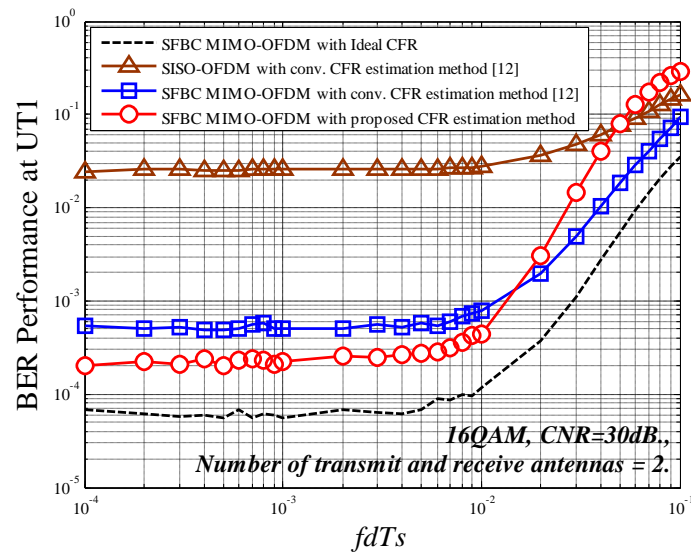
Figure 7.3: BER Performance at UT_1 of proposed method vs f_dT_s.
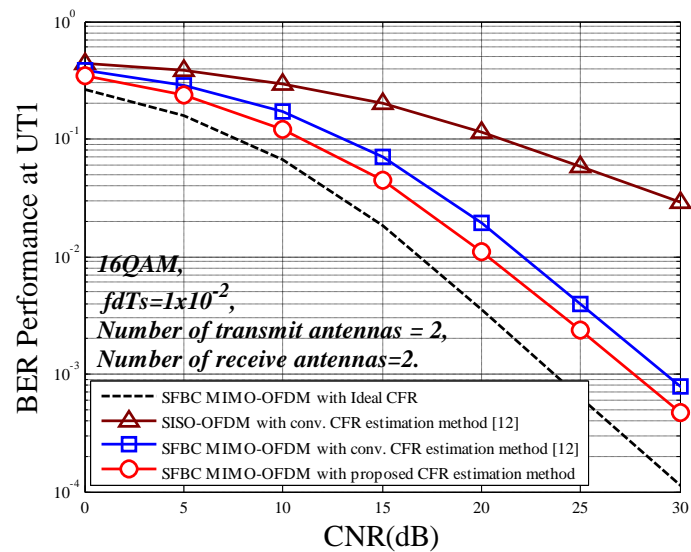
Figure 7.4: BER Performance at UT_1 of proposed method vs C/N.

Figure 7.4 shows the BER performance for the SFBC MIMO-OFDM system with the proposed CFR estimation method when changing C/N. In the simulation, the f_dT_s is 1×10^{-2} (Corresponds to 200km/h). From the figure, it can be seen that the proposed CFR estimation method shows better BER performance than the SISO-OFDM and SFBC MIMO-OFDM systems with the conventional CFR estimation method.

7.6   Conclusions

This chapter proposed the channel estimation (CE) method for SFBC MIMO-OFDM based two-way relay system by using the scattered pilot subcarriers with Walsh codes. The salient features of proposed CE method are to employ the scattered pilot subcarriers with the Walsh code to achieve the higher transmission efficiency and to employ the SFBC for data subcarriers both in the pilot symbols and data symbols to achieve the better BER performance in higher time-varying fading channel. The proposed CE method also employs the Maximum Likelihood (ML) and Cubic Spline Interpolation methods in the estimation of CFR in the frequency and time axes, respectively to improve the CFR estimation accuracy even in higher time-varying fading channel. Simulation results showed that the SFBC MIMO-OFDM system with the proposed CFR estimation method can achieve better BER performance with keeping higher transmission efficiency even in higher time-varying fading channel.

CHAPTER 8

CONCLUSIONS

As OFDM technique has an influence in the next generation wireless communication systems which has been widely employed in several wireless communication systems. Two solutions based OFDM techniques are studied and evaluated in this chapter. One is the PAPR reduction technique which is studied to solve the problem of time domain OFDM signal due to the larger PAPR which cause the undesirable spectrum re-growth and degradation of BER performance in the non-linear channel. The other solution is the channel estimation technique which is studied to improve the signal quality for the wireless communication based OFDM system.

This chapter proposes a new PAPR reduction method based on the packet-switched transmission systems in which all the clusters within the certain number of OFDM symbols have the sequential cluster ID numbers embedded in the header of each cluster. The proposed method enables the reduction of PAPR performance by re-ordering of clusters (ROC) in the frequency domain at the transmitter and reconstructs the original ordering of clusters by using the cluster ID numbers demodulated from each cluster at the receiver which requests no side information.

As the MBWA which has been received considerable attentions which could provide the drivers for the various multimedia internet based communications on the vehicle, one of the promising technologies for realizing the MBWA in the ITS is MIMO technique which can provide higher transmission data rate with high signal quality. This chapter proposes a RVC system of using the STBC (Space Time Block Coding) MIMO-OFDM technique which can achieve better BER performance even in higher time-varying fading channel. To achieve the potential capability in the proposed RVC system, it is the essential to realize the accurate channel estimation method. This chapter proposes a novel channel frequency response (CFR) estimation method by using the scattered pilot subcarriers in the frequency domain. From computer simulation results, this chapter demonstrates that the STBC MIMO-OFDM based RVC system of using the proposed CFR estimation method can achieve higher channel estimation accuracy and better BER performance even in the time varying fading channel.

In practical MIMO-OFDM system, the enhancement of system performance is depended on the efficient and accurate channel estimation method. This chapter proposes the ML based time domain channel estimation (TD-CE) method for MIMO-OFDM system which can achieve higher estimation accuracy even when the non-Nyquist rate and increasing the number of transmit antennas. From computer simulation results, this chapter demonstrates the effectiveness of propose ML based TD-CE method for MIMO-OFDM system.

To accommodate multiple users flexibly and efficiently in the uplink OFDMA system, this chapter also applies the proposed ML based TD-CE method for the uplink OFDMA which can achieve higher estimation accuracy even when the non-Nyquist rate in higher time-varying fading channel.

Broadband ANC based on OFDM has been widely investigated to increase capacity of two-way relay communication. In the ANC-OFDM system, the efficient and accurate channel estimation method is the mandatory requirement to achieve the potential system performance. This chapter proposes the ML based combined CFR estimation method for two-way relay

communication system by using a novel scattered pilot assignment method including the null subcarriers to avoid the collision of pilot subcarriers sent from both UTs. From the various computer simulation results, this chapter demonstrates the effectiveness of proposed ML based combined CFR estimation method which can achieve higher estimation accuracy and better BER performance even in higher time-varying fading channel.

This chapter also demonstrates the effectiveness of proposed ML based combined CFR estimation method when employing the two-way communication system of using the SFBC (Space-Frequency Block Coding) MIMO-OFDM technique to improve the BER performance. The salient feature of proposed CFR estimation method is to employ the pilot subcarriers with Walsh code to differentiate the pilot subcarriers sent from both UTs. From computer simulation results, this chapter confirms that the proposed SFBC MIMO-OFDM system of using the ML based combined CFR estimation method can achieve higher CFR estimation accuracy and better BER performance with higher transmission efficiency even in higher time-varying fading channel.

The several computer simulation results were presented in the thesis in order to confirm and verify the effectiveness of above proposed methods. Form the various simulation results, it could be confirmed that the estimation accuracy, channel capability, transmission signal quality and computational complexity could be improved and enhanced by using the proposed methods. As a conclusion of researches in this chapter, the proposed PAPR reduction and channel estimation methods have a capability to provide various practical solutions for the next generation wireless communications systems OFDM based technique.

APPENDIX A

RELATED PUBLICATIONS

A.1 TRANSACTIONS

(1)   Tanairat Mata, Katsuhiro Naito, Pisit Boonsrimuang, Kazuo Mori and Hideo Kobayashi, "Proposal of Channel Estimation Method for ITS systems by using STBC MIMO-OFDM," *ECTI Transactions on Computer and Information Technology*, Vol.8, No.1, pp.36-44, May 2014.

(2)   Tanairat Mata, Katsuhiro Naito, Pisit Boonsrimuang, Kazuo Mori and Hideo Kobayashi, "Proposal of PAPR Reduction Method for OFDM Signal by Re-Ordering of Clusters in Frequency Domain," *International Journal of Communications, Network and System Sciences*, Vol.6, No.9, pp.388-394, Sept. 2013.

(3)   Tanairat Mata, Pornpawit Boonsrimuang, Pisit Boonsrimuang and Hideo Kobayashi, "Proposal of Improved PTS Method for STBC MIMO-OFDM Systems", *IEICE Transactions on Communications*, Vol.E93-B, No.10, pp.2673-2676, Oct. 2010.

(4)   Tanairat Mata, Pisit Boonsrimuang, Kazuo Mori and Hideo Kobayashi, "Proposal of Channel Estimation Method for Wireless Two-way Relay System of using SFBC MIMO-OFDM Technique," *Springer Journal of Telecommunication Systems* (Conditional Acceptance).

A.2 INTERNATIONAL PROCEEDINGS

(1)   Tanairat Mata, Pisit Boonsrimuang, Kazuo Mori and Hideo Kobayashi, "Proposal of Time Domain Channel Estimation Method for MIMO-OFDM Systems," *in Proc. of 7th EAI International Conference on Wireless and Satellite Systems* (*WiSATS*2015), LNICST Vol.154, pp.215-228, Bradford, UK, July 2015.

(2)   Tanairat Mata, Mio Hourai, Pisit Boonsrimuang, Kazuo Mori and Hideo Kobayashi, "Time Domain Channel Estimation Method for Uplink OFDMA System," *in Proc. of the 22nd IEEE International Conference on Telecommunications* (*ICT*2015), pp.363-367, Sydney, Australia, Apr.2015.

(3)   Tanairat Mata, Pisit Boonsrimuang, Kazuo Mori and Hideo Kobayashi, "Channel Estimation Method for SFBC MIMO-OFDM Based Wireless Two-Way Relay System in Time-Varying Fading Channel," *in Proc. of the 5th IEEE International Conference on Communications and Electronics* (*ICCE*2014), pp.71-76, Danang, Vietnam, Jul.2014.

(4)   Tanairat Mata, Katsuhiro Naito, Pisit Boonsrimuang, Kazuo Mori and Hideo Kobayashi, "Proposal of Channel Estimation Method for Bi-directional OFDM Based ANC in Higher Time-varying Fading Channel," *in Proc. of the 79th IEEE Vehicular Technology Conference* (*VTC-Spring*2014), pp.1-5, Seoul, South Korea, May2014.

(5)   Tanairat Mata, Katsuhiro Naito, Pisit Boonsrimuang, Kazuo Mori and Hideo Kobayashi, "Proposal of PAPR Reduction Method for OFDM Signal by Re-Ordering of Clusters," *in Proc. of Asia-Pacific Conference on Communications* (*APCC*2013), pp.231-236, Denpasar, Indonesia, Aug.2013.

(6)   Tanairat Mata, Katsuhiro Naito, Pisit Boonsrimuang, Kazuo Mori and Hideo Kobayashi, "Re-Ordering of Clusters Method with Split-Radix IFFT for PAPR Reduction of OFDM Signal," *in Proc. of the 2nd KMITL International Conference on Engineering, Applied Sciences, and Technology* (*ICEAST*2013), pp.148-153, Bangkok, Thailand, Aug.2013.

(7)   Tanairat Mata, Katsuhiro Naito, Pisit Boonsrimuang, Kazuo Mori and Hideo Kobayashi, "Proposal of STBC MIMO-OFDM for ITS Systems," *in Proc. Of the 10th IEEE International Conference on Electrical Engineering/Electronics, Computer, Telecommunications and Information Technology* (*ECTICON*2013), pp.1-6, Krabi, Thailand, May2013.

(8)   Panus Pantiko, Tanairat Mata, Pisit Boonsrimuang, and Hideo Kobayashi, "A Low Complexity Improved-PTS Phase Coefficient Searching Algorithm for OFDM System," *in Proc. of the 8th International Conference on Electrical Engineering/Electronics Computer, Telecommunications and Information Technology* (*ECTICON*2011), pp.365-368, KhonKaen, Thailand, May 2011.

(9)   Jaturong Sarawong, Tanairat Mata, Pisit Boonsrimuang, and Hideo Kobayashi, "Interleaved Partitioning PTS with New Phase Factors for PAPR Reduction in OFDM Systems," *in Proc. of the 8th International Conference on Electrical Engineering/Electronics Computer, Telecommunications and Information Technology* (*ECTICON*2011), pp.361-364, KhonKaen, Thailand, May 2011.

(10)   Athid Mung-in, Tanairat Mata, Pisit Boonsrimuang, and Hideo Kobayashi, "Sub-optimum Improved-PTS for PAPR reduction of OFDM signals," *in Proc. of the 3rd Joint International Information & Communication Technology, Electronics and Electrical Engineering* (*JICTEE*2010), pp.331-334, Vientiane, Laos, Dec.2010.

(11)   Tanairat Mata, Pornpawit Boonsrimuang, Pisit Boonsrimuang, and Hideo Kobayashi, "A New Weighting Factor with Concurrent PAPR Reduction Algorithm for STBC MIMO-OFDM," *in Proc. of the 9th Malaysia International Conference on Communications* (*MICC*2009), pp.136-140, Kuala Lumpur, Malaysia, Dec.2009.

(12)   Tanairat Mata, Pornpawit Boonsrimuang, Pisit Boonsrimuang, and Hideo Kobayashi, "Proposal of improved PTS method for STBC MIMO-OFDM in the non-linear channel," *in Proc. of International Symposium on Antenna and Propagation* (*ISAP*2009), pp.715-718, Bangkok, Thailand, Oct.2009.

A.3 DOMESTIC CONFERENCES

(1)   Tanairat Mata, Pisit Boonsrimuang, Kazuo Mori and Hideo Kobayashi, "Time-Domain Channel Estimation Method for MIMO-OFDM Systems," *in Proc. of IEICE General Conference* 2015, No.B-5-155, pp.510, Mar.2015.

(2)   Tanairat Mata, Mio Hourai, Pisit Boonsrimuang, Kazuo Mori, and Hideo Kobayashi, "Proposal of Channel Estimation Method for Uplink OFDMA System under Time-varying Fading Environments," *Technical Report of IEICE*, Vol.114, No.372, pp.201-206, RCS2014-254, Dec.2014.

Appendix A

(3)   Tanairat Mata, Pisit Boonsrimuang, Kazuo Mori and Hideo Kobayashi, "Proposal of Channel Estimation Method for Uplink OFDMA Systems," *in Proc. of Tokai Conference* 2014 (*English session*), No.K2-3, Sept.2014.

(4)   Tanairat Mata, Katsuhiro Naito, Pisit Boonsrimuang, Kazuo Mori and Hideo Kobayashi, "Proposal of Channel Estimation Method for OFDM Based Analogue Network Coding in Higher Time-varying Fading Channel," *Technical Report of IEICE*, Vol.113, No.385, pp.181-186, RCS2013-286, Jan.2014.

(5)   Tanairat Mata, Katsuhiro Naito, Pisit Boonsrimuang, Kazuo Mori and Hideo Kobayashi, "Proposal of Channel Estimation Method for Two-timeslots OFDM Based Analog Network Coding in Higher Time-varying Fading Channel," *in Proc. of IEICE General Conference* 2013, No.B-5-41, pp.404, Sept.2013.

(6)   Tanairat Mata, Katsuhiro Naito, Pisit Boonsrimuang, Kazuo Mori and Hideo Kobayashi, "Study on Road to Vehicle Communication System by using STBC MIMO-OFDM," *in Proc. of IEICE General Conference* 2013, No.B-5-17, pp.427, Mar.2013.

APPENDIX B

AWARDS

(1) 2014 Young Researcher's Encouragement Award from IEEE Vehicular Technology Conference (VTC 2014-spring), IEEE VTS Japan Chapter.
(2) 2015 International Conference Research Presentation Award, IEEE Nagoya Section.

BIBLIOGRAPHY

[1]   ETSI TR 101 190, v1.3.1, Digital Video Broadcasting (DVB); Implementation guidelines for DVB terrestrial television service; Transmission aspects, 2008-10.

[2]   ETSI TS 102 831, v1.2.1, Digital Video Broadcasting (DVB); Implementation guidelines for the second generation digital terrestrial television broadcasting system (DVB-T2), 2012.

[3]   IEEE Std. 802.11a, Part 11: Wireless LAN Medium Access Control (MAC) and Physical Layer (PHY) specifications: High-speed Physical Layer in the 5GHz Band, 1999.

[4]   ETSI TR 101 683 v.1.1.1, Broadband Radio Access Network (BRAN); HIPERLAN Type 2; System Overview, 2000-02.

[5]   https://en.wikipedia.org/wiki/IEEE_802.20.

[6]   ARIB Std-T97, Mobile Broadband Wireless Access Systems (IEEE 802.20 TDD Wideband and 625k-MC Modes Application in Japan), 2008-11.

[7]   S.H.Muller and J.B.Huber, "OFDM with reduce peak-to-average power ratio by optimum combination of partial transmit sequences," *IEEE Electron. Letters*, Vol.33, No.5, pp.368-369, Feb.1997.

[8]   L.J.Cimini and N.R.Sollenberger, "Peak-to-average power ratio reduction of an OFDM signal using partial transmit sequences," *IEEE Communications Letters*, Vol.4(3), pp.86 - 88, Mar.2000.

[9]   R.W.Bauml, R.F.H.Fischer and J.B.Huber, "Reducing the peak-to-average power ratio of multicarrier modulation by selected mapping," *IEEE Electron. Letters*, Vol.32, No.22, pp.2056-2057, Oct.1996.

[10]   S.Y.L.Goff, S.S.Al-Samahi, B.K.Khoo, C.C.Tsimenidis and B.S.Sharif, "Selected mapping without side information for PAPR reduction in OFDM," *IEEE Transaction Wireless Communications*, Vol.8, No.7, pp.3320-3325, Jul.2009.

[11]   H.Ochiai and H.Imai, "Performance analysis of deliberately clipped OFDM signals," *IEEE Transactions on Communications*, Vol.50, pp.89-101, Jan.2002.

[12]   S.H.Han and J.H.Lee, "An Overview of Peak-to-Average Power Ratio Reduction Techniques for Multicarrier Transmission," *IEEE Transaction on Wireless Communications*, Vol.12, pp.56-65, Apr.2005.

[13]   H.G.Ryu, J.E.Lee and J.S.Park, "Dummy Sequence Insertion (DSI) for PAPR Reduction in the OFDM Communication System," *IEEE Transactions on Consumer Electronics*, Vol.50, pp.89-94, Feb.2004.

[14]   P.Boonsrimuang, K.Mori, T.Paungma and H.Kobayashi, "Proposal of Simple PAPR Reduction Method for OFDM Signal by Using Dummy Sub-Carriers," *IEICE Transactions on Communications*, Vol.E91-B, pp.784-794, Mar.2008.

[15]   L.K.Kook, K.Y.Gok and K.J.Hyuk, "A simple adaptive switching scheme between STBC-OFDM and SFBC-OFDM systems," *IEICE Transactions on Communications*, Vol.E92-B, No.11, pp.3546-3549, Nov.2009.

[16]   M.J.Dehghani, R.Aravind, S.Jam and K.M.M.Prabhu, "Space-Frequency Block Coding in OFDM Systems," *in Proc. of IEEE Region 10 Conference* (*TENCON*2004), pp.543-546, Nov.2004.

[17] S.A.Mujtaba, "Standardization of MIMO-OFDM Technology," *in Proc. Of IEEE International Conference on Networking and Communications* (*INCC*2008), pp.7-8, May2008.

[18] I.Baig and V.Jeoti, "A Zadoff-Chu Matrix Transform Precoding based Localized-OFDMA Uplink System: A PAPR analysis with RRC pulse shaping," *Acta Electrotechnica et informatica*, Vol.11, No.2, pp.64-69, Jun.2011.

[19] A.V.Oppenheim, A.S.Willsky and S.H.Nawas, "Signals and Systems," *2nd edition*, *Prentice Hall*, Feb.2008.

[20] B.A.Olshausen, "Aliasing," *PSC 129–Sensory Processes*, Oct.2000.

[21] P.Boonsrimuang, "Study on Mitigation Methods of Non-Linear Distortion for OFDM based Wireless Communications Systems," T*hesis for Doctor Degree, Division of System Engineering, Department of Electrical and Electronic Engineering*, Mie university, Mar.2007.

[22] IEEE Std. 802.11a, "High-speed Physical Layer in the 5GHz Band", 1999.

[23] H.Sari, G.Karam and I.Jeanclaude, "Transmission Techniques for Digital Terrestrial TV Broadcasting," *IEEE Communications Magazine*, Vol.33, pp.100-109, Feb.1995.

[24] A.Molisch, "3GPP Long Term Evolution," *Wireless Communication 2nd Edition*, *Wiley-IEEE Press*, pp.665-698, Nov.2010.

[25] J.Gozalvez, "Long-Term Evolution Advanced Demonstrations [Mobile Radio]," *IEEE Vehicular Technology Magazine*, Vol.6, pp.4-9, Dec.2011.

[26] D.Dardari, V.Tralli and A.Vaccari, "A Theoretical Characterization of Nonlinear Distortion Effects in OFDM Systems," *IEEE Transactions on Communications*, Vol.48, No.10, pp.1775-1764, Oct.2000.

[27] J.Tellado, "Multicarrier Modulation with Low PAR," *Kluwer Academic Publishers*, *Springer US*, 2000.

[28] X.Zhong, J.Qi and J.Bao, "Using Clipping and Filtering Algorithm to Reduce PAPR of OFDM System," *in Proc. of International Conference on Electronics, Communications and Control* (*ICECC*2011), pp.1763-1766, Sept.2011.

[29] Z.X.Dong, P.W.Sheng, L.Hong and T.Youxi, "Simplified Approach to Optimized Iterative Clipping and Filtering for PAPR Reduction of OFDM Signals," *IEEE Transactions on Communications*, Vol.11, pp.1891-1901, Feb.2013.

[30] H.B.Mishra, M.Mishra and S.K.Patra, "Selected Mapping based PAPR Reduction in WiMAX without Sending the Side Information," *in Proc. of Recent Advances in Information Technology* (*RAIT*2012), pp.182-184, Mar.2012.

[31] B.K.Taek, S.C.Yong and E.J.Powers, "Performance Analysis of OFDM Systems with Selected Mapping in the Presence of Nonlinearity," *IEEE Transactions on Wireless Communications*, Vol.12, pp.2314-2322, Apr.2013.

[32] J.Gao, J.Wang, B.Wang and X.Song, "Minimizing PAPR of OFDM Signals using Suboptimal Partial Transmit Sequences," *in Proc. of International Conference on Information Science and Technology* (*ICIST*2012), pp.776-779, Mar.2012.

[33] M.Gouda and M.Hussien, "Partial Transmit Sequence PAPR Reduction Method for LTE OFDM Systems," *in Proc. of Intelligent Systems Modeling and Simulation* (*ISMS*2013), pp.507-512, Jan.2013.

[34] C.Tellambura, "Computation of the Continuous-Time PAPR of an OFDM Signal with BPSK Sub-carriers," *IEEE Communications Letters*, Vol.5, pp.185-187, Jun.2001.

[35] T.Mata, K.Naito, P.Boonsrimuang, K.Mori and H.Kobayashi, "Proposal of PAPR Reduction Method for OFDM Signal by Re-Ordering of Clusters," *in Proc. of Asia-Pacific Conference on Communications* (*APCC*2013), pp.231-236, Aug.2013.

[36] P.Boonsrimuang, P.Reangsuntea, P.Boonsrimuang and H.Kobayashi, "Proposal of Improved PTS Method Based on Split-Radix IFFT for OFDM Signal," *David Publishing Computer Technology and Application 3*, pp.425-430, Jun.2012.

[37] W.Y.Shieh, C.C.J.Hsu, S.L.Tung, P.W.Lu, T.H.Wang and S.L.Chang, "Design of Infrared Electronic-Toll-Collection Systems with Extended Communication Areas and Performance of Data Transmission," *IEEE Transaction on Intelligent Transportation Systems*, Vol.12, pp.25-35, Mar.2011.

[38] Y.Hattori, T.Shimoda and M.Ito, "Development and Evaluation of ITS Information Communication System for Electric Vehicle," *in Proc. of IEEE 75th Vehicular Technology Conference (VTC-Spring*2012), pp.1-6, May2012.

[39] A.Ono, K.Naito, K.Mori and H.Kobayashi, "Roadside to Vehicle Communication System with OFDM Cooperative Transmission," *in Proc. of the 8th IEEE VTS Asia Pacific Wireless Communications Symposium (APWCS*2011), MP2-7, Aug.2011.

[40] D.Jiang and L.Delgrossi, "IEEE802.11p: Towards and International Standard for Wireless Access in Vehicular Environments," *in Proc. of IEEE 67th Vehicular Technology Conference (VTC-Spring*2008), pp.2036-2040, May2008.

[41] S.M.Alamouti, "A Simple Transmit Diversity Technique for Wireless Communications," *IEEE Journal on Selected Areas in Communications.*,Vol.16, pp.1451-1458, Oct.1998.

[42] T.Mata, P.Boonsrimuang, P.Boonsrimuang and H. Kobayashi, "Proposal of Improved PTS Method for STBC MIMO-OFDM Systems," *IEICE Transaction Communication Letter*, Vol.E93-B, No.10, Oct.2010.

[43] T.Mata, K.Naito, P.Boonsrimuang, K.Mori and H.Kobayashi, "Proposal of STBC MIMO-OFDM for ITS Systems," *in Proc. Of 10th International Conference on Electrical Engineering/Electronics, Computer, Telecommunications and Information Technology (ECTICON*2013), pp.1-6, May2013.

[44] G.Mkrtchyan, "Estimation, "Parameter Learning and Prediction of Time-varying Communication Channels," T*hesis for Doctor Degree, Division of System Engineering, Department of Electrical and Electronic Engineering*, Mie university, Sept.2006.

[45] H.Kobayashi and K.Mori, "Proposal of Channel Estimation Method for OFDM Systems under Time-Varying Fading Environments," *IEICE Transaction Communications*, Vol.J90-B, No.12, pp.1249-1262, Dec.2007.

[46] G.Santella, R.De Martino and M.Ricchiuti, "Single Frequency Network (SFN) Planning for Digital Terrestrial Television and Radio Broadcast Services: The Italian Frequency Plan for T-DAB," *in Proc. of IEEE 51st Vehicular Technology Conference (VTC-Spring*2004), pp.2307-2311, May2004.

[47] K.S.Ahn and R.W.Heath, "Performance Analysis of Maximum Ratio Combining with Imperfect Channel Estimation in the Presence of Co-channel Interferences," *IEEE Wireless Communications*, Vol.8, pp.1080-1085, Mar.2009.

[48] "Radio Broadcasting Systems Digital Audio Broadcasting (DAB) to Mobile, Portable and Fixed Receivers," ETS 300 401, v1.4.1, 2006.

[49] "Digital Video Broadcasting (DVB) Implementation Guidelines for the Second Generation Digital Terrestrial Television Broadcasting System (DVB-T2) ," ETSI TS 102 831, v1.2.1, 2012

[50] "IEEE Standard for Local and Metropolitan Area Networks Part 16: Air Interface for Fixed Broadband Wireless Access Systems," IEEE Std. 802.16, 2004

[51] J.Kim and I.Lee, "802.11 WLAN History and New Enabling MIMO Techniques for Next Generation Standards," *IEEE Communication Magazine*, Vol.53(3), pp.134-140, Mar.2015.

[52] M.Jiang and L.Hanzo, "Multi-user MIMO-OFDM for Next Generation Wireless Systems," *in Proc. of the IEEE*, Vol. 95(7), pp.1430-1469, Jul.2007.

[53] P.Sure and C.M.Bhuma, "A Pilot Aided Channel Estimator using DFT based Time Interpolation for Massive MIMO-OFDM Systems," *International Journal of Electronics and Communications* (*AEU*), Vol.69(1), pp.321-327, 2015.

[54] T.Mata, P.Boonsrimuang, K.Mori and H.Kobayashi, "Time-Domain Channel Estimation Method for MIMO-OFDM Systems," *IEICE General Conference 2015*, B-1-155, Mar.2015.

[55] M.Diallo, M.Hélard, L.Cariou and R.Rabineau, "Chapter6: DFT based Channel Estimation Methods for MIMO-OFDM Systems," *Vehicular Technologies*, *InTech*, pp.97-114, Apr.2011.

[56] T.Mata, M.Hourai, P.Boonsrimuang, K.Mori and H.Kobayashi, "Time Domain Channel Estimation Method for Uplink OFDMA System," *in Proc. of the 22nd International Conference on Telecommunications* (*ICT*2015), pp.363-367, Apr.2015.

[57] S.C.Yang, "OFDMA System Analysis and Design," *Artech House*, *Norwood*, MA 2010.

[58] O.Popescu and D.C.Popsescu, "On the Performance of 4G Mobile Wireless System with Multiple Antennas," *in Proc. of IEEE 10th International Conference on Communications* (*COMM*2014), pp.1-4, May 2014.

[59] W.C.Huang, Y.S.Yang and C.P.Li, "A New Pilot Architecture for Sub-band Uplink OFDMA Systems," *IEEE Transactions on Broadcasting*, Vol.59(3), pp.461-470, Sept. 2013.

[60] W.C.Huang, X.Z.He, C.P.Li and H.J.Li, "On Pilot Design for Channel Estimation and MUI Reduction in Uplink OFDMA Systems," *in Proc. of IEEE Wireless Communications and Networking Conference* (*WCNC*2009), pp.1-6, Apr2009.

[61] K.Hayashi and H.Sakai, "Uplink Channel Estimation for OFDMA System," *in Proc. of IEEE International Conference on Acoustics, Speech and Signal Processing* (*ICASSP*2007), pp.(III)285-(III)288 , Apr.2007.

[62] Y.Wang, Li.Lihua, P.Zhang and Z.Liu,"DFT-Based Channel Estimation with Symmetric Extension for OFDMA Systems," *EURASIP Journal on Wireless Communications and Networking* 2009, Jan.2009.

[63] H.Kobayashi and K.Mori, "Proposal of OFDM Channel Estimation Method using Discrete Cosine Transform," *IEICE Transaction on communications* (*Japanese edition*), Vol.J88-B, No.2, Jan.2005.

[64] M.T.Tran, J.S.Wang, I.Song and Y.H.Kim, "Channel Estimation and Optimal Training with the LMMSE Criterion for OFDM-based Two-Way Relay Networks," *EURASIP Journal on Wireless Communications and Networking* 2013, Vol.2013, May 2013.

[65] R.Ahlswede, N.Cai, S.Y.R.Li and R.W.Yeung, "Network Information Flow," *IEEE Transactions on Information Theory*, Vol.46(4), pp.1204-1216, Jul 2000.

[66] S.Katti, S.S.Gollakota and D.Katabi, "Embracing Wireless Interference: Analog Network Coding," *in Proc. of the Conference on Applications, Technologies, Architectures, and Protocols for Computer Communications* (*ACM SIGCOM*2007), pp.397-408, Aug. 2007.

[67] H.Gacanin. T.Sjodin and F.Adachi, "On Channel Estimation for Analog Network Coding in a Frequency-Selective Fading Channel," *EURASIP Journal on Wireless Communications and Networking* 2011, Vol.2011, 2011.

[68] I.Prodan, T.Obara, F.Adachi and H.Gacanin, "Performance of pilot-assisted channel estimation without feedback for broadband ANC systems using OFDM access," *EURASIP Journal on Wireless Communications and Networking*, 2012.

[69] Y.Koshimizu and E.Okamoto, "An effective channel estimation scheme for bi-directional two-timeslots OFDM relay transmission using analog network coding," *in Proc. of IEEE 75th Vehicular Technology Conference* (*VTC*2012-*spring*), pp.1-5, May2012.

[70] Y.Koshimizu and E.Okamoto, "An effective channel estimation scheme using Walsh pilots in bi-directional wireless OFDM relay systems with analog network coding," *IEICE Transactions on Communications*, E96-B, No.8, pp.2119-2130, 2013.

[71] F.Gao, R.Zhang, and Y. C.Liang, "On Channel Estimation for Amplify-and-Forword Two-Way Relay Networks," *in Proc. of IEEE Global Telecommunications Conference* (*Globecon*2008), pp.1-5, Dec 2008.

[72] T.Mata, K.Naito, P.Boonsrimuang, K.Mori and H.Kobayashi, "Proposal of Channel Estimation Method for ITS systems by using STBC MIMO-OFDM.," *ECTI Transactions on Computer and Information Technology*, Vol.8, No.1, pp.36-44, 2013.

[73] F.K.Gong, J. K.Zhang and J.H.Ge, "Distributed Concatenated Alamouti Codes for Two-Way Relaying Networks," *IEEE Wireless Communication Letter,* Vol.1, No.3, pp.197-200, 2012.

[74] V.T.Muralidharan and B.S.Rajan, "Distributed Space Time Coding for Wireless Two-Way Relaying," *IEEE Transactions on Signal Processing,* Vol.61, No.4, pp.981-991, 2013.

[75] T.Mata, K.Naito, P.Boonsrimuang, K.Mori and H.Kobayashi, "Proposal of Channel Estimation Method for Bi-directional OFDM Based ANC in Higher Time-varying Fading Channel," *in Proc. of IEEE 79th Vehicular Technology Conference* (*VTC*2014-*spring*), pp.1-5, May2014.